

# O Analytical and Numerical Methods in Acoustics

with M. Ochmann

Numerous analytical and numerical methods are displayed in this book together with the solutions for special tasks. This chapter contains analytical and numerical methods to be applied in acoustics, going beyond the scope of single examples. The description of a method unavoidably needs more textual explanations than the representation of just the resulting formulas. ➤ *Sect. O.1* describes a procedure for optimisation of the parameters of a sound absorber; ➤ *Sect. O.2* outlines a method for the evaluation of many concatenated transfer matrices. ➤ *Section O.3* will present five standard problems of numerical acoustics which frequently occur in practical applications. In ➤ *Sects. O.4–O.6* three important methods for the numerical solution of these problems will be described. The source simulation technique and the boundary element method are mainly used for exterior problems such as the radiation or the scattering problem (see ➤ *Sects. O.4* and *O.5*). The finite element method is especially suited for computing sound fields in interior spaces (see ➤ *Sect. O.6*). The fluid–structure interaction problem can be treated by a combined finite element and boundary element approach, for example with the method of ➤ *Sect. O.6*. The transmission problem can be formulated in terms of boundary integral equations (see ➤ *Sect. O.5*). Analytical field solutions for benchmark models are given in ➤ *Sects. O.7, O.8*.

## O.1 Computational Optimisation of Sound Absorbers

---

► See also: ➤ *Sect. J.34* for a similar task with duct lining absorbers.

*The situation:*

There exist precise and fast computing algorithms for the evaluation of a variety of absorbers, even those with complicated structures (e.g. multi-layer absorbers with foils and/or resonator neck plates in front of and/or between the layers of the absorber; see ➤ *Chs. D, G, H*). If one intends to design an absorber with a good performance in some aspect (e.g. sound absorption), one has to optimise by trial and error. This is an optimisation in the space of the absorber parameters which often becomes a 10- to 20-dimensional space, if all parameters are to be optimised in one run.

### The task:

Write a computer program which performs this optimisation of the absorber parameters.

What does “optimisation” mean ?

First, one has to fix the absorber quantity which should be improved by variation, e.g. the sound absorption coefficient  $\alpha$ .

Second, optimisation is generally understood with respect to a frequency response curve of that quantity. This introduces a frequency interval ( $f_{lo}, f_{hi}$ ) for optimisation, and a stepping through the interval, with either linear or logarithmic steps. Logarithmic stepping may be preferable, because it accentuates lower frequencies, which is often wanted.

Third, optimisation cannot be understood as a general optimisation of all parameters, because then the result can be found in most cases without any computation. For example, the general optimisation with respect to sound absorption of a multi-layer absorber would produce a porous layer with a huge thickness and a tiny flow resistivity of the material, with no surface cover. Therefore a reasonable optimisation supposes some given *structure* of the absorber (e.g. multi-layer absorber with locally reacting layers and possibly layer covers, or multiple-layer absorbers with bulk reacting layers, or locally reacting and bulk reacting layers in a mixed sequence, or resonators of different structures, etc.).

The following description of the method uses as a special example (just for illustration) a multi-layer absorber with locally reacting layers (in fact the layers must not be partitioned if the flow resistivity values of porous materials come out with sufficiently high values). Next, a “parallel” absorber will be optimised.

### Fundamentals:

The acoustical evaluation begins with the computation of the normalised input admittance  $Z_0 G$  of the arrangement. This evaluation needs as input most of the absorber parameters. The next step is the evaluation of the reflection coefficient  $|r|^2$  from which the absorption coefficient follows as  $\alpha = 1 - |r|^2$ .

$$\alpha(\Theta) = 1 - |r(\Theta)|^2; \quad r(\Theta) = \frac{\cos\Theta - Z_0 G}{\cos\Theta + Z_0 G}. \quad (1)$$

The absorption coefficient  $\alpha_{\text{dif}}$  for diffuse sound incidence on locally reacting absorbers is obtained with  $Z_0 G = g' + j \cdot g''$  by:

$$\begin{aligned} \alpha_{\text{dif}} &= 8g' \left[ 1 + \frac{g'^2 - g''^2}{g''} \arctan \left( \frac{g''}{g' + g'^2 + g''^2} \right) - g' \ln \left( 1 + \frac{1 + 2g'}{g'^2 + g''^2} \right) \right], \\ &\xrightarrow{g'' \rightarrow 0} 8g' \left[ 1 + \frac{g'}{1 + g'} - g' \ln \left( 1 + \frac{1 + 2g'}{g'^2} \right) \right]. \end{aligned} \quad (2)$$

If the absorber is bulk reacting, or has mixed bulk and locally reacting layers,  $\alpha_{\text{dif}}$  is obtained from  $\alpha(\Theta)$  by evaluation for a set of incidence angles  $\Theta$  and numerical list integration of the intermediate results. We further write  $\alpha$  and  $|r|^2$  commonly for the different possible kinds of incidence.

It is important that one knows an “ideal value” for  $\alpha$ , i.e.  $\alpha = 1$  (this value can be used as the goal, even knowing that for locally reacting absorbers the highest possible absorption coefficient for diffuse incidence is  $\alpha \approx 0.95$ ). Then in the relation  $\alpha = 1 - |r|^2$  the reflection coefficient  $|r|^2$  can be interpreted as a squared “error” of the actual value  $\alpha$  compared with the ideal value  $\alpha = 1$ . The algorithm for optimisation minimises the averaged square error

$$\langle |r|^2 \rangle = q(a_1, a_2, \dots; b_1, b_2, \dots) \\ = \sum_n w_n \cdot |r(f_n; a_1, a_2, \dots; b_1, b_2, \dots)|^2 / \sum_n w_n \stackrel{!}{=} \text{Min}, \quad (3)$$

where  $f_n$  are sampling frequencies over  $(f_{lo}, f_{hi})$ ;  $w(f)$  is a weight function;  $w_n = w(f_n)$ ; the  $\{a_i\}$  are the variable absorber parameters; the  $\{b_k\}$  are fixed parameters. The minimisation is performed by variation of the  $\{a_i\}$ .

The use of a weight function  $w(f)$  introduces the possibility to perform either a broad-banded optimisation over  $(f_{lo}, f_{hi})$ , e.g. with  $w(f) = 1$ , or a centred optimisation, if  $w(f)$  has a central maximum in  $(f_{lo}, f_{hi})$  (this form of optimisation can be used, for example, for the down-tuning of resonators, together with an improvement).

There exist algorithms in the literature for finding a minimum of a real function in the multi-dimensional space (e.g. W.H. Press et al. “Numerical Recipes”, Cambridge University Press). A principal distinction must be made in such algorithms whether the partial derivatives  $\partial q / \partial a_i$  can be evaluated or not. This generally is not possible in the present task. Some start values  $\{a_i\}_{\text{start}}$  must be given for the start of the minimum search. Most algorithms described for minimisation extend the search over the whole (real) space of the  $\{a_i\}$ , i.e. also to negative values. In our case, however, the parameters  $a_i$  represent geometrical lengths or material data which should be positive; some of them, like the porosity  $\sigma$ , have to respect lower and higher limits ( $0 < \sigma < 1$ ). Thus range limits for the  $a_i$  must be transmitted to the minimisation algorithm.

The procedure for optimisation of the absorption coefficient  $\alpha$  (and similarly for other target quantities) works as follows:

1. Make the decision for the target quantity (e.g. the sound absorption coefficient  $\alpha$  for diffuse incidence).
2. Make the decision for a structure of the absorber (e.g. a multi-layer absorber with locally reacting layers with (possibly) porous cover foils and/or perforated plates on the front sides of the layers). This decision determines the theoretical description of the absorber.
3. Fix the frequency interval  $(f_{lo}, f_{hi})$ , the kind of frequency steps (linear  $\Delta f$  or logarithmic  $\Delta \lg(f)$ , which often is preferable), the step width (it should not be too large, otherwise  $\langle |r|^2 \rangle = q(a_1, a_2, \dots; b_1, b_2, \dots)$  may not be steady enough for finding a minimum); fix the type of the weight function  $w(f)$  (see above).
4. Conceive a “start configuration” of the absorber, i.e. select values for all required absorber parameters (they define what will be called here the “original absorber”).

It is supposed that at this stage the data input is structured as follows (just for giving an example for a two-layer absorber; entries *(\*text\*)* indicate comment text):

```
(*Input frequency*)
flo= 50.; fhi= 2000. ;      lgfstep= 0.1 ;
(*Input layers*)
gn= 2 ;                    (*number N of layers*)
matlist= {1, 1} ;          (*types of porous material*)
Ξlist= {10000., 10000.};   (*flow resistivities Ξ *)
tlist= {0.05, 0.05 } ;     (*layer thickness t in meter*)
(*Input foils*)
pflist= {2700., 2700.};    (*foil material density pf in kg/m³*)
```

```

dflist= {0.0002, 0.0002}; (*foil thickness  $d_f$  in meter *)
Rflist= {1000., 2. }; (*normalised foil flow resistance  $R_f$  *)
(*Input perforates*)
shapelist= {1, 1}; (*perforation shape; 1= hole; 2= slit *)
 $\sigma$ list= {0., 0. }; (*porosity  $\sigma$  *)
dialist= {0., 0. }; (*diameter of perforation in meter*)
dplist= {0., 0. }; (*plate thickness  $d_p$  in meter *)

```

(Values  $d_f = 0$  or  $d_p = 0$  indicate that there is no foil or plate in that position; the other foil or plate parameter entries in that position then are neglected).

5. Determine which absorber parameters should be varied for optimisation. Some parameters evidently cannot be varied, such as the number  $N$  of layers, the layer material type (in `matlist`), the shape of the perforations (in `shapelist`); others should be kept constant, because a variation could lead to values which cannot be realised (such as the foil material density  $\rho_f$  in `pflist`).

The variable parameters could be signalled by lists of flags like:

```

(*Input layers*)
 $\Xi$ flag= {1 , 1 }; (*flow resistivities  $\Xi$  *)
tflag= {0 , 0 }; (*layer thickness  $t$  in meter*)
(*Input foils*)
dfflag= {0 , 0 }; (*foil thickness  $d_f$  in meter *)
Rfflag= {1 , 1 }; (*normalised foil flow resistance  $R_f$  *)
(*Input perforates*)
 $\sigma$ flag= {0 , 0 }; (*porosity  $\sigma$  *)
diaflag= {0 , 0 }; (*diameter of perforation in meter*)
dpflag= {0 , 0 }; (*plate thickness  $d_p$  in meter *)

```

A value 1 indicates that the corresponding parameter belongs to the  $\{a_i\}$ , a value 0 signals that the parameter belongs to the  $\{b_k\}$ . The number of unit values determines the dimension of the space of variables for the minimisation.

6. Some algorithms for minimisation need more than one set of start parameters, for example to indicate the direction of the search, or to fix the search range limits. They can, for example, be entered by lists like (where `xx` stands for suitable values at the list positions of the variable parameters  $a_i$ ; entries 0 signal constant parameters):

```

(*Input layers*)
 $\Xi$ lo= {xx , xx }; (*flow resistivities  $\Xi$  *)
tlo= {0 , 0 }; (*layer thickness  $t$  in meter*)
(*Input foils*)
dflo= {0 , 0 }; (*foil thickness  $d_f$  in meter *)
Rflo= {xx , xx }; (*normalised foil flow resistance  $R_f$  *)
(*Input perforates*)
 $\sigma$ glo= {0 , 0 }; (*porosity  $\sigma$  *)
dialo= {0 , 0 }; (*diameter of perforation in meter*)
dplo= {0 , 0 }; (*plate thickness  $d_p$  in meter *)

```

and

```

(*Input layers*)
 $\Xi$ hi= {xx , xx }; (*flow resistivities  $\Xi$  *)
thi= {0 , 0 }; (*layer thickness  $t$  in meter*)
(*Input foils*)
dfhi= {0 , 0 }; (*foil thickness  $d_f$  in meter *)
Rfhi= {xx , xx }; (*normalised foil flow resistance  $R_f$  *)

```

(\*Input perforates\*)

$\sigma_{ghi} = \{0, 0\}$ ; (\*porosity  $\sigma$  \*)

$d_{iahi} = \{0, 0\}$ ; (\*diameter of perforation in meter\*)

$d_{phi} = \{0, 0\}$ ; (\*plate thickness  $d_p$  in meter \*)

7. If one writes a general algorithm for minimisation of a function  $q(\{a_i\}, \{b_k\})$ , which should be usable for a changing number and composition of the  $\{a_i\}, \{b_k\}$ , then one should write a subroutine which transmits the variable absorber parameters to the variables  $\{a_i\}$ .
8. One needs correspondingly a subroutine which transmits the improved  $\{a_i\}$  back to the right positions of the variable absorber parameters (the information comes from the lists of flags).

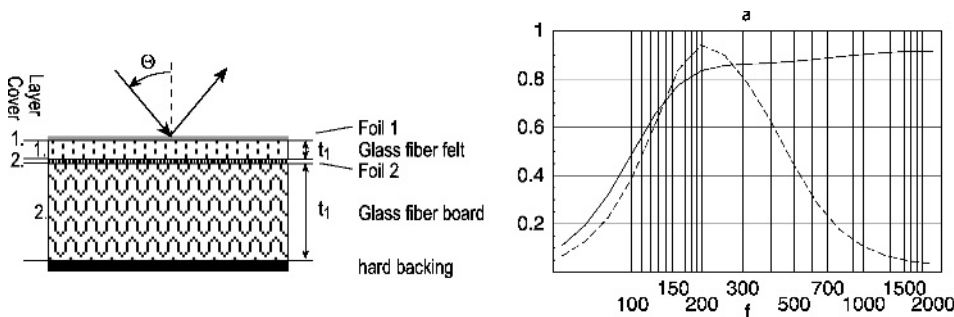
This subroutine, at the same time, takes care of the range limits for the parameters. A lower limit zero, for example, will be respected, if the subroutine transmits  $|a_i|$ . A lower or a higher non-zero limit can be introduced by the replacement of  $a_i$  by the limit values  $\dots lo$  or  $\dots hi$  whenever  $a_i$  exceeds a limit; this procedure replaces the variable function  $q(a_i; b_k)$  outside the limits by a constant value with respect to  $a_i$  (the minimisation program consequently will avoid ranges outside the limits).

### Examples of 2-layer absorbers:

Some examples will illustrate the procedure. The absorber is a two-layer absorber with locally reacting layers, possibly with foils and/or perforated plates (resonator neck plates) at the front sides of the layers. Diffuse sound incidence is applied.

#### First example:

This example uses the data input for the “original absorber” as given in the above lists; the variable parameters are  $\Xi list[[1]]$ ,  $\Xi list[[2]]$ ,  $Rnlist[[1]]$ ,  $Rnlist[[2]]$  ( $list[[n]]$  indicates the list element at position  $n$  of the list). The diagram below shows  $\alpha_{dif}$  for both the original absorber (dashed curve) and the optimised absorber (full line); the print-out of the input data indicates the optimised parameters with bold printing.



Input & optimised parameters

(\*Input frequency\*)

$f_{lo}=50.$ ,  $f_{hi}=2000.$ ,  $\Delta lg(f)=0.1$

(\*Flags\*)

Reflection=diffuse, Weight=no

(\*Number of layers & dimensions\*)



```

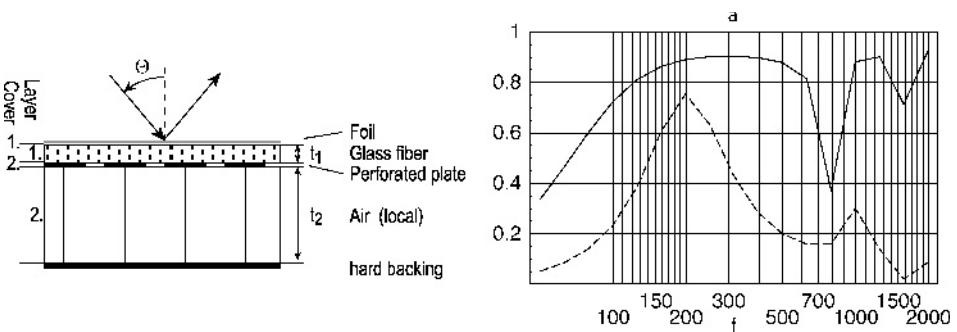
Nlayer=2, dim=4
(*Layer parameters*)
mat={1,1}
Ξ={13468.5, 4435.31}
t={0.05,0.05}
(*Foil parameters*)
ρf={2700.,2700.}
df={0.0002,0.0002}
Rf={1.28767, 1.67335}
(*Perforate parameters*)
shapes={1,1}
σ={0.,0.}
dia={0.,0.}
d={0.,0.}
(*Minimum value of <|r|^2>*)
<|r|^2>min=0.2783
(*Varied parameters*){Ξlist[[1]],Ξlist[[2]],Rflist[[1]],Rflist[[2]]}

```

The loss of absorption in the resonance maximum could be reduced by choosing a smaller frequency interval ( $f_{lo}, f_{hi}$ ) and a weight function  $w(f)$  with a central weighting (e.g. in the form of a cosine arc).

### Second example:

The second example uses a resonator neck plate between the layers; its porosity is constant with  $\sigma = 0.15$ . The second layer makes up the resonator volumes; it consists of air ( $mat = 0$ ). The Helmholtz resonance is marked by a rather low maximum of  $\alpha$  of the original absorber at higher frequencies. Varied parameters are  $\Xi_{list}[[1]]$ ,  $t_{list}[[2]]$ ,  $R_{flist}[[1]]$ ,  $d_{ialist}[[2]]$ ,  $d_{plist}[[2]]$ .



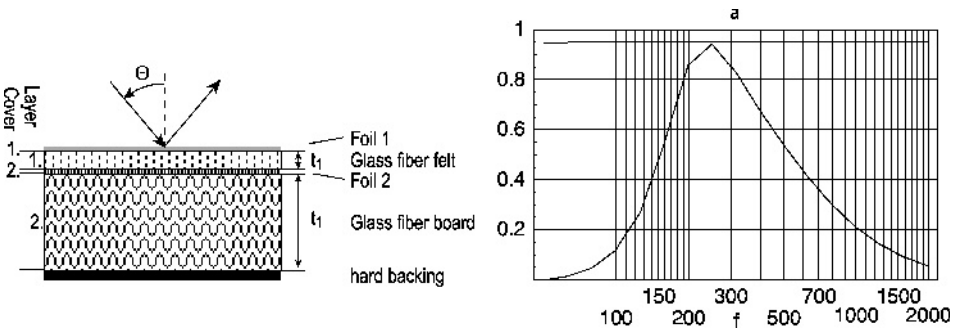
```

Input & optimised parameters (in bold)
(*Input frequency*)
flo=50., fhi=2000., Δlg(f)=0.1
(*Flags*)
Reflection=diffuse, Weight=no
(*Number of layers & dimensions*)
Nlayer=2, dim=5

```

```
(*Layer parameters*)
mat={1,0}
Ξ={32183.4, 0.}
t={0.02, 0.185033}
(*Foil parameters*)
ρf={2700.,0.}
df={0.0002,0.}
Rf={0.903345, 0.}
(*Perforate parameters*)
shapes={0,1}
σ={0.,0.15}
dia={0., 0.000174437}
d={0., 0.00628449}
(*Minimum value of <|r|^2>*)
<|r|^2>min=0.233324
(*Varied
parameters*){Ξlist[[1]],tlist[[2]],Rfist[[1]],dialist[[2]],dlist[[2]]}
```

The **third example** is more of a theoretical than a practical interest. Thickness and flow resistance of the cover foil and of the first layer are variable. The absorption coefficients  $\alpha$  for diffuse incidence of the original absorber displays a resonance (curve) and the optimised absorber shows the upper nearly horizontal line.



Input & optimised parameters (in bold)

```
(*Input frequency*)
flo=50., fhi=2000., Δlg(f)=0.1
(*Flags*)
Reflection=diffuse, Weight=no
(*Number of layers & dimensions*)
Nlayer=2, dim=4
(*Layer parameters*)
mat={1,1}
Ξ={328.465, 10000.}
t={3.26549, 0.05}
(*Foil parameters*)
ρf={2700.,2700.}
```

```

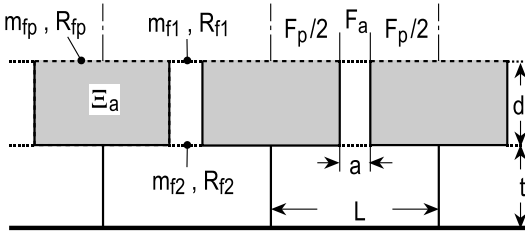
df={0.000328666, 0.0002}
Rf={0.513109, 2.}
(*Perforate parameters*)
shapes={1,1}
σ={0.,0.}
dia={0.,0.}
d={0.,0.}
(*Minimum value of <|r|^2>*)
<|r|^2>min=0.0492101
(*Varied parameters*){Ξlist[[1]],tlist[[1]],dfist[[1]],Rfist[[1]]}

```

As one could have anticipated the result with this choice of the set of variable parameters. The front layer has an enormous thickness and a very small flow resistivity, and the cover foil is thin with a low flow resistance. It is of some interest that the average reflection coefficient  $\langle |r|^2 \rangle$  obtained by optimisation is very precisely the theoretical minimum for diffuse sound incidence on locally reacting absorbers.

### Example of a “parallel” absorber:

The examples of multi-layer absorbers, shown above, can be named “series” absorbers. A “parallel” absorber, in contrast, is composed of different elementary absorbers which are placed side by side. As long as the lateral dimensions of the component absorbers and the composition are small compared to the wavelength, only the average admittance  $\langle G \rangle$  counts.



Boxes of width  $L - a$  and depth  $d$  contain a porous absorber material (e.g. glass fibres) with flow resistivity  $\Xi$ . Between the boxes are gaps of width  $a$  which form the necks of Helmholtz resonators. The boxes and/or one or both neck orifices may be covered with foils having a surface mass density  $m_f = \rho_f \cdot d_f$  and a normalised flow resistance  $R_f$ . With  $G_p$  for the input admittance of the boxes, and  $G_a$  for the input admittance of the resonator necks, the average admittance is:

$$\langle G \rangle = \frac{G_p + \beta \cdot G_a}{1 + \beta}; \quad \beta = \frac{F_a}{F_p} = \frac{a/L}{1 - a/L}. \quad (4)$$

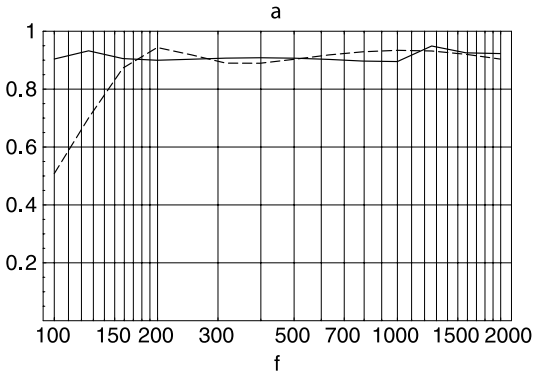
Possibly varied parameters are:

```
pars= {L, a/L, d/L, t/L, Ξ, d_fp, R_fp, d_f1, R_f1, d_f2, R_f2}
```

i.e. up to 11 variables in the search for a minimum.



The dashed curve of the “original” absorber in the following diagram for the sound absorption coefficient with diffuse sound incidence was obtained after “manual” optimisation. The full curve was obtained after application of the optimisation algorithm on the printed input data.



Input & optimised parameters

(\*Input frequency\*)

f<sub>lo</sub>=100. [Hz], f<sub>hi</sub>=2000. [Hz],  $\Delta \lg(f)=0.1$

(\*Flags\*)

Reflection=diffuse, Weight=no

(\*Dimensions\*)

L=0.2 [m], a/L=0.1, d/L=0.3, t/L=0.5

(\*Layer parameters\*)

Mat=1

$\Xi$  =10000. [Pa·s/m<sup>2</sup>]

(\*Foil parameters\*)

$\rho_{fp}$ =2700. [kg/m<sup>3</sup>]

d<sub>fp</sub>=0.0005 [m]

R<sub>fp</sub>=1.

Foil Position=1

$\rho_{f1}$ =2700. [kg/m<sup>3</sup>]

d<sub>f1</sub>=0.0002 [m]

R<sub>f1</sub>=0.2

$\rho_{f2}$ =0.

d<sub>f2</sub>=0.

R<sub>f2</sub>=0.

(\*Minimum value of  $\langle |r|^2 \rangle$ \*)

$\langle |r|^2 \rangle_{\min}=0.0886165$

(\*Varied parameters\*)

{a/L, d/L, d<sub>f1</sub>, R<sub>f1</sub>}={0.0862694, 0.554809, 0.0000810588, 0.35581}

### Post-processing:

One should notice that the algorithms for finding a minimum generally search for local minima, a number of which may exist in the range of the variable parameters, especially if the dimension of the parameter space is large.



9. You may try to find other minima either by starting with a different “original absorber” and/or by using other parameter ranges.
10. You may modify the optimum found, for example by an exchange of a large resonator volume depth with a smaller neck plate porosity. Then put the other optimised parameter values among the  $\{b_k\}$  and append a run of optimisation with the parameters between which a “trading” shall be tried.
11. It is a good practice to evaluate the target quantity with some “manual” modifications of the optimised parameter values, in order to see whether the absorber is sensitive with respect to small changes of the parameter values. In a similar procedure it can be tested, whether parameter values which are evaluated by optimisation, but which are not available in reality, can be replaced by nearby values of available absorber components.
12. Do not forget that the optimum found may depend also on the frequency range used  $\{f_{lo}, f_{hi}\}$ .

A final remark should be made. The program for finding the minimum may make wide excursions in the parameter space. Therefore the evaluations for the input admittance  $Z_0 G$  and the reflection coefficient  $|r|^2$  should apply formulas with analytical foundations, in order to avoid false or even nonsense results. This implies that the evaluation of characteristic data of porous materials should not use formulas which stem of regressions through experimental data (like the Delany–Bazley approximation), because the range of the flow resistivity, for example, in which the data were measured may be exceeded. Evaluations are recommended which are based either on analytical models of porous materials or on analytical models which are fitted to experimental data. Further, the diameter of resonator necks may become very small within the search for a minimum. It is recommended to use the propagation constant and wave impedance in capillaries, which include viscous and thermal losses and which go to  $j \cdot k_0$ ,  $Z_0$  for wider necks.

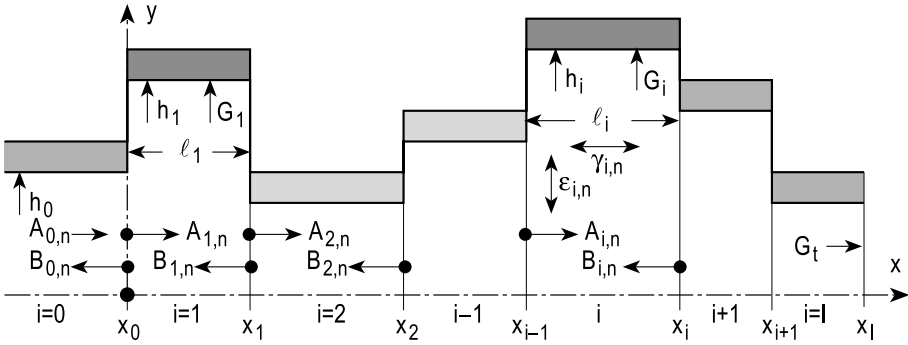
## 0.2 Computing with Mixed Numeric-Symbolic Expressions, Illustrated with Silencer Cascades

---

► See also: 🔍 Sects. J.19, J.20 dealing with silencer cascades, where the problem of this Section is avoided by neglecting acoustical feedback in the ducts, and 🔍 Sect. J.29 with a more simple application, due to the monotonic variation of cross-sections.

There are many tasks in acoustics which lead to iterative linear systems of equations. Such tasks are, for example, duct cascades, mufflers, conical ducts, wedges, a medium with spatial variation, etc. In principle one could consider the system of systems of linear equations as a large system for the combined vector of variables of those systems. However, this procedure mostly fails in its numerical realisation.

On the other hand, there exist mathematical programs which support both numerical and symbolic computations. This feature can be used to design straightforward solutions for the mentioned tasks, avoiding large systems of equations and many inversions of matrices. The method will be explained and illustrated with the example of a cascade of sections of lined ducts with different cross-sections and/or linings.



A sequence  $i = 1, 2, \dots, I$  of two-dimensional, flat duct sections follow each other, with half heights  $h_i$ , lengths  $\ell_i$ , and lined with locally reacting absorbers with input admittances  $G_i$ . The fields in the sections are formulated as mode sums of forward propagating modes with amplitudes  $A_{i,n}$  and backward propagating modes with amplitudes  $B_{i,n}$ . The lateral wave numbers  $\epsilon_{i,n}$  follow from the characteristic equations of the sections, the axial propagating constants  $\gamma_{i,n}$  from the secular equation. Some kinds of excitation at the entrance  $x = x_0$  will be considered, and some kinds of terminations at  $x = x_l$ . The “heads” of duct steps are assumed to be hard.

Field formulations:

$$p_i(x, y) = \sum_n [A_{i,n} \cdot e^{-\gamma_{i,n}(x-x_{i-1})} + B_{i,n} \cdot e^{+\gamma_{i,n}(x-x_i)}] \cdot q_{i,n}(y), \quad (1)$$

$$Z_0 v_{i,x}(x, y) = -j \sum_n \frac{\gamma_{i,n}}{k_0} [A_{i,n} \cdot e^{-\gamma_{i,n}(x-x_{i-1})} - B_{i,n} \cdot e^{+\gamma_{i,n}(x-x_i)}] \cdot q_{i,n}(y)$$

$$\text{with the mode profiles: } q_{i,n}(y) = \cos(\epsilon_{i,n}y) \quad (2)$$

and the lateral wave numbers  $\epsilon_{i,n}$  being solutions of the characteristic equations:

$$(\epsilon_{i,n}h_i) \cdot \tan(\epsilon_{i,n}h_i) = jk_0h_i \cdot Z_0G_i \quad (3)$$

and the axial propagation constants from the secular equations:

$$\gamma_{i,n}h_i = \sqrt{(\epsilon_{i,n}h_i)^2 - (k_0h_i)^2}; \quad \text{Re}\{\gamma_{i,n}h_i\} \geq 0. \quad (4)$$

Mode norms  $N_{i,m}$ :

$$\frac{1}{h_i} \int_0^{h_i} q_{i,m}(y) \cdot q_{i,n}(y) dy = \delta_{m,n} \cdot N_{i,m}; \quad N_{i,m} = \frac{1}{2} \left( 1 + \frac{\sin(2\epsilon_{i,m}h_i)}{2\epsilon_{i,m}h_i} \right). \quad (5)$$

Mode coupling coefficients  $C(i, m; k, n)$ :

$$C(i, m; k, n) = \frac{1}{h_i} \int_0^{h_i} q_{i,m}(y) \cdot q_{i,n}(y) dy; \quad k = \begin{cases} i-1 \\ i+1 \end{cases}, \quad (6)$$

$$C(i, m; k, n) = \frac{1}{2} \left( \frac{\sin((\epsilon_{i,m} - \epsilon_{k,n})h_i)}{(\epsilon_{i,m} - \epsilon_{k,n})h_i} + \frac{\sin((\epsilon_{i,m} + \epsilon_{k,n})h_i)}{(\epsilon_{i,m} + \epsilon_{k,n})h_i} \right).$$

Boundary conditions at  $x = x_i$  for sound pressure and axial particle velocity:

*expanding duct:* ( $h_{i+1} \geq h_i$ )

$$\begin{aligned} p_i(x_i, y) &\stackrel{!}{=} p_{i+1}(x_i, y) \quad \text{in } y = (0, h_i), \\ Z_0 v_{i+1,x}(x_i, y) &\stackrel{!}{=} \begin{cases} Z_0 v_{i,x}(x_i, y) & \text{in } y = (0, h_i) \\ 0 & \text{in } y = (h_i, h_{i+1}) \end{cases}, \end{aligned} \quad (7)$$

*contracting duct:* ( $h_{i+1} < h_i$ )

$$\begin{aligned} p_i(x_i, y) &\stackrel{!}{=} p_{i+1}(x_i, y) \quad \text{in } y = (0, h_{i+1}), \\ Z_0 v_{i,x}(x_i, y) &\stackrel{!}{=} \begin{cases} Z_0 v_{i+1,x}(x_i, y) & \text{in } y = (0, h_{i+1}) \\ 0 & \text{in } y = (h_{i+1}, h_i) \end{cases}. \end{aligned} \quad (8)$$

Notations (for ease of writing):

$$\gamma_{i,n} h_{i+1} = \gamma h_{i,n}; \quad \gamma_{i,n} \ell_i = \gamma \ell_{i,n}; \quad A_{i,n} \cdot N_{i,n} = \bar{A}_{i,n}; \quad B_{i,n} \cdot N_{i,n} = \bar{B}_{i,n}. \quad (9)$$

By use of the orthogonality, with  $m = \text{any mode order}$ :

*expanding duct:* ( $h_{i+1} \geq h_i$ )

$$\begin{aligned} [\bar{A}_{i,m} \cdot e^{-\gamma \ell_{i,m}} + \bar{B}_{i,m}] &= \sum_n [\bar{A}_{i+1,n} + \bar{B}_{i+1,n} \cdot e^{-\gamma \ell_{i+1,n}}] \\ &\quad \cdot \frac{C(i, m; i+1, n)}{N_{i+1,n}}, \\ \gamma h_{i+1,m} \cdot [\bar{A}_{i+1,m} - \bar{B}_{i+1,m} \cdot e^{-\gamma \ell_{i+1,m}}] &= \sum_n \gamma h_{i,n} \cdot [\bar{A}_{i,n} \cdot e^{-\gamma \ell_{i,n}} - \bar{B}_{i,n}] \\ &\quad \cdot \frac{C(i, n; i+1, m)}{N_{i,n}}, \end{aligned} \quad (10)$$

*contracting duct:* ( $h_{i+1} < h_i$ )

$$\begin{aligned} [\bar{A}_{i+1,m} + \bar{B}_{i+1,m} \cdot e^{-\gamma \ell_{i+1,m}}] &= \sum_n [\bar{A}_{i,n} \cdot e^{-\gamma \ell_{i,n}} + \bar{B}_{i,n}] \\ &\quad \cdot \frac{C(i+1, m; i, n)}{N_{i,n}}, \\ \gamma h_{i,m} \cdot [\bar{A}_{i,m} \cdot e^{-\gamma \ell_{i,m}} - \bar{B}_{i,m}] &= \sum_n \gamma h_{i+1,n} \cdot [\bar{A}_{i+1,n} - \bar{B}_{i+1,n} \cdot e^{-\gamma \ell_{i+1,n}}] \\ &\quad \cdot \frac{C(i+1, n; i, m)}{N_{i+1,n}}. \end{aligned} \quad (11)$$

The ratios of mode coupling coefficients and mode norms on the right-hand sides form matrices  $\{\text{matrix}\}$ ; we symbolise with  $\{\text{matrix}\}^{-1}$  the inverse of a matrix. Then the above systems (of couples of systems) of linear equations for the mode amplitudes lead to the iterative systems:

expanding duct:  $(h_{i+1} \geq h_i)$

$$\begin{aligned} \bar{A}_{i+1,m} = \frac{1}{2} \sum_n \bar{A}_{i,n} \cdot e^{-\gamma \ell_{i,n}} \left( \left\{ \frac{C(i, n; i+1, m)}{N_{i+1,m}} \right\}^{-1} + \frac{\gamma h_{i,n}}{\gamma h_{i+1,m}} \frac{C(i, n; i+1, m)}{N_{i,n}} \right) \\ + B_{i,n} \left( \left\{ \frac{C(i, n; i+1, m)}{N_{i+1,m}} \right\}^{-1} - \frac{\gamma h_{i,n}}{\gamma h_{i+1,m}} \frac{C(i, n; i+1, m)}{N_{i,n}} \right), \end{aligned} \quad (12)$$

$$\begin{aligned} \bar{B}_{i+1,m} \cdot e^{-\gamma \ell_{i+1,m}} = \frac{1}{2} \sum_n \bar{A}_{i,n} \cdot e^{-\gamma \ell_{i,n}} \\ \cdot \left( \left\{ \frac{C(i, n; i+1, m)}{N_{i+1,m}} \right\}^{-1} - \frac{\gamma h_{i,n}}{\gamma h_{i+1,m}} \frac{C(i, n; i+1, m)}{N_{i,n}} \right) \\ + \bar{B}_{i,n} \left( \left\{ \frac{C(i, n; i+1, m)}{N_{i+1,m}} \right\}^{-1} + \frac{\gamma h_{i,n}}{\gamma h_{i+1,m}} \frac{C(i, n; i+1, m)}{N_{i,n}} \right), \end{aligned} \quad (13)$$

contracting duct:  $(h_{i+1} < h_i)$

$$\begin{aligned} \bar{A}_{i+1,m} = \frac{1}{2} \sum_n \bar{A}_{i,n} \cdot e^{-\gamma \ell_{i,n}} \left( \frac{C(i+1, m; i, n)}{N_{i,n}} + \frac{\gamma h_{i,n}}{\gamma h_{i+1,m}} \left\{ \frac{C(i+1, m; i, n)}{N_{i+1,m}} \right\}^{-1} \right) \\ + \bar{B}_{i,n} \left( \frac{C(i+1, m; i, n)}{N_{i,n}} - \frac{\gamma h_{i,n}}{\gamma h_{i+1,m}} \left\{ \frac{C(i+1, m; i, n)}{N_{i+1,m}} \right\}^{-1} \right), \end{aligned} \quad (14)$$

$$\begin{aligned} \bar{B}_{i+1,m} \cdot e^{-\gamma \ell_{i+1,m}} = \frac{1}{2} \sum_n \bar{A}_{i,n} \cdot e^{-\gamma \ell_{i,n}} \\ \cdot \left( \frac{C(i+1, m; i, n)}{N_{i,n}} - \frac{\gamma h_{i,n}}{\gamma h_{i+1,m}} \left\{ \frac{C(i+1, m; i, n)}{N_{i+1,m}} \right\}^{-1} \right) \\ + B_{i,n} \left( \frac{C(i+1, m; i, n)}{N_{i,n}} + \frac{\gamma h_{i,n}}{\gamma h_{i+1,m}} \left\{ \frac{C(i+1, m; i, n)}{N_{i+1,m}} \right\}^{-1} \right). \end{aligned} \quad (15)$$

There are more unknown mode amplitudes  $A_{i,n}$ ,  $B_{i,n}$  than equations at the duct section limits. One needs *source conditions* and *termination conditions*.

Alternative *source conditions*:

Sound pressure source:

At the entrance  $x = x_0$  a sound pressure profile  $P(y)$  is given (over the full height  $h_1$ , else the task would be ill posed). Expand the pressure profile in modes of the section  $i = 1$ :

$$P(y) = \sum_n a_n \cdot \cos(\epsilon_{1,n} y); \quad \bar{a}_n = N_{1,n} \cdot a_n = \frac{1}{h_1} \int_0^{h_1} P(y) \cdot \cos(\epsilon_{1,n} y) dy. \quad (16)$$

The boundary condition for the sound pressure at  $x = x_0$  gives:

$$\bar{A}_{1,n} + \bar{B}_{1,n} \cdot e^{-\gamma \ell_{1,n}} = \bar{a}_n. \quad (17)$$

One of the amplitudes  $\bar{A}_{1,n}$ ,  $\bar{B}_{1,n}$  of the first section can be expressed by the other amplitude and a known number  $\bar{a}_n$ .

*Particle velocity source:*

At the entrance  $x = x_0$  a particle velocity profile  $V(y)$  is given; the source may cover a height  $h_0 \leq h_1$ , assuming the other part  $(h_0, h_1)$  of the entrance plane is hard. Expand in modes of the section  $i = 1$ :

$$Z_0 v_{1,x}(x_0, y) = \begin{cases} Z_0 V(y) & \text{in } y = (0, h_0) \\ 0 & \text{in } y = (h_0, h_1) \end{cases} = \sum_n a_n \cdot \cos(\epsilon_{1,n} y),$$

$$\bar{a}_n = N_{1,n} \cdot a_n = \frac{1}{h_1} \int_0^{h_1} \begin{cases} Z_0 V(y) \\ 0 \end{cases} \cdot \cos(\epsilon_{1,n} y) dy. \quad (18)$$

The boundary condition at  $x = x_0$  for the particle velocity gives:

$$\bar{A}_{1,n} - \bar{B}_{1,n} \cdot e^{-\gamma \ell_{1,n}} = \frac{j k_0 h_1}{\gamma h_{1,n}} \bar{a}_n. \quad (19)$$

Again one of the amplitudes  $\bar{A}_{1,n}$ ,  $\bar{B}_{1,n}$  of the first section can be expressed by the other amplitude and a known number containing  $\bar{a}_n$ .

*Incident wave from the entrance duct  $i = 0$ :*

A sound wave with given mode amplitudes  $A_{0,n}$  is incident from the entrance duct  $i = 0$  which is supposed to be anechoic or infinite for  $x \rightarrow -\infty$ .

Setting formally  $\ell_0 = 0$ , i.e. defining the amplitudes  $A_{0,n}$  in the plane  $x = x_0$ , the above equations can also be used for that cross-section. The right-hand sides contain only the amplitudes  $B_{0,n}$  as unknown quantities.

Depending on the selected source condition, the above systems of equations will have the general forms (imagine the iteration to be performed up to  $i$ ):

*for pressure or velocity source:*

$$\bar{A}_{i+1,m} = \frac{1}{2} \sum_n \bar{B}_{1,n} \cdot \alpha_{i,n} + \beta_{i,n},$$

$$\bar{B}_{i+1,m} = \frac{1}{2} \sum_n \bar{B}_{1,n} \cdot \alpha'_{i,n} + \beta'_{i,n} \quad (20)$$

with numerical values  $\alpha_{i,n}$ ,  $\beta_{i,n}$ ,  $\alpha'_{i,n}$ ,  $\beta'_{i,n}$  and symbolic  $\bar{B}_{1,n}$ ,

*for incident wave:*

$$\bar{A}_{i+1,m} = \frac{1}{2} \sum_n \bar{B}_{0,n} \cdot \alpha_{i,n} + \beta_{i,n},$$

$$\bar{B}_{i+1,m} = \frac{1}{2} \sum_n \bar{B}_{0,n} \cdot \alpha'_{i,n} + \beta'_{i,n} \quad (21)$$

with numerical values  $\alpha_{i,n}$ ,  $\beta_{i,n}$ ,  $\alpha'_{i,n}$ ,  $\beta'_{i,n}$  and symbolic  $\bar{B}_{0,n}$ .

Alternative *termination conditions*:

Section  $i + 1 = I$  *anechoic*: i. e.  $\bar{B}_{I,m} = 0$ .

Then the last of the above equations (12)–(15) is a system of linear inhomogeneous equations for either  $\bar{B}_{I,n}$  or  $\bar{B}_{0,n}$ . After its solution, all other mode amplitudes follow by insertion in the former systems of equations.

Section  $i + 1 = I$  *terminated with an admittance*  $G_t$ :

This termination condition gives the relations between  $\bar{A}_{I,n}$ ,  $\bar{B}_{I,n}$ :

$$\gamma h_{I,n} [\bar{A}_{I,n} \cdot e^{-\gamma \ell_{I,n}} - \bar{B}_{I,n}] = jk_0 h_I \cdot Z_0 G_t \cdot [\bar{A}_{I,n} \cdot e^{-\gamma \ell_{I,n}} + \bar{B}_{I,n}] \quad (22)$$

so one of the amplitudes  $\bar{A}_{I,n}$ ,  $\bar{B}_{I,n}$  can be expressed by the other (e.g.  $\bar{A}_{I,n}$  by  $\bar{B}_{I,n}$ ). Thus the last of the above iterative systems of equations will give two coupled systems of equations for the amplitudes  $\bar{B}_{I,n}$ ,  $\bar{B}_{0,n}$  or  $\bar{B}_{I,n}$ ,  $\bar{B}_{1,n}$  (depending on the source condition). After the solution, all other amplitudes follow by insertion.

*General termination*:

With other terminations, e.g. a radiating duct end of the section  $i = I$ , one always gets a relation of the form (the termination with an admittance  $G_t$  is a special case thereof with a diagonal matrix):

$$\{\bar{A}_{I,m}\} = \{\{\text{matrix}\}\} \bullet \{\bar{B}_{I,n}\}, \quad (23)$$

so one will end again in the two coupled systems of equations mentioned above.

The general problem with cascades of ducts and layers comes from the fact that one gets enough systems of equations only after the source condition has been concatenated with the termination condition. And one gets solvable systems of equations after the amplitudes  $\bar{A}_{i,n}$ ,  $\bar{B}_{i,n}$  for the intermediate sections are eliminated. This elimination can be done in an analytical manner only for a low number  $I$  of sections. A solution which is suited for numerical evaluation is obtained if the systems of equations from the boundary conditions are transformed to iterative systems, and a mixed numerical-symbolic evaluation (“hybrid” evaluation) is applied to that system.

The hybrid evaluation makes use of the ability of mathematical programs (like *Mathematica*® or *Maple*®) to handle hybrid expressions. They automatically simplify numerical terms in the expressions and give them canonical forms, so that the numerical coefficients or the symbolic factors can be extracted. Thus the final system(s) of equations for the numerical evaluation can easily be obtained. And if the right-hand sides of the intermediate equations are saved, one gets the numerical values of the left-hand sides (after solution of the final system(s)) just by calling them, because the key solutions ( $\bar{B}_{I,n}$ ,  $\bar{B}_{0,n}$ ,  $\bar{B}_{1,n}$ ) then are automatically inserted.

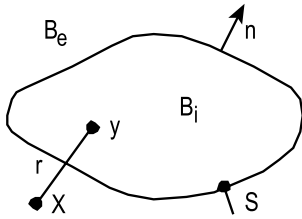
### O.3 Five Standard Problems of Numerical Acoustics

Five standard problems of numerical acoustics are presented below which frequently occur in practical applications.

#### O.3.1 The Radiation Problem

A vibrating structure radiates sound into the surrounding space. The radiated sound field is characterized by the sound pressure  $p$ , particle velocity  $\vec{v}$ , and derived quantities such as the sound intensity  $\vec{I}$ , the radiated sound power  $\Pi$ , the radiation efficiency  $\sigma$  etc., which will be calculated by numerical methods.

As shown in the figure, the bounded volume of the radiating structure in three-dimensional space is denoted by  $B$  (like Body). The interior of  $B$  is called  $B_i$  and the exterior  $B_e$ . The surface normal  $n$  should be directed into the exterior  $B_e$ .



The complex sound pressure  $p$ , radiated into the free, three-dimensional space has to satisfy the Helmholtz equation

$$\Delta p + k_0^2 p = 0 \quad \text{in } B_e, \quad (1)$$

where  $k_0 = \omega/c_0$  is the wave number,  $\omega$  is the angular frequency,  $c_0$  the speed of sound, and  $\Delta$  is the Laplace operator. All time-varying quantities should obey the time dependence  $\exp(j\omega t)$  with  $j = \sqrt{-1}$ . The fluid in the outer space is assumed to be loss-free, homogeneous, and at rest. For a complete description of the problem, boundary conditions on the surface of the radiator and at infinity are needed. If the body has edges corner conditions must be applied also, see [Sect. B.16](#). The most important *Neumann* boundary value problem describes a body, which vibrates with a given normal velocity  $v$ . Therefore, the pressure gradient

$$\frac{\partial p}{\partial n} = -j\omega\rho_0 v \quad \text{on } S \quad (2a)$$

is prescribed on  $S$ . Here,  $\rho_0$  is the fluid density and  $\partial/\partial n$  is the derivative in the direction of the outward normal  $n$ . Sometimes, the sound pressure

$$p = p_0 \quad \text{on } S \quad (2b)$$

is given, which is called the *Dirichlet* problem. The most general form of a local boundary condition is the *Robin* or impedance problem with

$$R(p) := \frac{\partial p}{\partial n} + j\omega\rho_0 G p = f(S) \quad \text{on } S, \quad (2c)$$



where  $f(S)$  is a function defined on  $S$ .  $R(p)$  is a linear boundary operator.  $G$  is the field admittance in the direction of the normal  $n$ . For  $G \rightarrow 0$ , we obtain the Neumann problem, for  $G \rightarrow \infty$  the Dirichlet problem is obtained. If  $Z := 1/G$  is a nonzero but finite quantity, the general impedance problem results, which describes locally reacting absorbing surfaces.

In addition, the physical requirement that all radiated waves are outgoing leads to the Sommerfeld radiation condition

$$\lim_{R \rightarrow \infty} R \left[ \frac{\partial p}{\partial R} + jk_0 p \right] = 0, \quad (3)$$

which can be interpreted as a boundary condition at infinity. Here,

$$R = |x| = \sqrt{x_1^2 + x_2^2 + x_3^2}$$

denotes the distance from  $x$  to the origin, where points in space are denoted by simple letters such as  $x = (x_1, x_2, x_3)$ . The Sommerfeld condition generally leads to the choice of functions among different mathematically possible alternatives (like the corner condition does); therefore it decides about the sign of exponents and of roots, and if a field function has branch points, it gives rules about which branch of multi-valued functions should be selected.

Equations O.3.(1), O.3.(2a, 2b, or 2c), and O.3.(3) describe the radiation problem for the radiated pressure  $p$ . With the knowledge of  $p$  and  $\vec{v}$  the effective sound intensity

$$\vec{I} = \frac{1}{2} \text{Re} \{ p \vec{v}^* \}, \quad (4)$$

the effective sound power

$$\Pi(p, v) = \frac{1}{2} \iint_S \text{Re} \{ p v^* \} ds, \quad (5)$$

and the radiation efficiency

$$\sigma = \Pi(p, v) / \Pi(\rho_0 c_0 v, v) \quad (6)$$

can be easily calculated. Here,  $\Pi(\rho_0 c_0 v, v)$  is the power of a plane wave with

$$p = \rho_0 c_0 v \quad (7)$$

on  $S$  [Junger/Feit (1972)]. The asterisk denotes the complex conjugate and  $\text{Re}\{\dots\}$  the real part of the quantity in brackets.

Due to definition O.3.(6), the quantity  $\Pi(\rho_0 c_0 v, v)$  can be considered as a sound power with radiation efficiency  $\sigma = 1$ . Hence, the numerical computation of the radiated sound field allows a numerical sound intensity method to be used. Such a method can be used for the localisation of acoustical sources on the surface of the vibrating machine structure or for detecting cracks that cause changes of the acoustical surface intensity [Koopmann/Perraud (1981)].

### 0.3.2 The Scattering Problem

► See also: ➤ Chap. E for scattering.

For the related scattering problem, an incident wave  $p_{in}$  is impinging on the body B and causes a scattered wave  $p_s$ . The scattering problem for the scattered pressure  $p_s$  is again described by the Helmholtz equation

$$\Delta p_s + k_0^2 p_s = 0 \quad \text{in } B_e \quad (8)$$

and the corresponding radiation condition

$$\lim_{R \rightarrow \infty} R \left[ \frac{\partial p_s}{\partial R} + j k_0 p_s \right] = 0. \quad (9)$$

Now, the boundary condition is homogeneous, since the body is at rest, and it must be formulated for the total pressure  $p_T = p_{in} + p_s$ . Similar to the radiation problem, the Neumann problem for an acoustically rigid scatterer is given by:

$$\partial p_T / \partial n = 0 \quad \text{on } S. \quad (10a)$$

A perfectly (acoustically) soft scatterer leads to the Dirichlet condition

$$p_T = 0 \quad \text{on } S. \quad (10b)$$

The general form of the impedance boundary condition is described by:

$$R(p_T) := \frac{\partial p_T}{\partial n} + j \omega \rho_0 G p_T = 0, \quad (10c)$$

where again  $G$  is the field admittance at the surface  $S$ .

The scattering problem can be formulated as an equivalent radiation problem by the following procedure: considering the hard scatterer, the normal velocity  $v_{in}$  of the incident pressure wave  $p_{in}$  will be evaluated at the surface  $S$  where the scatterer is assumed (for the moment) to be sound transparent. If  $B$  is now vibrating with the negative normal velocity  $(-v_{in})$ , the radiated sound pressure is identical to the pressure  $p_s$  scattered from  $B$  due to the incident wave  $p_{in}$ . Hence, instead Eq. O.3.(10a), we simply have:

$$\frac{\partial p_s}{\partial n} = -j \omega \rho_0 (-v_{in}) \quad (11a)$$

for the scattering problem, which again is an inhomogeneous boundary condition like Eq. O.3.(2a). Analogously, the impedance boundary condition O.3.(10c) can be written as

$$R(p_s) = f, \quad (11b)$$

where  $f$  is the known function  $f = -R(p_{in})$ . Equations O.3.(8), O.3.(9), O.3.(11a/11b) describe the scattering problem as an equivalent “radiation problem” for the scattered pressure  $p_s$ . In conclusion, the radiation and the scattering problem can be treated by numerical methods in a uniform way.

Having calculated the main quantities  $p_s$  and  $\vec{v}_s$ , the scattered effective intensity (or intensity of return) is given by:

$$\vec{I}_s = \frac{1}{2} \text{Re} \{ p_s \vec{v}_s^* \}. \quad (12)$$

Assuming that the incident wave is a plane wave with incident intensity  $I_{\text{in}}$  (in the direction of incidence), the target strength TS is defined by:

$$TS = 10 \lg \frac{I_s(r = 1 \text{ m})}{I_{\text{in}}} [\text{dB}], \quad (13)$$

where  $I_s(r = 1 \text{ m})$  is the effective intensity of the sound returned by the scatterer at a distance of 1 m from its acoustical center in some specified direction. In Eq. O.3.(13),  $\lg$  denotes the logarithm to the base 10. The target strength is often used in the context of underwater sound (see [Urick (1983)], for more details).

### O.3.3 The Sound Field in Interior Spaces

If a sound field in an interior space  $B_i$  is considered, the Helmholtz equation O.3.(1) must be satisfied in  $B_i$ . This is a classical problem of room acoustics. At the boundary  $S$  of the enclosure, there may exist a rigid part  $S_1$  with  $\partial p / \partial n = 0$ , an acoustically soft part  $S_2$  with  $p = 0$ , and an absorbing surface  $S_3$  with  $\partial p / \partial n + j\omega\rho_0 G p = 0$ , such that  $S = S_1 \cup S_2 \cup S_3$ . In contrast to exterior radiation or scattering problems, a finite volume is considered, and no radiation condition is necessary.

If no acoustical sources such as vibrating walls or bodies are inside the room, the Helmholtz equation together with the boundary conditions represents an eigenvalue problem for the determination of the eigenfrequencies and eigenmodes of the enclosed fluid.

On the other hand, sources such as vibrating parts of the boundary, point sources, etc. lead to forced vibrations of the fluid.

Sometimes, interior and exterior acoustic problems can be coupled. Such a situation occurs when an interior acoustic space is connected to an exterior one through openings [Seybert/Cheng/Wu (1990)]. A simple example is a duct with an open end rising into the surrounding infinite space.

The problem of a half space belongs to the class of exterior problems rather than to interior problems (see ➤ Sect. O.5.5).

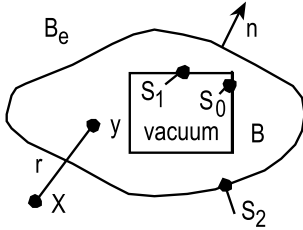
Numerical methods based on the solution of the wave equation or Helmholtz equation (reduced wave equation) are only useful for the treatment of small enclosures at low frequencies, i.e. for small  $k_0 a$  numbers, where  $a$  is a characteristic dimension of the room (for example the diameter or one side of the room). For problems with high  $k_0 a$  numbers, it is more convenient to use methods of geometrical acoustics (see ➤ Ch. M).

### O.3.4 The Coupled Fluid–Elastic Structure Interaction Problem

If the radiating or scattering structure  $B$  consists of an elastic material, the interaction between the body and the surrounding fluid must be taken into account. In addition, the structure can be coupled with an internal acoustic cavity. The problem is significantly simplified if the acoustic loading of sound inside the cavity can be neglected.

Following Soize [Soize (1998)], the boundary value problem can be described as follows:  $B$  is the bounded domain occupied by the linearly elastic structure. The boundary  $S$

is divided into three parts:  $S = S_0 \cup S_1 \cup S_2$ . On  $S_0$  the boundary is fixed. This means that  $u = 0$  on  $S_0$  where  $u = (u_1, u_2, u_3)$  denotes the displacement field. On  $S_1 \cup S_2$ , it is free (see the figure).



For simplicity, we only consider the coupling between a structure and an external fluid. Systems coupled with internal acoustic cavities are described in [Soize (1999)]. The structure is subject to a body force  $f = (f_1, f_2, f_3)$  and a surface force  $f_{S_1} = (f_{S_{1,1}}, f_{S_{1,2}}, f_{S_{1,3}})$ . The steady state response of the linearly elastic structure is given by:

$$-\omega^2 \rho_s u_i - \sigma_{ij,j} = f_i \quad \text{in } B, \quad (14a)$$

$$\sigma_{ij} n_j = -p n_i \quad \text{on } S_2, \quad (14b)$$

$$\sigma_{ij} n_j = f_{S_{1,i}} \quad \text{on } S_1, \quad (15)$$

$$u_i = 0 \quad \text{on } S_0, \quad (16)$$

where the summation convention over repeated indices is used.  $\rho_s$  is the mass density of the structure and

$$\sigma_{ij,j} = \sum_{j=1}^3 \frac{\partial \sigma_{ij}}{\partial x_j}.$$

For a linear viscoelastic material, the stress tensor is given by:

$$\sigma_{ij} = a_{ijkh}(x, \omega) \varepsilon_{kh}(u) + b_{ijkh}(x, \omega) \varepsilon_{kh}(j\omega u),$$

where summation over indices  $k$  and  $h$  must be performed, and the linearized strain tensor is:

$$\varepsilon_{kh}(u) = \left( \frac{\partial u_k}{\partial x_h} + \frac{\partial u_h}{\partial x_k} \right) / 2.$$

The coefficients  $a_{ijkh}(x, \omega)$  and  $b_{ijkh}(x, \omega)$  are real and depend on the properties of the elastic medium.

The coupling term between the external fluid and the structure is the pressure  $p$  that acts like a fluid load. Introducing the velocity potential  $\psi$  by:

$$\text{grad } \psi = \vec{v}, \quad (17)$$

the external fluid is described by the Helmholtz equation for the potential

$$\Delta \psi + k_0^2 \psi = 0. \quad (18)$$

According to Newton's law the external pressure is given by:

$$p = -j\omega\rho_0\psi. \quad (19)$$

At the outer boundary  $S_2$  the normal velocity of the structure  $\partial u_n / \partial t = j\omega u_n$  and of the fluid  $v_n = \partial\psi / \partial n$  must be equal

$$\partial\psi / \partial n = j\omega u_n. \quad (20)$$

In addition, the potential  $\psi$  has to fulfill the Sommerfeld radiation condition O.3.(3). For solving the coupled fluid-structure problem, Eqs. O.3.(14), O.3.(15), O.3.(16), O.3.(18), O.3.(20) have to be solved. Clearly, the vibrating structure can be coupled to an external fluid and to an internal acoustic cavity leading to very similar equations.

### O.3.5 The Transmission Problem

► *See also: Chap. I on sound transmission.*

The transmission problem is characterized by the fact that the incident sound wave  $p_{in}$  can penetrate into the body  $B$ , which is assumed to have acoustic constants (sound speed  $c_i$  and density  $\rho_i$ ) different from those of the surrounding medium  $c_0$  and  $\rho_0$ .

The total pressure  $p = p_{in} + p_s$  in  $B_e$  and the interior pressure  $p_i$  in  $B_i$  have to satisfy the Helmholtz equations

$$\Delta p + k_0^2 p = 0 \quad \text{in } B_e, \quad p_i + k_i^2 p_i = 0 \quad \text{in } B_i \quad (21)$$

with  $k_i = \omega/c_i$ , the radiation condition

$$\lim_{R \rightarrow \infty} R \left[ \frac{\partial p}{\partial R} + jk_0 p \right] = 0 \quad (22)$$

and the transmission conditions for the pressure and normal velocities


$$p - p_i = f \quad \text{on } S, \quad (23)$$

$$v - v_i = g \Leftrightarrow \frac{j}{\omega\rho_0} \frac{\partial p}{\partial n} - \frac{j}{\omega\rho_i} \frac{\partial p_i}{\partial n} = g \quad \text{on } S, \quad (24)$$

where  $f$  and  $g$  are given continuous functions on  $S$ . For  $f = g = 0$  pressure and velocity are continuous at the boundary. It can be shown (see [Colton/Kress (1983), p. 101]) that the transmission problem has a unique solution.

## 0.4 The Source Simulation Technique (SST)

The source simulation technique is a general tool for calculating the sound radiation or scattering from complex-shaped structures into the three-dimensional space, [Kress/Mohsen (1986); Ochmann, *Acustica* (1990); Ochmann (1995); Ochmann (1999); Ochmann (2000); Ochmann/Wellner (1991)]. Hence, it can be used for the numerical solution of the first and second standard problem (see  Sect. 0.3, problem 1 and problem 2). It should be noted that many names are in use for the same or similar methods such as *source simulation method*, *multipole method*, *superposition method*, *spherical wave synthesis*, etc. [Attala/Winckelmans/Sgard (1999); Bobrovnikskii/Tomilina (1990); Bobrovnikskii/Tomilina (1995); Cremer/Wang (1988); Cunefare/Koopmann/Brod (1989); Fahnline/Koopmann (1991); Hwang/Chang (1991); Heckl (1989); Jeans/Mathews (1992); Johnson/Elliott/Bæk/Garcia-Bonito (1998); Karageorghis/Fairweather (1998); Kress/Mohsen (1986); Koopmann/Song/Fahnline (1989); Masson/Redon/Priou/Gervais (1994); Ochmann, *Acustica* (1990); Ochmann (1995); Ochmann (1998); Ochmann (1999); Ochmann (2000); Ochmann/Homm (1994); Ochmann/Wellner (1991)]. The basic idea of the method consists in replacing the structure by a system of acoustical sources placed in the interior of the structure. By definition, these source functions have to satisfy the Helmholtz equation and the radiation condition. For solving the radiation or scattering problem completely, the source system also has to fulfil the boundary conditions on the surface of the body or, equivalently, a certain boundary equation. The better the system of sources satisfies the boundary condition on the surface of the structure, the closer is the agreement between the original and the simulated sound field. Spherical wave functions are often used as sources, since they can easily be calculated. Bodies of arbitrary shape are treated by taking into account spherical wave functions with different source locations. To solve the boundary equation, which minimizes the boundary error, the method of weighted residuals is applied. Depending on the choice of the weighting functions, different variants of the source simulation technique are obtained, for example, the *null-field equations* and the *full-field equations*. The full-field equations often lead to better conditioned sets of equations than the null-field equations. The null-field and the full-field equations can also be derived from the interior or exterior Helmholtz integral equation, respectively (see [Ochmann (1999); Ochmann (2000)]). This illustrates the close relationship between the source simulation technique and the boundary element method (see  Sect. 0.5). This presentation follows the lines given in the review article [Ochmann (2000)], where more details and examples of calculations for several radiation and scattering problems can be found. In the list of references many different aspects of the SST can be found: for instance, the calculation of sound fields in the interior of enclosures containing scattering objects, [Johnson/Elliott/Bæk/Garcia-Bonito (1998)], the treatment of scattering and radiation from bodies of revolution, [Stepanishen (1997)], a formulation in the time domain, [Kropp/Svensson (1995)], or the use of special surface sources weighted according to a Gaussian distribution, [Guyader (1994)].

In  Sect. 0.3.2 it is shown that the scattering problem can be considered as an equivalent radiation problem. Thus, it is sufficient to treat only the radiation problem in the following. Exceptionally, only in this chapter, the time convention  $e^{-i\omega t}$  is used, in order to be in agreement with most of the related literature about the SST.

### 0.4.1 General Description of the Source Simulation Technique

The basic idea of the SST consists of replacing the vibrating body by a system of sources placed in the interior of the body. The sources are denoted by  $q(x, y)$  where  $x$  is an arbitrary point in space and  $y$  is the position of the singularity, i.e., the location of the source point. Now, for the SST in its most general form, it is assumed that the pressure can be presented in the form

$$p(x) = \iiint_Q c(y)q(x, y)dy, \quad (1)$$

where  $Q$  is a region which is fully contained in  $B_i$  and embodies all sources;  $c(y)$  is the yet unknown source density, which gives every source a certain source strength. Every single source function (also called trial function)  $q(x, y)$  itself can consist of a finite or infinite sum of elementary sources such as monopoles, dipoles, etc.:  $q(x, y) = d_0 q_0(x, y) + d_1 q_1(x, y) + \dots$ . The volume integral in Eq. O.4.(1) reduces to a surface integral or a contour integral if the region  $Q$  is a surface or a line, respectively. The integral turns into a finite sum if isolated point sources are used or if the integral must be discretized for numerical reasons, since we cannot work with infinitely many sources. The system of functions  $c(y)q(y)$  with  $y \in Q$  will be called the source system. All functions of the source system have by definition to satisfy Eqs. O.3.(1) and O.3.(3) (with respect to  $x$ ). The source system also has to satisfy the boundary condition on the surface  $S$ . As a consequence of the present time convention  $e^{i\omega t}$ , the boundary conditions O.3.(2a) and O.3.(2c) must be written with a different sign

$$\frac{\partial p}{\partial n} = i\omega\rho_0 v, \quad (2a)$$


$$R(p) = \frac{\partial p}{\partial n} - i\omega\rho_0 Gp = f \quad \text{on } S. \quad (2b)$$

Hence, by substituting Eq. O.4.(1) into Eq. O.4.(2a) or into the general radiation boundary condition O.4.(2b), one gets for the rigid radiator

$$\iiint_Q c(y) \frac{\partial}{\partial n} q(x, y) dy - j\omega\rho_0 v = 0 \quad \text{on } S \quad (2c)$$

or, in the general case

$$R \left[ \iiint_Q c(y)q(x, y)dy \right] - f = 0 \quad \text{on } S. \quad (2d)$$

These equations “live” on the boundary, and they are called the boundary equations of the SST. Thus by using sources as trial functions, the original domain problem can be transformed into a boundary problem. This illustrates that the SST can be considered as a counterpart to the finite element method (FEM, see  Sect. O.6), which solves the original domain problem. If the boundary equations can be solved exactly, the coefficients  $c(y)$  are determined such that the sound field generated by the vibrating

structure is identical to the field produced by the source system. This follows from the unique solvability of the exterior problems described in ► Sect. 0.3 (see [Colton/Kress (1983)]). Such a source system is called an *equivalent source system*. Consequently, the exact solution of the radiation problem can be found if it is possible to construct an equivalent source system. However, such exact solutions are only known for special geometries in standard coordinate systems (e.g. in spherical coordinates). For nearly all relevant practical problems the surface  $S$  has a complicated shape. Therefore, we are only looking for approximate solutions of the boundary equations by minimizing the so-called *boundary error* or *residual*

$$\epsilon(x) = \iiint_Q c(y) \frac{\partial}{\partial n(y)} q(x, y) dy - i\omega\rho_0 v \quad \text{on } S \quad (3a)$$

or

$$\epsilon(x) = R \left[ \iiint_Q c(y) q(x, y) dy \right] - f \quad \text{on } S. \quad (3b)$$

The minimization process can be performed by means of the method of weighted residuals, which is a very general approach (see [Ochmann, *Acustica* (1990)]). It consists in choosing a complete family of weighting functions  $w_n$ ;  $n = 1, 2, 3, \dots$  and demanding that

$$\iint_S \epsilon(x) w_\ell(x) ds = \iint_S \left\{ R \left[ \iiint_Q c(y) q(x, y) dy \right] - f \right\} w_\ell(x) ds = 0; \quad \ell = 1, 2, 3, \dots \quad (4)$$

The completeness ensures that the residual will go to zero if the number of weighting functions tends to infinity. Equation 0.4.(4) is called the *weighted residual equations* of the SST for the determination of the source density  $c(y)$ . It can be seen that different variants of the SST stem from different choices of sources and weighting functions. For example, the kind, number, and locations of source and corresponding weighting functions are important parameters of the method. Important source functions are the spherical wave functions, which will be introduced in the next section together with corresponding symmetry relations.

#### 0.4.2 Spherical Wave Functions and Symmetry Relations

By definition, sources must be radiating wave functions. However, analytical solutions of the Helmholtz equation can only be constructed explicitly in separable coordinate systems, [Morse/Feshbach (1953), p. 494]. In three-dimensional space, the spherical wave functions present the simplest form of such solutions. Hence they are the type of sources most often used, and they are given by

$$\psi_{nm}^{c,s}(x) = \Gamma_{nm} h_n^{(1)}(k_0 r) P_n^m(\cos \vartheta) \begin{cases} \cos(m\varphi) \\ \sin(m\varphi) \end{cases}, \quad (5)$$



where the  $P_n^m(\cos \vartheta)$  are the associated Legendre polynomials, [Abramowitz/Stegun (1972)]. Here, spherical co-ordinates  $\{r, \vartheta, \varphi\}$  are introduced by  $\mathbf{x} = \{r \sin \vartheta \cos \varphi, r \sin \vartheta \sin \varphi, r \cos \vartheta\}$ . The superscript  $c$  (or  $s$ ) in the equations below indicates that the cosine (or sine) is used. The cylindrical functions  $h_n^{(1)}(z)$  are the spherical Hankel functions of the first kind (with the choice  $e^{-i\omega t}$ ), [Abramowitz/Stegun (1972)]. The normalizing factors

$$\Gamma_{nm} = \left[ \frac{\varepsilon_m}{4\pi} (2n+1) \frac{(n-m)!}{(n+m)!} \right]^{1/2}; \quad \varepsilon_m = \begin{cases} 1; & m=0 \\ 2; & m>0 \end{cases} \quad (6)$$

are chosen in such a way that the spherical harmonics

$$y_{nm}^{c,s}(\mathbf{x}) = \Gamma_{nm} P_n^m(\cos \vartheta) \cdot \begin{cases} \cos(m\varphi) \\ \sin(m\varphi) \end{cases} \quad (7)$$

are orthonormal with respect to the integration over the unit sphere:

$$\int_0^{2\pi} \int_0^\pi y_{mn}^\alpha \cdot y_{\mu\nu}^\beta \sin \vartheta d\vartheta d\varphi = \begin{cases} 1; & \text{if } \alpha = \beta, \mu = m, \text{ and } \nu = n \\ 0; & \text{else} \end{cases} \quad (8)$$

where  $\alpha$  and  $\beta$  stand for  $c$  or  $s$ , respectively. Taking into account that there are only wave functions of cosine type for  $m=0$ , the number of different spherical wave functions up to an index  $n_0$  is given by

$$\sum_{j=0}^{n_0} (2j+1) = (n_0+1)^2. \quad (9)$$

For simplicity, we denote the  $\psi_{nm}^{c,s}$  and  $y_{nm}^{c,s}$  by  $\psi_\ell$  and  $y_\ell$ , respectively, where the index  $\ell = 0, 1, 2, \dots$  runs through all combinations of  $m$  and  $n$  for  $c$  and  $s$ . The regular wave functions

$$\chi_1 = \text{Re}\{\psi_1\} \quad (10)$$

present standing waves, where  $\text{Re}\{\}$  denotes the real part of the quantity in brackets. The regular wave functions contain spherical Bessel functions  $j_n(z)$  instead of Hankel functions like the radiating wave functions, since

$$h_n^{(1)}(z) = j_n(z) + iy_n(z) \quad (11)$$

with  $y_n(z)$  spherical Neumann functions.

For deriving the null-field and the full-field equations from the weighted residual Eq. O.4.(4), the following symmetry relations are very important

$$\iint_S \left( \psi_\ell \frac{\partial \psi_m}{\partial n} - \psi_m \frac{\partial \psi_\ell}{\partial n} \right) ds = 0, \quad (12a)$$

$$\iint_S \left( \chi_\ell \frac{\partial \psi_m}{\partial n} - \psi_m \frac{\partial \chi_\ell}{\partial n} \right) ds = \delta_{\ell m} \frac{i}{k_0}, \quad (12b)$$

$$\iint_S \left( \psi_\ell^* \frac{\partial \psi_m}{\partial n} - \psi_m \frac{\partial \psi_\ell^*}{\partial n} \right) ds = \delta_{\ell m} \frac{2i}{k_0}, \quad (12c)$$

where the asterisk denotes the complex conjugate, and  $\delta_{\ell m}$  is the Kronecker Delta. Equation O.4.(12a) is valid for all radiating wave functions as shown in [Ochmann, *Acustica* (1990)]. The proofs for Eqs. O.4.(12a)–O.4.(12c) can be found in [Ochmann (1999)] together with [Ochmann (1995)]. Since the bilinear form

$$[u, v, ] := \iint_S uv dy \quad (13)$$

is symmetric, i.e.  $[u, v, ] = [v, u, ]$ , all three symmetry relations O.4.(12) for the operator  $D = \partial/\partial n$  can be extended to the more general boundary operator  $R$  (see Eq. O.4.(2b)):

$$[\psi_\ell, R\psi_m] - [R\psi_\ell, \psi_m] = 0, \quad (14a)$$

$$[\chi_\ell, R\psi_m] - [R\chi_\ell, \psi_m] = \delta_{\ell m} \frac{i}{k_0}, \quad (14b)$$

$$[\psi_\ell^*, R\psi_m] - [R\psi_\ell^*, \psi_m] = \delta_{\ell m} \frac{2i}{k_0}. \quad (14c)$$

It is well-known that the spherical wave functions can be interpreted as multipoles. Hence in related works the name *multipole method* or *multipole radiator synthesis* is used, especially in the case when a sum of multipoles is located at a few isolated points in the interior  $B_i$ . By combining the results of ► Sects. O.2 and O.3, the SST with spherical wave functions is obtained.

### O.4.3 Variants of the SST with Spherical Wave Functions

In the following, spherical wave functions are used as equivalent sources. Only sparsely scattered attempts can be found in the literature, in which other types of source functions are used. For example, functions in prolate spheroidal coordinates were applied in [Hackman (1984)], and surface sources weighted according to a Gaussian distribution were employed in [Guyader (1994)]. The reason is that it is more difficult to deal with such functions than with spherical wave functions. Fortunately, working with spherical functions is adequate, since the use of several source locations distributed over the interior  $B_i$  enables us to treat complex non-spherical geometries. This is shown in ► Sects. O.5 and O.6. In the present section, only spherical wave functions with respect to one source location (placed in the origin) as defined in Eq. O.4.(5) will be considered. Hence, the source area is simply  $Q = \{0\}$ , and the source function  $q(x, 0)$  (see Eq. O.4.(1)) consists of a series of spherical wave functions with increasing order in the most general case. Hence, in accordance with Eqs. O.4.(1) and O.4.(5) it can be written


$$p(x) = c(0)q(x, 0) = \sum_{m=0}^{\infty} c_m \psi_m. \quad (15)$$

By introducing expansion O.4.(15) into the weighted residuals O.4.(4) one gets the weighted residual equations with spherical wave functions as sources:


$$\sum_{m=0}^{\infty} c_m \iint_S R[\psi_m(y)] w_\ell(y) ds = \iint_S f(y) w_\ell(y) ds; \quad \ell = 0, 1, 2, 3 \dots \quad (16)$$

These equations are called *spherical weighted residual equations*. Three important variants of the SST result from specifying the weighting functions in Eq. O.4.(16). All other parameters are fixed.

### O.4.3.1 Null-Field-Like Equations

As mentioned in  Sect. O.3, the family of weighting functions has to form a complete system in the Hilbert space  $H = L_2(S)$  of square integrable functions over the surface  $S$  equipped with the usual scalar product

$$(u, v) = \iint_S uv^* ds \quad \text{for } u, v \in H. \quad (17)$$

Recall that a system of functions is complete if the only function orthogonal to all other functions is the null function (see for example [Higgins (1977), p. 15]). In [Vekua (1953)] Vekua has shown that the spherical wave functions are complete in the Hilbert space  $H$  for every wave number  $k$  if  $S$  is a Lyapunov surface as assumed in  Sect. O.2.1 (see Theorem 1 of [Ochmann (1995)]). Hence, the spherical wave functions are also admissible as weighting functions:

$$w_\ell = \psi_\ell. \quad (18)$$

Such an approach is known as the *Galerkin method* where trial and weighting functions are identical. By introducing these weighting functions into the spherical weighted residual equations O.4.(16), we obtain

$$\sum_{m=0}^{\infty} c_m \iint_S R[\psi_m(y)] \psi_\ell(y) ds = \iint_S f(y) \psi_\ell(y) ds; \quad \ell = 0, 1, 2, \dots \quad (19)$$

The symmetry relation O.4.(14a) yields

$$\iint_S \sum_{m=0}^{\infty} c_m \psi_m(y) R[\psi_\ell(y)] ds = \iint_S f(y) \psi_\ell(y) ds; \quad \ell = 0, 1, 2, \dots \quad (20)$$

or equivalently

$$\iint_S p(y) R[\psi_\ell(y)] ds = \iint_S f(y) \psi_\ell(y) ds; \quad \ell = 0, 1, 2, \dots \quad (21)$$

by taking into account expansion O.4.(15). Choosing  $R = \partial/\partial n$  and  $f = j\omega\rho_0 v$  yields exactly the null-field equations for Neumann data (see [Kleinman/Roach/Ström (1984)], Eq. O.3.(3)). Hence, the following result is obtained: the null-field equations for Neumann data use the spherical wave functions as weighting functions. If in addition the pressure  $p$  is expanded into spherical wave functions, then the null-field equations and the spherical SST are identical. Similarly, the null-field equations for Dirichlet data (see [Kleinman/Roach/Ström (1984), Eq. (2)]) are obtained if the weighting functions  $w_1 = \partial\psi_n/\partial n$  are used. The null-field equations were described in many papers (see for example [Colton/Kress (1983); Kleinman/Roach/Ström (1984); Martin (1982); Stupfel/

Lavie/Decarpigny (1988)]). Theorem 6 of [Ochmann (1995)] shows that the the null-field equations minimise the amplitude of the reactive power of the error field

$$\Delta p = \sum_{m=0}^N c_m \psi_m - p, \quad (22)$$

but not the sound power radiated by this error field (the error disappears if  $N \rightarrow \infty$ , see Eq. O.4.(15)).

For most radiation problems it would be more desirable to minimise the sound power of the radiated error wave directly. Unfortunately, to the author's knowledge, such a variational principle has not yet been found (see [Ochmann (1995)]).

In Sect. 6 of [Ochmann (2000)] the null-field equations were derived from the Helmholtz integral equation for the interior field, which is an ill-posed integral equation of the first kind. This shows that the null-field equations and the related T-matrix approach of Waterman, [Waterman (1969)], can lead to unstable systems of equations. Hence, alternative formulations of the SST can be found by choosing other sets of weighting functions.

### 0.4.3.2 The Full-Field Equations

If the regular wave functions  $\chi_\ell = \text{Re}\{\psi_\ell\}$  are selected as weighting functions and introduced into the spherical weighted residual equations O.4.(16) one obtains

$$\sum_{m=0}^{\infty} c_m \iint_S R[\psi_m(y)] \chi_\ell(y) ds = \iint_S f(y) \chi_\ell(y) ds; \quad \ell = 0, 1, 2, \dots \quad (23)$$

By employing the symmetry relation O.4.(14b) we find

$$\frac{i}{k_0} c_\ell + \sum_{m=0}^{\infty} c_m \iint_S \psi_m(y) R[\chi_\ell(y)] ds = \iint_S f(y) \chi_\ell(y) ds; \quad \ell = 0, 1, 2, \dots \quad (24)$$

These equations are called *full-field equations of the first kind*. They are derived and discussed in [Ochmann (1999)]. In [Ochmann (1999); Ochmann (2000)], the full-field equations of the first kind are also derived from the exterior Helmholtz integral equation for the “full” outer space, which clarifies the term “full-field equations” in contrast to the “null-field equations”. It can be shown that the diagonal elements  $\text{diag} 1 = i/k_0$  on the left-hand side of Eq. O.4.(24) have a stabilizing effect on the resulting system of equations.

However, the full-filled equations of the first kind have the following disadvantage: The family of weighting functions  $\{\chi_\ell\}$  is not complete and hence does not constitute a basis for the Hilbert space  $L_2(S)$  whenever  $k_0$  is an eigenvalue of the interior Dirichlet problem (see [Waterman (1969), Appendix A]). This problem is closely related to the appearance of critical frequencies in the boundary element method (see [Schenck (1968)] and ▶ Sect. O.5.4). However, the completeness of weighting functions is necessary for

inverting the system of equations O.4.(16) (see [Kleinman/Roach/Ström (1984), Appendix 2]). To avoid such difficulties at certain critical frequencies, it is recommended to use the complex conjugate spherical wave functions (see [Ochmann (1999)])

$$w_\ell = \psi_\ell^* \quad (25)$$

as weighting functions. Since the  $\psi_\ell$  are complete, it follows that the  $\psi_\ell^*$  are also complete and constitute a basis for  $L_2(S)$  at every wave number  $k_0$ . On the other hand, the symmetry relation O.4.(14c) also contains a diagonal element on the right-hand side similar to Eq. O.4.(14b). Hence, by inserting the functions O.4.(25) into Eq. O.4.(16) and applying Eq. O.4.(14c) one finds the equations

$$\frac{2i}{k_0} c_\ell + \sum_{m=0}^{\infty} c_m \iint_S \psi_m R[\psi_\ell^*] ds = \iint_S f \psi_\ell^* ds; \quad \ell = 0, 1, 2, \dots \quad (26)$$

As suggested in [Ochmann (1999)], Eq. O.4.(26) were called *full-field equations of the second kind*. Again, the diagonal elements

$$\text{diag}2 = 2\text{diag}1 = 2 \frac{i}{k_0} \quad (27)$$

arising from the application of Eq. O.4.(14c), have a stabilizing effect. This was demonstrated in Sect. 10.3 of [Ochmann (2000)]. The idea of using the complex conjugate functions for constructing energy expressions goes back to Cremer and Wang [Cremer/Wang (1988)].

### O.4.3.3 The Least Squares Minimization Technique

Finally, we consider the weighting functions

$$w_\ell = \frac{\partial \psi_\ell^*}{\partial n}. \quad (28)$$

It is known that these functions are complete in  $L_2(S)$  (see [Ochmann (1995), p. 517]). By introducing these functions into the spherical weighted residual equations O.4.(16) with Neumann data ( $R = \partial/\partial n$ ,  $f = i\omega\rho_0 v$ ) one gets

$$\sum_{m=0}^{\infty} c_m \iint_S \frac{\partial \psi_m}{\partial n} \frac{\partial \psi_\ell^*}{\partial n} ds = \iint_S f(y) \frac{\partial \psi_\ell^*}{\partial n} ds; \quad \ell = 0, 1, 2, \dots \quad (29)$$

Equation O.4.(29) has the advantage that the corresponding matrix is Hermitian since

$$a_{m\ell} := \frac{\partial \psi_m}{\partial n} \frac{\partial \psi_\ell^*}{\partial n} = a_{\ell m}^*. \quad (30)$$

It can be shown that Eq. O.4.(29) minimise the surface velocity error  $E/i\omega\rho_0$  with

$$E = \iint_S \left| \sum_{m=0}^{\infty} c_m \frac{\partial \psi_m}{\partial n} - i\omega\rho_0 v \right|^2 ds \quad (31)$$

in the mean square sense (see [Ochmann (1995), Ch. 6.2]). Hence, Eq. O.4.(31) can be interpreted as the normal equations of the *least squares method*. It is also possible to consider the least squares method as an orthogonalization method and to employ the Gram-Schmidt technique as described briefly in [Ochmann (1995), p. 519]. An approach which deals directly with orthonormalized functions can be found in [Wu/Yu (1998)].

For extending the least squares method to the mixed boundary conditions O.4.(2b) we suggest using the weighting functions

$$w_\ell = (R\psi_\ell)^* = \frac{\partial \psi_\ell^*}{\partial n} - G^* \psi_\ell^* . \quad (32)$$

According to Millar ([Millar (1983)], see also [Colton/Kress (1983), p. 97]), these functions are complete in the space  $L_2(S)$  if the assumption

$$\text{Im}\{G\} \leq 0 \quad (33)$$

is satisfied. Then, the weighting functions O.4.(32) are admissible and again lead to a set of equations with a corresponding Hermitian matrix

$$\sum_{m=0}^{\infty} c_m \iint_S R\psi_m (R\psi_\ell)^* ds = \iint_S f (R\psi_\ell)^* ds; \quad \ell = 0, 1, 2, \dots \quad (34)$$

As before, Eq. O.4.(34) are the normal equations of the least squares method which now minimize the error functional

$$E = \iint_S \left| \sum_{m=0}^{\infty} c_m R\psi_m - f \right|^2 ds . \quad (35a)$$

#### **O.4.3.4 Summary: Weighting Functions and Corresponding Methods**

► Table 1 provides an overview of all the variants of the spherical SST described, depending on the weighting functions chosen. In all cases only spherical wave functions with respect to one source location are used as source functions (cf. Eq. O.4.(15)).

**Table 1** Methods and weighting functions

Method	Weighting functions
Null-field equations for Neumann data	$\psi_\ell$
Null-field equations for Dirichlet data	$\partial \psi_\ell / \partial n$
Full-field equations of the first kind	$\chi_\ell = \text{Re}\{\psi_\ell\}$
Full-field equations of the second kind	$\psi_\ell^*$
Least squares method	$(\partial \psi_\ell / \partial n)^*$ or $(R\psi_\ell)^*$

### 0.4.3.5 Extension of the SST by Using Equivalent Sources with Complex Source Points

It is possible to shift the coordinates of the singularities of the equivalent sources from real values into the complex plane. For example, if point sources (to the time factor  $e^{+j\omega t}$ )

$$g(\mathbf{x}, \mathbf{y}) = A \exp(-jkR)/(4\pi R); \quad R = \sqrt{(x - x_S)^2 + (y - y_S)^2 + (z - z_S)^2} \quad (35b)$$

are used, the new sources are obtained by adding imaginary parts to the real source coordinate  $\mathbf{y} = (x_S, y_S, z_S)$ :

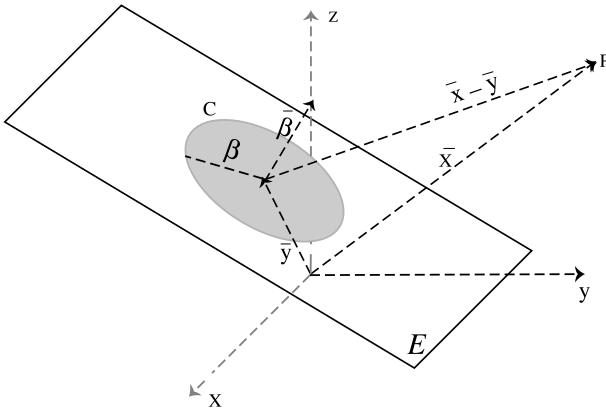
$$\mathbf{y}_c = (x_S - ja, y_S - jb, z_S - jc) = \mathbf{y} - j\boldsymbol{\beta}, \quad \boldsymbol{\beta} = (a, b, c). \quad (35c)$$

Here,  $A$  is the complex amplitude,  $\mathbf{x} = (x, y, z)$  is the receiver position, and  $\mathbf{y}_c$  is the complex source position.

Such a monopole with a complex source point is also a solution of the Helmholtz equation with respect to the spatial coordinates  $\mathbf{x} = (x, y, z)$  for a fixed complex source position  $\mathbf{y}_c$ . The proof can be found in [Ochmann (2005)]. However, it must be taken in account that the singularities of the complex source are different from the point singularity  $\delta(\mathbf{x}, \mathbf{y})$  of the ordinary monopole. The complex distance  $R = R_r + jR_i$  becomes zero on the circle

$$C = \{\mathbf{x} \in E / |\mathbf{x} - \mathbf{y}| = \beta\}, \quad \beta = |\boldsymbol{\beta}|$$

that lies in the plane  $E = \{\mathbf{x} / (\mathbf{x} - \mathbf{y}) \cdot \boldsymbol{\beta} = 0\}$  with center in  $\mathbf{y} = (x_S, y_S, z_S)$ . This is shown in the Fig. 1.



**Figure 1** Complex source point and corresponding geometry

By adding such complex source point solutions to the system of equivalent sources, strongly focused sound field similar to sound beams could be computed with promising accuracy. For example, the radiation from a circular piston in an infinite rigid baffle, which is vibrating in phase with the normal velocity  $v_0$ , was investigated in [Ochmann (2006)]. Only at the axis through the piston, an analytical solution for the sound pressure can be obtained by:

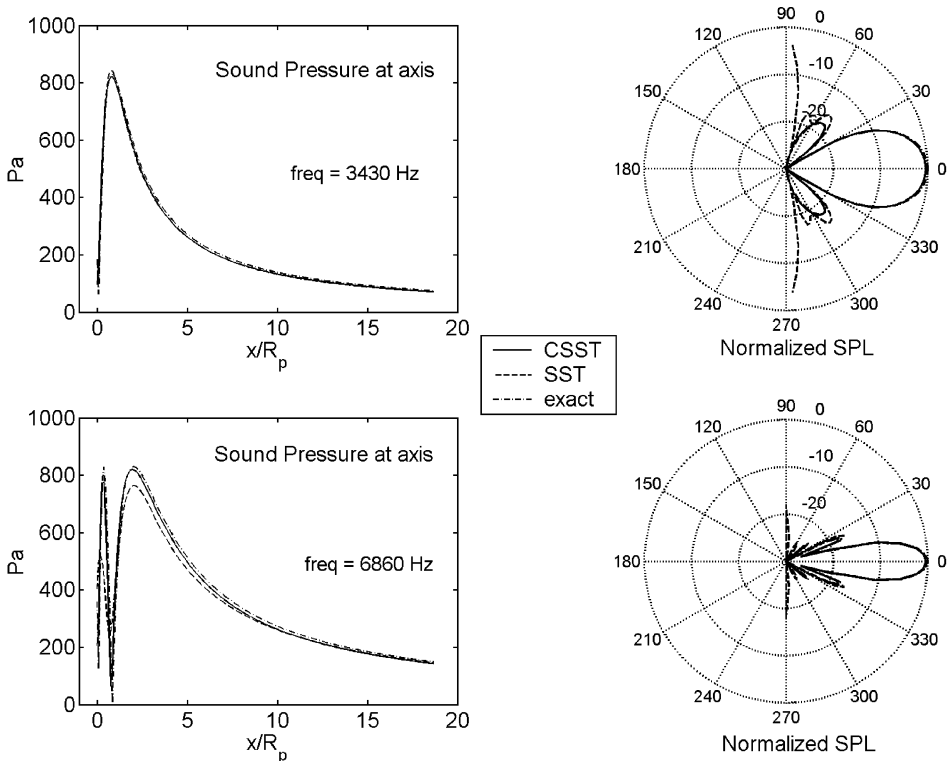
$$p_{\text{axis}}(x) = \rho c v_0 \left( e^{-jk\sqrt{R_0^2 + x^2}} - e^{-jkx} \right), \quad (35d)$$

where  $R_p$  is the radius of the piston. In the far-field ( $kr \gg 1$ ), an approximate solution is given by

$$p_{\text{far}}(r, \theta) = \frac{j\rho c k^2 R_p^2 v_0 e^{-jkr}}{2kr} \left[ \frac{2J_1(kR_p \sin \theta)}{kR_p \sin \theta} \right], \quad (35e)$$

where  $\theta$  is the angle between the field point  $r$  and the axis of radiation.  $J_1$  is the Bessel function of first order.

As a numerical example, a circular piston with radius  $R_p = 0.1$  m was imbedded in a square plate with a side length of 2 m. The elements are squares with a side length of 0.0167 m, so that six points per wavelength up to 3430 Hz are ensured. However, we have used this model also for 6860 Hz, and good results were still obtained. The total number of elements is 14 400. In order to simulate a circular piston, the elements whose centres lie within an area with radius 0.1 m are assumed to vibrate with the constant normal velocity amplitude of 1 m/s. A series of calculations shows that an appropriate source system consists of ten complex monopoles, which lie directly behind the piston in a distance of 0.005 m. The x-component of the source positions possesses a growing imaginary part which varies from 0.015 up to 0.15 m. To achieve a comparable accuracy,



**Figure 2** Comparison of the analytical sound pressure with the results of the “complex SST” (CSST) and the “real SST” at the axis (*left*) and in the far-field (*right*)



only ten complex monopoles are needed in contrast to 216 real multipoles (monopoles, dipoles and quadrupoles). This decreases the time of calculation on an ordinary PC about more than 20 times. The results are shown in the Fig. 2.

In the figure, the amplitude of the exact sound pressure at the axis (see Eq. O.4.(35d)) and at a circle of radius 100 m in a plane perpendicular to the piston (see Eq. O.4.(35e)) is compared with the amplitude of the sound pressure calculated with the complex (abbreviation CSST) and real source systems (SST) for the two frequencies. The radiation patterns at the right are normalized with respect to the value at  $0^\circ$ . The agreement is excellent. The error of the sound pressure at the axis at 6840 Hz is slightly bigger when using the SST instead of the CSST. The radiation pattern of the SST is incorrect in the plane of the baffle, which indicates that this type of radiator is difficult to handle with the SST using only “real sources”. More details can be found in [Ochmann (2006)]. In [Piscocya/Ochmann (in preparation)], the radiation from a sphere cap and a vibrating wheel is simulated by using the SST with complex source points.

#### 0.4.3.6 Extension of the SST to Bodies of Arbitrary Geometry

Up to now only spherical wave functions with a singularity at the origin of the coordinate system as defined in Eq. O.4.(5) are used. This kind of SST is called *one-point multipole method*, [Ochmann (1995)], and is well suited for sphere-like radiators. But the more the shape of the body deviates from a sphere the slower the rate of convergence of the one-point multipole expansion O.4.(15) will become. For this reason a more flexible source system can be constructed by using spherical wave functions with several source locations  $\mathbf{x}_q$  located in the interior  $B_i$  as source functions (multi-point multipole method, [Ochmann (1995)]):

$$\psi_\ell^q(\mathbf{x}) = \psi_\ell(\mathbf{x} - \mathbf{x}_q); \quad q = 1, \dots, Q; \ell = 0, \dots, N. \quad (36)$$

Such source systems allow the boundary conditions to be satisfied on complex-shaped structures. For example, by choosing  $N = 0$  the source system consists of  $Q$  monopoles distributed over an interior auxiliary surface. Such an approach can be considered as derived from an acoustic single layer potential (see O.5.(1) and [Kress/Mohsen (1986)]). Also, it can be found in American [Koopmann/Song/Fahline (1989); Fahline/Koopmann (1991)], French [Guyader (1994)], and Russian papers [Bobrovnikskii/Tomilina (1990); Bobrovnikskii/Tomilina (1995)] under the names *superposition method* or *equivalent source method*. Now, instead of Eq. O.4.(15) the pressure is expanded into the double series

$$p(\mathbf{x}) = \sum_{q=1}^Q \sum_{m=0}^{\infty} c_m^q \psi_m^q(\mathbf{x}). \quad (37)$$

First, the null-field equations are extended by using the  $\psi_\ell^q$  as source and weighting functions. Proceeding along the same lines as in ➤ Sect. O.4.1, we obtain the generalized null-field equations

$$\iint_S \sum_{q=1}^Q \sum_{m=0}^{\infty} c_m^q \psi_m^q(\mathbf{x}) R[\psi_\ell^s(\mathbf{y})] ds = \iint_S f(\mathbf{y}) \psi_\ell^s(\mathbf{y}) ds; \quad s = 1, \dots, Q; \ell = 0, 1, \dots \quad (38)$$

instead of the null-field equations O.4.(20). Here we have taken into account the symmetry relation O.4.(14a), which is valid for all kinds of radiating wave functions.

However, in deriving generalized full-field equations some care is needed since the symmetry relations O.4.(14b, O.4.14c) are only valid for wave functions with the same source location. For example, instead of O.4.(14b) one gets

$$\iint_S (\chi_\ell^S R \psi_m^q - \psi_m^q R \chi_\ell^S) ds = \begin{cases} \frac{j}{k_0} & \text{for } l = m \text{ and } s = q \\ 0 & \text{for } l \neq m \text{ and } s = q \\ ? & \text{for } s \neq q \end{cases} \quad (39a)$$

$$\iint_S (\chi_\ell^S R \psi_m^q - \psi_m^q R \chi_\ell^S) ds = \begin{cases} 0 & \text{for } l \neq m \text{ and } s = q \end{cases} \quad (39b)$$

$$\iint_S (\chi_\ell^S R \psi_m^q - \psi_m^q R \chi_\ell^S) ds = \begin{cases} ? & \text{for } s \neq q \end{cases} \quad (39c)$$

Equations O.4.(39a, 39b) follow directly from Eq. O.4.(14b), which does not depend on the special choice of the source location  $x_q \in B_i$ . For wave functions with different source locations, the present author has not found analogous symmetry relations. This does not matter since the symmetry relations have only to be applied to the diagonal  $l = m$  and  $s = q$  which yields the generalized full-field equations of the first kind

$$\frac{j}{k_0} c_\ell^S + \sum_{q=1}^Q \sum_{m=0}^{\infty} c_m^q \iint_S g_{\ell,m}^{s,q} ds = \iint_S f \chi_\ell^S ds; \quad s = 1, \dots, Q; \ell = 0, 1, \dots \quad (40a)$$

with

$$g_{\ell,m}^{s,q} = \begin{cases} \psi_m^q R [\chi_\ell^S], & \text{for } \ell = m \text{ and } s = q \\ R [\psi_m^q] \chi_\ell^S, & \text{elsewhere.} \end{cases} \quad (40b)$$

Analogously, the weighting functions  $(\psi_1^S)^*$  lead to the generalized full-field equations of the second kind

$$\frac{2j}{k_0} c_\ell^S + \sum_{q=1}^Q \sum_{m=0}^{\infty} c_m^q \iint_S h_{\ell,m}^{s,q} ds = \iint_S f (\psi_\ell^S)^* ds; \quad s = 1, \dots, Q; \ell = 0, 1, \dots \quad (41a)$$

$$h_{\ell,m}^{s,q} = \begin{cases} \psi_m^q R (\psi_\ell^S)^*, & \text{for } \ell = m \text{ and } s = q \\ (\psi_\ell^S)^* R [\psi_m^q]; & \text{elsewhere.} \end{cases} \quad (41b)$$

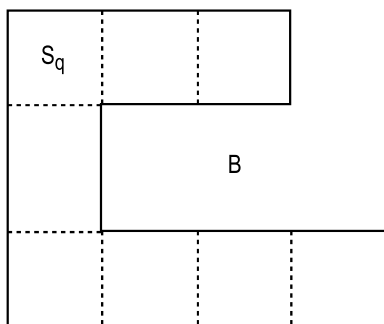
Equations O.4.(41) for Neumann data were derived in [Ochmann (1999)]. They possess the following advantages: the diagonal terms diag2 ensure an improved stability, no critical frequencies occur, and arbitrary surface geometries can be treated if the source locations are chosen in an appropriate manner. This will be considered in the next section.

The analogous derivation of the generalized least squares method is straightforward and hence will be omitted.

#### O.4.4 Position of Sources and Their Optimal Choice

In practical applications the important question arises of how to find optimal source locations in the interior  $B_i$  of the structure. Clearly, the main requirement is that the source locations have to be chosen such that the boundary error, for example the surface velocity error O.4.(31) for Neumann data, becomes minimal.

No general rule exists for achieving this, but a rule of thumb was given in [Ochmann (1990)]: The structure  $B$  should be divided into  $Q$  substructures as indicated by broken lines in the figure. Then, one multipole has to be placed at the centroid of each substructure. The shape of every substructure  $S_q$  ( $q = 1, \dots, Q$ ) should be as sphere-like as possible. In addition, it has to be star-like with respect to its centroid, which means that every part of the surface can be seen from the position of the centroid. Such a choice seems to make sense from an intuitive point of view since the “influence area” of each multipole represents a sphere-like substructure. Many numerical calculations confirm that such source systems may lead to smaller boundary errors than other source configurations. However, no strong mathematical proof has been given up to now.



In [Ochmann (1992)] an attempt was made to optimize numerically the source locations. For this purpose a nonlinear least squares problem has to be solved, which can be done iteratively by applying the Levenberg-Marquardt algorithm. The investigation of idealized radiating structures like cubes and cylinders showed that the additional optimization of the multipole locations had a strong effect on the boundary error and did improve the accuracy of the sound field approximation remarkably, [Ochmann (1992)]. On the other hand, such an automatic optimisation needs a greater amount of computer time, which may be justified if the manual choice as described above does not lead to satisfactory results.

After having presented the theory of the SST, numerical aspects and one example of the method will be considered.

## 0.4.5 Numerical Aspects

### 0.4.5.1 Numerical Implementation

In practical calculations, only a finite number  $N_W = (N + 1)Q$  of source functions  $\psi_m^q$  with  $m = 0, \dots, N$  and  $q = 1, \dots, Q$  can be used. For example, if only monopoles ( $N = 0$ ) and two source locations ( $Q = 2$ ) are used, the full-field equations of the second kind O.4.(41) for Neumann data O.4.(2a) lead to a system of equations  $Ac = f$  with

$$A = \begin{pmatrix} 2j/k_0 + \iint_S \psi_0^1 \frac{\partial (\psi_0^1)^*}{\partial n} ds & \iint_S \frac{\partial \psi_0^2}{\partial n} (\psi_0^1)^* ds \\ \iint_S \frac{\partial \psi_0^1}{\partial n} (\psi_0^2)^* ds & 2j/k_0 + \iint_S \psi_0^2 \frac{\partial (\psi_0^2)^*}{\partial n} ds \end{pmatrix}, \quad (42a)$$

and

$$c = \begin{pmatrix} c_0^1 \\ c_0^2 \end{pmatrix} \quad \text{and} \quad f = j\omega\rho_0 \iint_S \begin{pmatrix} v(\psi_0^1)^* \\ v(\psi_0^2)^* \end{pmatrix}. \quad (42b)$$

The solution of Eqs. O.4.(42) gives the unknown vector of coefficients  $c$  which determines the source strength of both monopoles. For performing the surface integration, the surface is divided into  $M$  boundary elements. The simplest integration scheme is obtained if one assumes that pressure and normal velocity are constant over a single surface element. Such constant elements are often used, but, as in BEM, linear, quadratic, or more sophisticated elements may lead to better numerical results (see [► Sect. 0.5.2](#)). One main advantage of the SST can be seen from Eqs. O.4.(42): In general, the number of equations will be much smaller than the number of boundary elements, i.e.  $N_W \ll M$ , especially if fine-meshed grids are used for the purpose of high-frequency calculations. Hence, the SST may lead to faster numerical algorithms than boundary element techniques, which work with  $N_W = M$  (if constant elements are used). On the other hand, the SST will give approximate solutions for  $N_W < M$ , whereas the BEM normally provides exact solutions limited only by the discretization error (see [Makarov/Ochmann (1998)]). An example may illustrate this situation: let us consider a body that vibrates like a pulsating sphere. Then only one equation has to be solved for finding the exact solution if the equivalent monopole is placed at the right position. In contrast, the BEM has to solve as many equations as the body has boundary elements. However, a complex shaped body with a complicated vibration pattern may require that nearly  $N_W \approx M$  sources should be taken into account.

The spherical wave functions involve the spherical Bessel and Hankel functions. Depending on order and argument, these functions may assume large numerical values. Hence, we recommend working with normalized functions  $\psi_\ell^q(x)/K_\ell^q$  instead of using the spherical wave functions directly. We have chosen the Hankel functions  $h_n^{(1)}(k_0 a)$  as normalizing constants in most calculations with  $a$  being a typical dimension of the structure.

### 0.4.5.2 Stability and Condition Number

The variants of the SST may be distinguished by their different stability behaviour, which is especially valid for the null-field equations and the full-field equations. The stability of a system of equations  $A \cdot x = b$  can be investigated by considering the condition number, [Pärt-Enander/Sjöberg/Melin/Isaksson (1996); Press/Flannery/Teukolsky/Vetterling (1990)]

$$\kappa = \text{cond}(A) = \|A\| \|A^{-1}\|, \quad (43)$$

where  $\|\dots\|$  is a matrix norm and  $\kappa$  is a real number greater than or equal to one. The condition number measures the sensitivity of the solution  $x$  with respect to perturbations in  $A$  or in  $b$ . An unstable or badly conditioned system has a large condition number, [Pärt-Enander/Sjöberg/Melin/Isaksson (1996); Press/Flannery/Teukolsky/Vetterling (1990)]. The condition number depends on the chosen matrix norm. The Euclidean (or spectral) condition number  $\kappa_{\text{spec}}$  is defined as the ratio of the largest and the smallest singular value of  $A$ . As suggested by Tobocman, [Tobocman (1985)], the matrix norm

$$\kappa_F = \frac{1}{n} \|A\|_F \|A^{-1}\|_F \quad (44a)$$

can also be used which is based on the Frobenius norm

$$\|A\|_F = \sqrt{\sum_{i=1}^{N_W} \sum_{j=1}^{N_W} |a_{ij}|^2}. \quad (44b)$$

Here again,  $A = (a_{ij})$  is the above mentioned  $N_W \times N_W$  matrix. However, the calculation of  $\kappa_{\text{spec}}$  or  $\kappa_F$  may be very time consuming due to the calculation of the singular values or the inverse matrix, respectively. For this reason, it is advisable to use approximations for the condition number as given in [Pärt-Enander/Sjöberg/Melin/Isaksson (1996)].

Numerical examples show that the null-field equations may lead to large condition numbers, especially if the number of sources is large, [Ochmann (1999); Ochmann (2000)]. This drawback can be removed by applying the singular-value decomposition or by using the full-field equations instead of the null-field equations.

### 0.4.5.3 Calculation of Field Quantities and Sound Power

After having determined the coefficients  $c_i$ , i.e. the source strengths of the equivalent sources by inverting the matrix  $A$ ,  $c = A^{-1}f$ , all field quantities in the exterior space  $B_e$  can easily be computed by a simple source superposition as indicated in Eqs. 0.4.(1), 0.4.(15), or 0.4.(37). For example, the acoustic pressure  $p$  is obtained from Eqs. 0.4.(1), 0.4.(15), or 0.4.(37) directly. Then, the velocity vector  $\mathbf{v} = (v_x, v_y, v_z)$  can be obtained from the well-known formula (for a time factor  $e^{-i\omega t}$ )

$$\mathbf{v} = (i\omega\rho_0)^{-1} \text{grad } p. \quad (45)$$

From the knowledge of  $p$  and  $v$  the sound intensity and the sound power can be calculated (see ► Sect. O.3.1). If the one-point multipole method is used, the radiated effective sound power  $\Pi$  is proportional to the sum of the source coefficients squared

$$\Pi = \Pi(p, v) = \frac{1}{2} \operatorname{Re} \left\{ \iint_{\Omega_{Ra}} p(x) v^*(x) dx \right\} = \frac{1}{2\rho_0 c_0 k_0^2} \sum_{m=0}^N |c_m|^2, \quad (46)$$

where  $\Omega_{Ra}$  is a sphere surrounding the radiating body. Formula O.4.(46) can be derived from Eqs. O.4.(5), O.4.(8), and O.4.(15). If the multi-point multipole method is used, the sound power cannot be expressed in such a simple manner, since the source functions  $\psi_m^q$  are not orthogonal over an exterior sphere. Therefore, the integration over a closed surface has to be performed numerically.

Some more useful definitions will be given for the Neumann problem where the normal velocity  $v$  is prescribed on the surface  $S$ . Clearly, the normal velocity  $w = v_{\text{sim}}$  simulated by the source system may differ from the real  $v$ , since the SST will only give approximate solutions (see ► Sect. O.2). Hence, the relative surface velocity error

$$F_{\text{rel}} = \iint_S |v - w|^2 ds / \iint_S |v|^2 ds \quad (47)$$

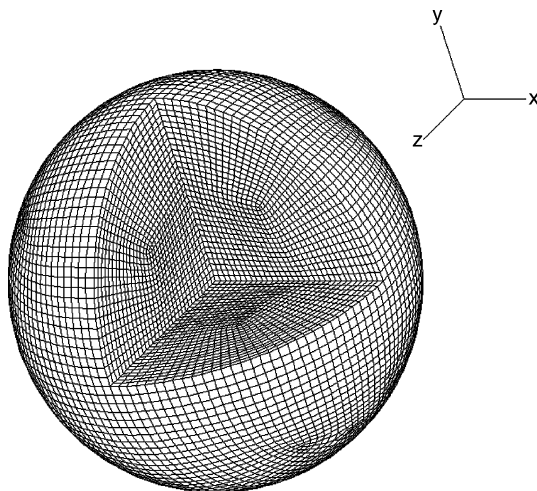
is a measure for the accuracy of the solution depending on the number and on the locations of the sources. For every calculation such a boundary error (Eq. O.4.(47) valid for Neumann data or a corresponding error for other boundary conditions) can be computed even if the solution is not known a priori. For Neumann data we can also differentiate between the sound power  $\Pi(p, v)$ , which is calculated, using the prescribed velocity  $v$  and the sound power  $\Pi(p, v_{\text{sim}})$  for the simulated velocity (see Eq. O.3.(5)). In both cases the pressure  $p$  is the simulated pressure since the true pressure is unknown.

#### O.4.6 A Numerical Example:

##### Sound Scattering from a Non-Convex Cat's-Eye Structure

To illustrate the theory of the SST numerical results for one specially chosen scattering problem will be presented. More results for additional radiation and scattering problems concerning idealized structures, a propeller, and a cylinder can be found in [Ochmann (2000)] and in [Homm/Ochmann (1996); Homm/Schneider (2000); Ochmann, VDI-Berichte (1990); Ochmann/Heckl (1994); Ochmann/Homm (1996)].

In the example shown the SST is used for treating the scattering from complex-shaped, non-convex structures. In [Makarov/Ochmann (1998); Ochmann (1999); Ochmann/Homm (1997)] such a structure was studied which consisted of a sphere where the positive octant, i.e. the part corresponding to  $x > 0$ ,  $y > 0$ ,  $z > 0$ , was cut out. The region of the missing octant is called “cat's-eye”, since it acts like a three-dimensional reflector. As shown in Fig. 3, the finite element model of the cat's-eye structure consists of 7911 boundary elements to achieve six elements per wavelength at  $k_0 a = 20.9$  ( $a$  is the radius of the corresponding sphere). The incidence direction  $n_i$  of the single frequency, plane wave is along the negative bisector of the angle between the  $x$  and  $y$  axes. Hence



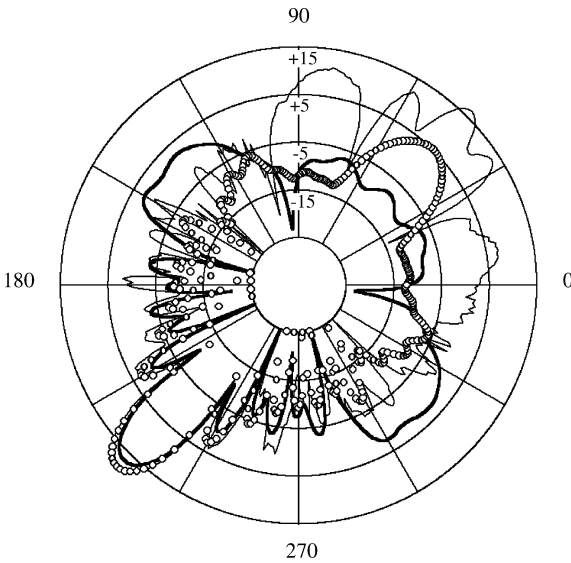
**Figure 3** Finite element model for the cat's eye structure with  $k_0 a = 20.9$

the incident wave illuminates the reflecting area of the cat's-eye and leads to multiple reflections. According to the "rule of thumb" of ► Sect. 0.6 the source system was constructed as follows: multipoles of order  $N$  were placed in the middle of each of the seven octants.

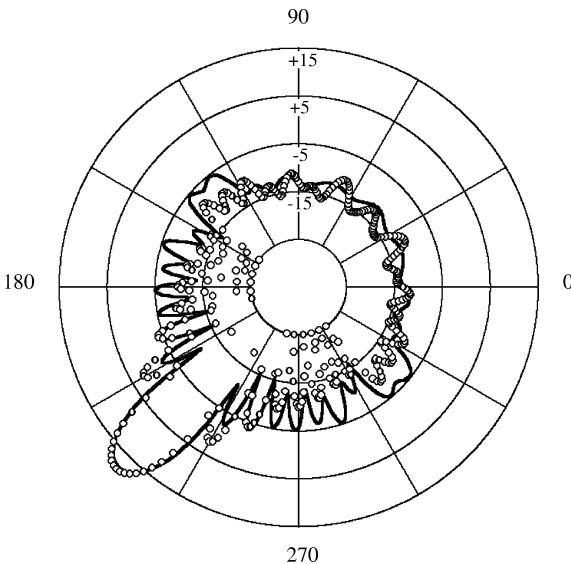
Only a few results are presented here. More details and results can be found in [Ochmann (1999)]. In Fig. 4 the directivity pattern of the target strength TS (see ► Sect. 0.3.2, Eq. 0.3.(13)) is shown in the  $xy$ -plane. (The target strength was calculated in the far-field and then projected back to the distance of 1 m from the scatterer.) The surface is assumed to be rigid. The total number of sources was 700, since multipoles of order up to  $N = 9$  at each of the seven source locations were taken into account. For the incidence direction  $n_i$  the maximum of the forward and backward scattering can be seen in the  $xy$ -plane. Obviously, the data of the null-field equations, full-field equations of 2nd kind, and the plane wave approximation (see ► Sect. 0.3.1) agree well at forward scattering. However, the backscattering maximum is only predicted by the full-field equations of 2nd kind ( $\kappa_{\text{spec}} = 4.6 \cdot 10^4$ ,  $F_{\text{rel}} = 23\%$ ). The null-field equations produce too large results since we have  $\kappa_{\text{spec}} = 1.1 \cdot 10^8$ ,  $F_{\text{rel}} = 700\%$ . The plane wave approximation could not find any backscattering since it principally neglects multiple reflections.

### 0.4.7 Concluding Remarks

A general assumption of the SST is that all sources must be located in the interior  $B_i$  of the structure. If the sources are placed on the boundary itself, the corresponding BEM is obtained (see ► Sect. R.5). In addition, the SST as well as the BEM can be considered as methods of weighted residuals, [Ochmann, Acustica (1990)]. Advantages and drawbacks of both methods are presented and compared in [Ochmann (1995)] with the following result: the application of the BEM is easier and more automatic than the SST, since no source system must be constructed explicitly. However, a BEM computation can become



**Figure 4** Directivity pattern of the target strength TS in the  $x, y$  plane for a rigid surface, direction of incidence along the negative bisector of the angle between the  $x$  and  $y$  axes; 700 sources were used; *thick curve*: plane wave approximation, *thin curve*: null-field equations, *circles*: full-field equations of the 2nd kind



**Figure 5** Directivity pattern of the target strength TS in the  $x, y$  plane for an absorbing impedance, direction of incidence along the negative bisector of the angle between the  $x$  and  $y$  axes; 567 sources were used; *thick curve*: plane wave approximation, *circles*: least squares method



extremely time-consuming for the treatment of complex structures involving a large number of elements. Consequently, the SST should be applied if the surface model of the structure is very finely discretized and the structural vibration shows a not too complicated pattern, such as a pulsating or oscillating body. This implies that the number of sources needed will be much smaller than the number of boundary elements, and a smaller system of equations has to be solved. Also, complex structures which vibrate in a complicated manner, can be treated by the SST in a very efficient way if one looks for an approximate solution with explicitly determined boundary errors.

The main topic of the presented overview is the application of the SST to the calculation of sound radiation or scattering into the unbounded, three-dimensional space. In addition, the SST can be used for the treatment of several other acoustical problems. For example, two-dimensional sound fields, problems with axisymmetric or cyclic symmetry, sound fields in interior spaces or in half spaces, or scattering and radiation from elastic structures can be investigated by means of the SST. Moreover, Leviatan and his co-workers have analyzed various scattering problems by means of a source-model technique in a series of papers (see, e.g. [Erez/Leviatan (1993)] where more references can be found).

## 0.5 The Boundary Element Method (BEM)

The BEM is mainly used for solving the radiation and scattering problem (see ➤ *Sect. 0.3*, standard problems 1 and 2). The interior problem (standard problem 3) can also be treated with the help of the BEM. The fluid-structure interaction problem can be solved by combining the BEM with the finite element method (see ➤ *Sect. 0.6.3*).

### 0.5.1 Boundary Integral Equations

The most frequently used integral equation formulation in acoustics is the well-known Helmholtz integral equation for exterior field problems. The Helmholtz integral equation is obtained by applying Green's second theorem to the Helmholtz equation 0.3.(1) (see for example [Schenck (1968)] or [Colton/Kress, *Integral Equations in Scattering Theory* (1983)]). Depending on the location of the field point  $x$ , the Helmholtz integral equation takes the form

$$\iint_S \left[ p(y) \frac{\partial g(x, y)}{\partial n(y)} - \frac{\partial p(y)}{\partial n(y)} g(x, y) \right] ds = \begin{cases} p(x), & x \in B_e \\ \frac{1}{2} p(x), & x \in S \\ 0, & x \in B_i \end{cases} \quad \begin{matrix} (1a) \\ (1b) \\ (1c) \end{matrix}$$

where (for a time factor  $e^{+j\omega t}$ )

$$g(x, y) = \frac{1}{4\pi\bar{r}} e^{-jk_0\bar{r}} \quad \text{with} \quad \bar{r} = \bar{r}(x, y) = \|x - y\| \quad (2)$$

is the free-space Green's function, and  $y$  is a spatial point on the structural surface  $S$ . The geometrical notations are chosen as described in ➤ *Sect. 0.3.1*. Eqs. 0.5.(1a), 0.5.(1b),

and O.5.(1c) are called exterior Helmholtz integral equation, the surface Helmholtz integral equation, and the interior Helmholtz integral equation, respectively. There also exists an analogous Helmholtz integral formulation for interior field problems, which will be considered in ► Sect. O.5.5. The interior Helmholtz integral equation O.5.(1c) considered here gives a null-field in  $B_i$  which obviously does not represent a physical solution, and should not be confused with the Helmholtz integral formulation for interior problems. Solutions of the Helmholtz integral equation automatically satisfy the radiation condition O.3.(3). Many boundary element formulations in acoustics use the surface Helmholtz integral equation as a starting point since it is a second kind Fredholm integral equation for the familiar Neumann boundary condition with satisfactory numerical stability, [Schenck (1968)]. Fast numerical solvers for the discretized version of the surface Helmholtz integral equation can be obtained by using, for example, iterative algorithms, [Makarov/Ochmann (1998)], or multigrid methods, [Ochmann/Wellner (1991)].

The Helmholtz formula O.5.(1) is valid if the surface  $S$  is assumed to be closed and sufficiently smooth, i.e. there is a unique tangent to  $S$  at every  $x \in S$ . For the general case, where no unique tangent plane exists at  $x \in S$  (for example, when  $x$  is lying on a corner or an edge), the surface Helmholtz integral equation has to be modified slightly, [Seybert/Soenarko/Rizzo/Shippy (1985)]

$$\iint_S \left[ p(y) \frac{\partial g(x, y)}{\partial n(y)} - \frac{\partial p(y)}{\partial n(y)} g(x, y) \right] ds = \frac{C(x)}{4\pi} p(x), \quad (3a)$$

where

$$C(x) = 4\pi + \iint_S \frac{\partial}{\partial n(y)} \left( \frac{1}{\tilde{r}(x, y)} \right) ds(y) \quad (3b)$$

is the solid angle seen from  $x$ , [Peter (2000)]. For a smooth surface  $C(x) = 2\pi$  is in agreement with Eq. O.5.(1b).

For calculating the quantities of the sound field, two steps are necessary. First, the surface Helmholtz integral equation O.5.(1b) has to be solved which gives pressure and normal velocity on the surface of the structure. This procedure requires the main effort, since a complex, fully populated, and unsymmetrical system of linear equations has to be solved. Second, the sound field in the whole outer space can be calculated with the help of the exterior Helmholtz integral equation by a simple integration over the surface  $S$ .

The numerical treatment of the surface Helmholtz integral equation involves two characteristic difficulties. The equation possesses a weakly singular kernel, and it has no unique solution at the so-called critical frequencies. The interior Helmholtz integral equation does not suffer from these disadvantages. However, as an integral equation of the first kind, it provides a less satisfactory basis for numerical calculations, [Schenck (1968)]. Its numerical treatment needs extreme care, and regularisation methods should be applied, [Colton/Kress, *Integral Equations in Scattering Theory* (1983); Colton/Kress (1992)].

Another formulation of acoustical boundary integral methods is the potential-layer approach. By representing the pressure  $p$  as a single-layer potential (i.e. a layer of monopoles)

$$p(x) = \iint_S \sigma(y) g(x, y) ds(y) ; \quad x \in B_e \quad \text{or} \quad x \in B_i \quad (4a)$$

one obtains the boundary integral equation

$$\frac{\sigma(x)}{2} - \iint_S \sigma(y) \frac{\partial g(x, y)}{\partial n(x)} ds(y) = j\omega\rho_0 v ; \quad x \in S \quad (4b)$$

for the determination of the density  $\sigma$ , if the exterior Neumann problem with

$$\partial p / \partial n = -j\omega\rho_0 v \quad (5)$$

is considered (see Theorem 3.16 of [Colton/Kress, Integral Equations in Scattering Theory (1983)]).

For the interior Neumann problem, one gets

$$\frac{\sigma(x)}{2} + \iint_S \sigma(y) \frac{\partial g(x, y)}{\partial n(x)} ds(y) = -j\omega\rho_0 v ; \quad x \in S . \quad (6)$$

The double-layer potential (i.e. a layer of dipoles)

$$p(x) = \iint_S \psi(y) \frac{g(x, y)}{\partial n(y)} ds(y) ; \quad x \in B_e \quad \text{or} \quad x \in B_i \quad (7a)$$

leads to the integral equation

$$\frac{\psi(x)}{2} + \iint_S \psi(y) \frac{\partial g(x, y)}{\partial n(y)} ds(y) = p_0(x) ; \quad x \in S \quad (7b)$$

for the exterior Dirichlet problem with

$$p = p_0 \text{ on } S . \quad (8)$$

It leads to

$$\frac{\psi(x)}{2} - \iint_S \psi(y) \frac{\partial g(x, y)}{\partial n(y)} ds(y) = -p_0(x) ; \quad x \in S \quad (9)$$

for the corresponding interior Dirichlet problem (Theorem 3.15 of [Colton/Kress, Integral Equations in Scattering Theory (1983)]).

Whereas the single- or double-layer approach can be interpreted as a layer of monopoles or dipoles, respectively, the Helmholtz integral equation contains both layers of monopoles and dipoles.

All the above presented layer approaches lead to boundary equations of the second kind. It is also possible to derive equations of the first kind. Following Colton and



Kress, [Colton/Kress, *Integral Equations in Scattering Theory* (1983)], the single-layer potential 0.5.(4a) solves the interior and exterior Dirichlet problem with boundary conditions 0.5.(8) if the density  $\sigma$  is a solution of the integral equation (Theorem 3.28 of [Colton/Kress, *Integral Equations in Scattering Theory* (1983)])

$$\iint_S \sigma(y) g(x, y) ds(y) = p_0; \quad x \in S. \quad (10)$$

The double-layer potential 0.5.(8) solves the interior and exterior Neumann problem with boundary condition 0.5.(6), provided the density  $\psi$  is a solution of the singular integral equation (Theorem 3.31 of [Colton/Kress, *Integral Equations in Scattering Theory* (1983)])

$$\frac{\partial}{\partial n(x)} \iint_S \psi(y) \frac{\partial g(x, y)}{\partial n(y)} ds(y) = -j\omega\rho_0 v; \quad x \in S. \quad (11)$$

Such integral equations of the first kind are improperly posed. The ill-posed nature of these equations is described in [Colton/Kress, *Integral Equations in Scattering Theory* (1983), p. 90]. However, there exist several attempts to deal with equations of the first kind too, and advances have been made in their numerical analysis. References can be found in [Colton/Kress, *Integral Equations in Scattering Theory* (1983); Colton/Kress (1992)].

In addition, Eq. 0.5.(11) contains the normal derivative of the double-layer potential, which in general does not exist on the boundary. Even if it exists, Eq. 0.5.(11) becomes strongly singular and a regularization is required.

Table 2 provides an overview about the exterior integral equations considered above, where the Neumann boundary conditions, [Seybert/Soenarko/Rizzo/Shippy (1985)], are taken into account. Only slight modifications are necessary if other boundary data, such as Dirichlet or Robin data, are prescribed (see [Angell/Kleinman (1982), Kleinman/Roach (1974)]). Table 2 shows the surface equation, which has to be solved first. The corresponding equation for the pressure in the exterior space is given in the right column.

**Table 2** Boundary integral formulations for the exterior domain;

HIE = Helmholtz integral equation;

SLP = Single-layer potential;

DLP = Double-layer potential

	Surface equation on $S$	Exterior equation for $p$ in $B_e$
HIE	$p = Kp + R(j\omega\rho_0 v)$	$p = \frac{1}{2} [Kp + R(j\omega\rho_0 v)]$
SLP	$\sigma - K'\sigma = 2j\omega\rho_0 v$	$p = \frac{1}{2} R\sigma$
DLP	$T\psi = -2j\omega\rho_0 v$	$p = \frac{1}{2} K\psi$

Here, the following abbreviations for integral operators (after [Colton/Kress, *Integral Equations in Scattering Theory* (1983)]) are used

$$(K\varphi)(x) := 2 \iint_S \varphi(y) \frac{\partial g(x, y)}{\partial n(y)} ds(y) , \quad (12)$$

$$(K'\varphi)(x) := 2 \iint_S \varphi(y) \frac{\partial g(x, y)}{\partial n(x)} ds(y) , \quad (13)$$

$$(R\varphi)(x) := 2 \iint_S \varphi(y) g(x, y) ds(y) , \quad (14)$$

$$(T\varphi)(x) := 2 \frac{\partial}{\partial n(x)} \iint_S \varphi(y) \frac{\partial g(x, y)}{\partial n(y)} ds(y) . \quad (15)$$

### 0.5.2 Discretization of the Boundary Integral Equation

In the following, only the exterior radiation problem with Neumann data is considered as the model problem. For the numerical solution of one of the above three surface integral equations, the continuous equation is discretised and transformed into a system of linear equations. For this reason, the surface of the radiator is approximated by a finite element model consisting of  $N$  finite surface elements  $F_k$  ( $k = 1, \dots, N$ ). The generation of such finite element grids for complex machine structures, which often consists of several thousand elements, requires an immense effort, even if special finite element model generators ("preprocessors") will be used.

The easiest approach to performing the surface integration in the Helmholtz integral equation 0.5.1(b) is to consider pressure and normal velocity as constant over each single element. This approach is called *collocation method*, since it means that a certain value of pressure and normal velocity is assigned to the centroid of each element. These simple and often used approaches are described by Rao and Raju, [Rao/Raju (1989)], under the name "method of moments".

The collocation method transforms the Helmholtz integral equation into the following system of  $N \times N$  linear equations

$$DP + MV = P/2 , \quad (16)$$

where the matrix  $D = (d_{ik})$  consists of the dipole terms

$$d_{ik} = \iint_{F_k} \frac{\partial g(x_i, y)}{\partial n(y)} ds(y) \quad (17a)$$

and the matrix  $M = (m_{ik})$  consists of the monopole terms

$$m_{ik} = j\omega\rho_0 \iint_{F_k} g(x_i, y) ds(y) . \quad (17b)$$

$P$  is the  $N$ -dimensional vector of pressure values in the centroids of the  $N$  elements, and  $V$  is the corresponding normal velocity vector.

For practical purposes, often plane triangular or rectangular elements are used. Hence, the discretised surface will be not smooth, but it will be equipped with several edges and corners. Nevertheless, it is not necessary to use modification O.5.(3), since the pressure is only evaluated in the element centroids. In addition, corners and edges can be considered as slightly rounded, which will not influence the sound radiation remarkably.

Higher order elements such as linear, quadratic or cubic elements are used, too. A quadratic isoparametric element formulation with six nodes for the triangular and eight nodes for the quadrilateral curvilinear element was suggested in [Seybert/Soenarko/Rizzo/Shippy (1985)], in which both the surface elements and the acoustic variables are represented by second-order shape functions.

Often, complex structures consisting of a large number of plane triangular and rectangular elements occur in practical industrial problems. For such finite element models it is recommended to perform the integrations appearing in Eq. O.5.(17) as follows: choose variables that are constant over a single element and transform each element  $F_k$  on to the unit triangular or rectangular element (see [Chen/Schweikert (1963); Schwarz (1980)]). Then use Gaussian integration rules of the desired order of accuracy.

The average size of the elements of a boundary grid determines the highest frequency that can be treated. A famous rule of thumb is the “six elements per wavelength rule”. It means that at least six elements per wavelength should be taken into account if constant or linear elements are used. This is approximately valid for  $k_0 d \leq 1$  where  $d$  is a typical dimension of the element. A detailed discussion about this rule can be found in [Marburg (acc. for publ.)]. Figure O.4.3 shows a boundary element mesh consisting of 7869 rectangular and 42 triangular elements, which can be used up to  $k_0 a \leq 21$ , where  $a$  is the radius of the corresponding sphere.

### O.5.3 Solution of the Linear System of Equations

One of the main problems of the BEM is that the matrix  $A$  of the system O.5.(16) written in the form

$$AP = F \quad (18)$$

with  $A = D - 0.5 I$  ( $I$  = unity matrix) and  $F = -MV$  ( $V$  = prescribed normal velocity vector) is fully occupied, complex and unsymmetrical. This is an essential disadvantage of the BEM in comparison with the FEM, which leads to symmetrical and weakly populated matrices with small bandwidth (see ➤ Sect. O.6.2). However, many technical structures consist of several thousands of elements leading to huge systems of equations. The numerical solution of such systems needs much computer time. Often, it is not possible to store the whole matrix  $A$  on the disk. In addition, if complete spectra should be calculated, a full system of equations has to be solved for every single frequency. For this reason, direct solvers such as the Gaussian elimination or the LU decomposition with backsubstitution, [Press/Flannery/Teukolsky/Vetterling (1990)], should only be used for systems up to a few hundreds of equations, [Stummel/Hainer (1971), p. 147], since the numerical effort is of order  $N^3$ .

For vibrating structures with symmetry, simplified boundary integral equations with a reduced number of unknowns can be derived leading to reduced computer costs. For example, the sound radiation from axisymmetric bodies is treated in [Akyol (1986); Seybert/Soenarko/Rizzo/Shippy (1986)]. Under the condition that the boundary conditions are axisymmetric too, the introduction of elliptic integrals leads to further simplifications, [Seybert/Soenarko/Rizzo/Shippy (1986)].

For larger systems without special symmetry properties, iterative solvers should be preferred, since they lead to a numerical cost of order  $N^2$  approximately. The shape of the system O.5.(16) suggests the iteration scheme (called Picard iteration)

$$\frac{1}{2}P^{(i+1)} = DP^{(i)} + MV \quad (19)$$

for a prescribed normal velocity vector  $V$ . Starting with an initial guess for the pressure vector  $P^{(0)}$ , a sequence of iteration vectors  $P^{(i)}$  is obtained. Such an iteration scheme corresponds to the basic iterative method of Jacobi, [Stummel/Hainer (1971), p. 148]. Unfortunately, the Jacobi iteration O.5.(19) does not converge generally. Convergence only takes place if the powers of the matrices  $D$  converge to a matrix of zeros, [Stummel/Hainer (1971), p. 148], or if the eigenvalues of the corresponding integral operators do not lie inside of the unit circle, [Chertock (1968)]. For example, this is not the case for the spheroid investigated by Chertock, [Chertock (1968)]. However, by introducing a suitable chosen relaxation parameter  $\beta$  into Eq. O.5.(19) and using

$$\frac{1}{2}P^{(i+1)} = \frac{1}{2}\beta P^{(i)} + (1 - \beta) [DP^{(i)} + MV] \quad (20)$$

Chertock achieved convergence in some cases. The iteration scheme O.5.(20) corresponds to the *Successive Overrelaxation* (SOR) method. But, Kleinman and Wendland, [Kleinman/Wendland (1977)], showed that a convergent series of successive approximations for the Helmholtz integral equation is only obtained by O.5.(20) if the wave number is sufficiently small. Hence, method O.5.(20) is not a satisfactory basis for practical applications.

In [Kleinman/Roach (1988)] Kleinman and Roach presented an iterative method, which is convergent for all wave numbers  $k_0$ . The key point of the method is a self-adjoint formulation of the Helmholtz integral equation which is obtained by multiplying Eq. O.5.(18) with the complex conjugate matrix  $A^*$

$$A^*AP = A^*F \quad (21)$$

Then again, a successive overrelaxation method is applied to Eq. O.5.(21) leading to

$$P^{(i+1)} = (P^{(i)} - \alpha A^*AP^{(i)}) + \alpha A^*F \quad (22)$$

with relaxation parameter  $\alpha$  for the radiation problem considered in this chapter. Makarov and Ochmann, [Makarov/Ochmann (1998)], applied a variant of this method to the high-frequency acoustic scattering from complex bodies consisting of up to 60 000 surface elements. One major problem arising from method O.5.(22) is to find the optimal parameter  $\alpha$ . Hence, it is more convenient to use parameter-free iterative methods such as the Generalized Minimum Residual Method, which was successfully applied to



acoustic and medium-to-high electromagnetic scattering in [Makarov/Ochmann (submitted); Makarov/Ochmann/Ludwig (submitted); Ochmann/Homm/Semenov/Makarov (2001)].

Another promising iterative method for the solution of the Helmholtz integral equation is the multigrid method, [Ochmann/Wellner (1991)]. It consists mainly of two steps, the smoothing step and the coarse grid correction. Starting with an initial value  $P_0$ , one Picard iteration 0.5.(19) is performed for determining the part  $P_{1/2}$  of the solution vector  $P$  that is highly oscillating with respect to the spatial coordinate on the surface  $S$ . This is the so-called smoothing step. It forces the solution of the system of equations for the error  $P - P_{1/2}$  to be smoother, so that it can be determined on a coarser finite element grid without significant loss of accuracy. For obtaining a coarser grid, two neighbouring grid points are condensed into one. The calculated error is projected by linear interpolation from the coarser grid to the finer one. If only two grids are used, the approach is called the *two-grid method*. The key idea of the multigrid method is as follows: The system for the error is not solved directly. Instead, a two-grid method is used again for obtaining an approximate solution, where one has to go over to an even coarser grid. This procedure is repeated until one arrives at a grid that contains only a small number of elements. Thus, the corresponding system of equation is small enough too, and can be solved with little effort by a direct solver. A detailed description of the multigrid method and corresponding calculations for radiating structures can be found in [Ochmann/Wellner (1991)].

#### 0.5.4 Critical Frequencies and Other Singularities

The integral equation formulation for the exterior problem involves a characteristic problem: At the so-called critical wave numbers  $k_c$  the integral equation is not solvable or not uniquely solvable. This phenomenon has been known for a long time (see Kupradze, [Kupradze (1956)], or Smirnow, [Smirnow (1977)]). Copley, [Copley (1968)], considered it in connection with the acoustical radiation problem and pointed out that the integral equation for the single-layer potential 0.5.(4b) does not possess a solution if the wave number  $k_c$  is an eigenvalue of the interior Dirichlet problem

$$\Delta p + k_c^2 = 0 \quad \text{in } B_i; \quad (23)$$

$$p = 0 \quad \text{on } S. \quad (24)$$

Physically, such a behaviour can be interpreted as a resonance phenomenon of the interior space, [Copley (1968)]. The surface Helmholtz integral equation, however, possesses solutions at the critical wave numbers, but these solutions are not uniquely determined. This was shown by Schenk, [Schenck (1968)], in detail, based on the general theory of Fredholm integral equations. He suggested to use the combined integral equation formulation.

##### 0.5.4.1 Combined Integral Equation Formulation (CHIEF)

The idea is as follows. At wave numbers  $k_c$  the surface Helmholtz integral equation 0.5.(1b) has infinitely many solutions (i.e. a nontrivial null-space). However, it can be



shown that the physically relevant solution of O.5.(1b) is the only one that satisfies the interior Helmholtz integral equation O.5.(1c) simultaneously. Hence, the idea of CHIEF is to solve the surface Helmholtz integral equation on  $S$  and the interior Helmholtz integral equation at certain selected interior points  $x_i$  (so-called CHIEF points) simultaneously:

$$\iint_S \left[ p(y) \frac{\partial g(x, y)}{\partial n(y)} - \frac{\partial p(y)}{\partial n(y)} g(x, y) \right] ds = \frac{1}{2} p(x); \quad x \in S \quad (25a)$$

$$\iint_S \left[ p(y) \frac{\partial g(x_i, y)}{\partial n(y)} - \frac{\partial p(y)}{\partial n(y)} g(x_i, y) \right] ds = 0; \quad x_i \in B_i. \quad (25b)$$

The discretization of both integral equations leads to an overdetermined system of equations. If  $N$  surface elements and  $M$  CHIEF points are used, then a  $(N+M) \times N$  system results. Such a system can be solved by a least-squares orthonormalising procedure. An alternative approach is that of Rosen et al., [Rosen/Canning/Couchman (1995)], who suggested to create a square matrix by introducing a vector  $\lambda$  of Lagrange multipliers:

$$\begin{pmatrix} A & B^* \\ B & I \end{pmatrix} \begin{pmatrix} P \\ \lambda \end{pmatrix} = \begin{pmatrix} F \\ F_C \end{pmatrix}. \quad (26)$$

$A$  (see Eq. O.5.(18)) and  $B$  are the matrices of coefficients resulting from the discretisation of Eqs. O.5.(25a) and O.5.(25b), respectively.  $F$  and  $F_C$  are the corresponding right-hand sides,  $B^*$  is the  $N \times M$  conjugate transpose of  $B$ , and  $I$  is the  $M \times M$  identity matrix. The Lagrange multipliers

$$\lambda = F_C - BP \quad (27)$$

are the residuals in satisfying the  $M$  CHIEF constraint equations.


The CHIEF method suffers from the fact that the interior points  $x_i$  are not allowed to lie on the node surfaces of the interior standing wave field. However, these nodes are not known for general radiator geometries, and their number increases with increasing frequency. On the other hand, the higher the frequency the more CHIEF points are needed, and no rules are known how to choose the number and locations of these points optimally. For avoiding this problem, the following similar method was proposed.

#### 0.5.4.2 Combination with the Null-Field Equation

Stupfel et al., [Stupfel/Lavie/Decarpigny (1988)], suggested the following method, originally based on an idea of Jones, [Jones (1974)]. The surface pressure  $p$  has simultaneously to satisfy the surface Helmholtz integral equation and additional  $M$  null-field equations of the form

$$\iint_S p(y) \frac{\partial \psi_\ell(y)}{\partial n(y)} ds(y) = \iint_S \frac{\partial p(y)}{\partial n(y)} \psi_\ell(y) ds(y); \quad \ell = 1, 2, \dots, \quad (28)$$

where the spherical wave functions  $\psi_\ell$  are defined in  $\blacktriangleright$  Sect. O.4.3. In this way, all critical wave numbers  $k \leq k_M$  are suppressed, where the eigenvalues of the interior Dirichlet problem O.5.(23), O.5.(24) are ordered so that  $k_1 \leq k_2 \leq k_3 \leq \dots$

A detailed description of the null-field equations can be found in  Sect. O.4.3.

The surface Helmholtz integral equation as an integral equation of the second kind is well-posed, and the null-field equations do not suffer from the non-uniqueness problem, [Colton/Kress, Q.J. Mech. Appl. Math. (1983); Martin (1988)]. Hence, the combination of both types of equations seems to be a promising approach – also for numerical calculations in the high-frequency regime.

### 0.5.4.3 Combination with the Differentiated Integral Equation

According to Table 2 the surface Helmholtz integral equation for the exterior Neumann problem in operator notation can be written as

$$p = Kp + R(j\omega\rho_0 v) . \quad (29a)$$

A second relationship can be obtained by formally differentiating the surface Helmholtz integral equation in the direction of the normal. This results in the boundary integral equation

$$-j\omega\rho_0 v = \frac{\partial p}{\partial n} = Tp + K'(j\omega\rho_0 v) \quad (29b)$$

of the first kind for the unknown boundary value  $p$  on  $S$ , where the integral operators  $T$  and  $K'$  are defined below in Eqs. O.5.(13), O.5.(15). Combining both equations leads to the equation

$$p - Kp + j\eta Tp = R(j\omega\rho_0 v) - j\eta(j\omega\rho_0 v + K'(j\omega\rho_0 v)) \quad (30)$$

of the second kind. Burton and Miller showed in reference [Burton/Miller (1971)] that the linear combination O.5.(30) has a unique solution for all real values of the wave number  $k$ , if the real coupling parameter  $\eta$  is not zero. This approach is called the *Burton and Miller method* or the *Composite Outward Normal Derivative Overlap Relation* (with acronym CONDOR). A drawback of the method is that Eq. O.5.(30) includes the derivative of the double-layer Helmholtz potential

$$(Tp)(x) := 2 \frac{\partial}{\partial n(x)} \iint_S p(y) \frac{\partial g(x, y)}{\partial n(y)} ds(y)$$

which is a hypersingular operator. This operator must be transformed to reduce the strength of the singularity, and two ways of regularisation are discussed in [Burton/Miller (1971)].

In a similar way, the solution of the exterior Neumann problem can be sought in the form of a combined single- and double-layer potential

$$p(x) = \iint_S \left\{ g(x, y) + j\eta \frac{\partial g(x, y)}{\partial n(y)} \right\} \sigma(y) ds(y) \quad (31)$$

leading to the hypersingular integral equation (see Table 2 and [Colton/Kress, Integral Equations in Scattering Theory (1983), p. 92])

$$\sigma - K'\sigma - j\eta T\sigma = 2j\omega\rho_0 v \quad (32)$$

for the unknown density  $\sigma$ , which is the adjoint of the combined Green's formula integral equation 0.5.(30). Again, it can be shown that the combined single- and double-layer integral equation 0.5.(32) is uniquely solvable for all wave numbers if  $\eta \neq 0$ , [Colton/Kress, *Integral Equations in Scattering Theory* (1983), Theorem 3.34]. Kress and Spassow, [Kress/Spassow (1983)], had analyzed how to choose the coupling parameter  $\eta$  appropriately in order to minimise the condition number of the integral operators appearing in Eq. 0.5.(32).

#### 0.5.4.4 Modified Green's Functions

Another approach leading to uniquely solvable integral equations for exterior boundary value problems was developed by Jones, [Jones (1974)], Ursell, [Ursell (1973); Ursell (1978)], and Kleinman and Roach, [Kleinman/Roach (1982), Kleinman/Roach (1988); Kleinman/Roach/Schuetz/Shirron (1988)]. They suggested to add a series of radiating wave functions  $\psi_\ell$  (all definitions are given in [Sect. 0.4.3](#)) to the free field Green's function  $g(x, y)$  resulting in a modified double-layer potential Green's function

$$g_m(x, y) := g(x, y) + \sum_{\ell=0}^{\infty} c_\ell \psi_\ell. \quad (33)$$

Now, all surface integral equations from Table 2 can be modified by using the Green's function  $g_m(x, y)$  instead of  $g(x, y)$  in the definition of the operators 0.5.(12)–0.5.(15). For example, the modified double-layer potential is of the form

$$p(x) = \iint_S \Psi(y) \frac{g_m(x, y)}{\partial n(y)} ds(y); \quad x \notin B_e \text{ or } x \notin B_i \quad (34)$$

with density  $\psi$ .

It can be shown that the corresponding surface integral equations are uniquely solvable for all wave numbers provided that the coefficients  $c_\ell$  appearing in 0.5.(33) satisfy certain inequalities (see [Colton/Kress, *Integral Equations in Scattering Theory* (1983), Theorem (3.35)] and [Kleinman/Roach (1988)]). In addition, it was shown by Jones, [Jones (1974)], (see also [Kleinman/Roach/Schuetz/Shirron (1988)]) that the integral equations will still be uniquely solvable for  $k_0 \leq k_N$ , where  $k_N$  is a certain critical wave number, if the  $c_k$  are chosen to vanish for  $\ell > N$ . Hence, the Green's function has only to be modified with a finite number of terms. However, this shows a drawback of the method: the higher the frequency the more terms in the series must be included, which may lead to numerical problems if high-frequency radiation or scattering is considered.

For a numerical analysis, it can be of advantage to get an estimate about the locations of the critical frequencies appearing in a certain frequency range. In [Stupfel/Lavie/Decarpigny (1988), p. 928] it was noted that the inequalities

$$\frac{K_n}{A} \leq k_n \leq \frac{K_n}{a} \quad (35)$$

are valid, where  $K_n$  is the  $n$ -th eigenvalue of the interior Dirichlet problem 0.5.(23), 0.5.(24) for the unit sphere.  $A$  and  $a$  are the radii of spheres lying completely in the exterior  $B_e$  and the interior  $B_i$ , respectively.

### 0.5.4.5 Treatment of Singularities

The integral equations considered involve singularities, since the Green's function  $g(x, y)$  and its normal derivations become singular for  $x \rightarrow y$ . First, the surface Helmholtz integral equation contains the weekly singular monopole terms  $m_{ii}$ , Eq. 0.5.(17b). This singularity is of order  $\tilde{r}^{-1} = \|x - y\|^{-1}$  and can be removed by introducing polar coordinates. Following Everstine, [Everstine/Henderson (1990)], it is assumed that  $v$  is constant over a small circular area of radius  $b_i$  with centroid  $x_i$  so that the monopole terms 0.5.(17b) can be written as

$$m_{ii} = j\omega\rho_0 \iint_{F_i} g(x_i, y) ds(y) = j\omega\rho_0 \int_0^{2\pi} \int_0^{b_i} \frac{e^{-jk_0 r}}{4\pi r} r dr d\phi \quad (36)$$


where  $b_i$  is such that  $\pi b_i^2 = F_i$  gives the total area of the element  $F_i$  assigned to the point  $x_i$ . Hence, the following result is obtained

$$m_{ii} = j\omega\rho_0 F_i / (2\pi b_i) \quad \text{with} \quad b_i = \sqrt{F_i / \pi} . \quad (37)$$

Second, the dipole self terms  $d_{ii}$  0.5.(17a) must be evaluated. It can be shown, [Koopmann/Brenner (1982)], that for plane elements  $d_{ii} = 0$ , [Koopmann/Benner (1982)], since  $\tilde{r} \perp n$  and hence  $\partial \tilde{r} / \partial n = 0$ . If the curvature  $c_i$  of the radiating surface element is taken into account, it can be shown that approximately, [Everstine/Henderson (1990)],

$$d_{ii} = -(1 + jk_0 b_i)(c_i F_i) / (4\pi b_i) . \quad (38)$$

### 0.5.5 The Interior Problem: Sound Fields in Rooms and Half-Spaces


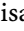

The numerical calculation of a sound field in an interior space  $B_i$  is the third standard problem of  Sect. 0.3.3. If a problem without acoustical sources in the interior  $B_i$  is considered, the application of Green's second theorem to the Helmholtz equation 0.3.(1) (see for example [Colton/Kress, Integral Equations in Scattering Theory (1983); [Skudrzyk (1971)], or [Seybert/Cheng (1987)]) leads to the interior Helmholtz integral formula

$$\iint_S \left[ p(y) \frac{\partial g(x, y)}{\partial n(y)} - \frac{\partial p(y)}{\partial n(y)} g(x, y) \right] ds = \begin{cases} 0, & x \in B_e \\ -\frac{1}{2} p(x), & x \in S \\ -p, & x \in B_i \end{cases} \quad (39a)$$

$$\iint_S \left[ p(y) \frac{\partial g(x, y)}{\partial n(y)} - \frac{\partial p(y)}{\partial n(y)} g(x, y) \right] ds = \begin{cases} -\frac{1}{2} p(x), & x \in S \end{cases} \quad (39b)$$

$$\iint_S \left[ p(y) \frac{\partial g(x, y)}{\partial n(y)} - \frac{\partial p(y)}{\partial n(y)} g(x, y) \right] ds = \begin{cases} -p, & x \in B_i \end{cases} \quad (39c)$$

for the pressure  $p$ . Again, the Green's function  $g(x, y)$  is given by Eq. 0.5.(2). The interior formula is very similar to the exterior Helmholtz integral formula 0.5.(1). Only the sign and the role of the interior and exterior space have changed. Now, the BEM can be applied to the solution of the interior problem in just the same way as described for the radiation problem (e.g. [Seybert/Cheng (1987)]). Boundary conditions for the pressure or the pressure gradient have to be inserted into the surface integral Eq. 0.5.(39b). Clearly, a radiation condition is not necessary. Discretisation of Eq. 0.5.(39b) leads to a system of equations for the determination of the second acoustic surface variable as described


in  Sects. 0.2 and 0.3. Fortunately, critical frequencies cannot occur, since the adjoint problem now is the exterior problem which does not possess any discrete eigenvalues. Hence, the regularisation procedures described in  Sect. 0.3 are not needed. However, fully interior problems are mainly the domain of the finite element method, which can deal with very general interior fluid-structure interactions problems (see  Sect. 0.6).

The BEM is well suited for the calculation of sound radiation into a half-space, [Ochmann (2000)], too. In many applications the radiator is situated on a locally reacting plane  $S_{\text{plane}}$ . Such an infinite plane can be taken into account by using a half-space Green's function

$$g_H(\mathbf{x}, \mathbf{y}) = \frac{1}{4\pi\tilde{r}} e^{-jk_0\tilde{r}} + R \frac{1}{4\pi\tilde{r}'} e^{-jk_0\tilde{r}'} \quad \text{with} \quad \tilde{r} = \|\mathbf{x} - \mathbf{y}\| \quad \text{and} \quad \tilde{r}' = \|\mathbf{x}' - \mathbf{y}\| \quad (40)$$

instead of the free-space Green's function  $g(\mathbf{x}, \mathbf{y})$  in the surface Helmholtz integral equation 0.5.(1b).

Here,  $\mathbf{x}'$  is the image point of  $\mathbf{x}$  behind the plane and  $R$  is the reflection coefficient of the plane. For a rigid plane  $R=1$  and for a free surface  $R = -1$ . For other values of  $R$ , Eq. 0.5.(40) is only an approximation.

The exact representation of the Green's function over an absorbing impedance plane is more complicated, and a detailed discussion of various formulas can be found in [Mechel (1989)]. Exact solutions and approximations are given in  Sects. D.14–D.20. In [Ochmann (2004)], the half-space Green's function above an impedance plane is formulated as a superposition of point sources which are located at complex source points (see Eq. 0.5.(42) in [Ochmann (2004)]). This Green's function is suitable for all kind of surface impedances and hence can be used as a building block for a boundary element method.

By using such half-space Green's function, one only has to extend the integration in Eq. 0.5.(1b) over the surface of the radiator  $S$ . The infinite impedance plane  $S_{\text{plane}}$  has not to be taken into account!

If the radiating body is in contact with the plane, a slightly modified version of the surface Helmholtz integral Eq. 0.5.(3a) has to be used, where the coefficient  $C(\mathbf{x})$  is now given by

$$C(\mathbf{x}) = (1 + R) \left[ 2\pi - \iint_{S_0 \cup S_c} \frac{\partial}{\partial n(\mathbf{y})} \left( \frac{1}{\tilde{r}} \right) d\mathbf{s}(\mathbf{y}) \right]. \quad (41)$$

Here  $S = S_0 \cup S_c$ , where  $S_c$  is the part of the radiator surface  $S$  that is in contact with  $S_{\text{plane}}$ . The derivation of  $C(\mathbf{x})$  and more details can be found in [Seybert/Wu (1989)]. Equation 0.5.(41) is valid for a normal pointing into the body.

The method of mirror sources for constructing the Green's function as a kernel for an appropriate integral equation can be generalized to regard additional plane boundaries around the radiating body. For example, if the vibrating structure is situated in a rectangular room, the resulting sound field can be computed by using two different representations of the Green's function for a rectangular enclosure with dimensions  $\ell_x \times \ell_y \times \ell_z$ , [Lam/Hodgson (1990)]. The first formula for the Green's function can be

constructed by mirror sources. Hence it consists of an infinite series of exponentials, and converges for small distances from the radiator.

For larger distances, the approximate Green's function

$$G_E(x, y) = \sum_{n=0}^{\infty} \frac{\Phi_n(x)\Phi_n(y)}{V\Gamma_n(k_n^2 - k_0^2 - j\tau_n)} \quad (42)$$

which is combined of the known eigenmodes of a rectangular room, [Lam/Hodgson (1990); Morse/Ingard (1968)], shows a better convergence behaviour.

The eigenfunctions are given by

$$\Phi_n(x) = \cos(k_{nx}x) \cos(k_{ny}y) \cos(k_{nz}z)$$

with

$$k_{nx} = \frac{\pi n_x}{\ell_x}, \quad k_{ny} = \frac{\pi n_y}{\ell_y}, \quad k_{nz} = \frac{\pi n_z}{\ell_z}.$$

The damping factor of the  $n$ -th mode is given by

$$\tau_n = k_0 \left[ \epsilon_{nx} \left( \frac{\beta_{xo} + \beta_{xl}}{\ell_x} \right) + \epsilon_{ny} \left( \frac{\beta_{yo} + \beta_{yl}}{\ell_y} \right) + \epsilon_{nz} \left( \frac{\beta_{zo} + \beta_{zl}}{\ell_z} \right) \right],$$

where  $\beta_{xl}$  (for example) is the specific acoustic admittance at the wall at  $x = \ell_x$ .  $\Gamma_n$  is given by  $\Gamma_n = 1 / (\epsilon_{nx}\epsilon_{ny}\epsilon_{nz})$ , where the Neumann symbol  $\epsilon_n$  is defined by

$$\epsilon_n = \begin{cases} 1, & \text{for } n = 0 \\ 2, & \text{otherwise} \end{cases}; \quad V \text{ is the volume of the room.}$$

This method seems to be superior to the FEM for complex structures in large rectangular rooms, since it only requires to divide the surface of the structure into elements, whereas the FEM has to discretise the whole interior volume of the room into finite elements.

The solution of coupled interior–exterior acoustics problems with the help of the BEM was investigated by Seybert et al. [Seybert/Cheng/Wu (1990)].

### 0.5.6 The Scattering and the Transmission Problem

As explained in ► Sect. 0.3.2, the scattering problem can be considered as an equivalent radiation problem with respect to the scattered pressure  $p_s$ . However, sometimes it is more convenient to have an explicit boundary integral equation for the total pressure  $p = p_T = p_s + p_{in}$  as the starting point for a numerical calculation. The scattered wave  $p_s$  has to fulfil the exterior Helmholtz formula 0.5.(1). The incident pressure  $p_{in}$  is assumed to have no singularities in  $B_i$ , and hence it must satisfy the interior Helmholtz formula 0.5.(39). By adding both Eqs. 0.5.(1) and 0.5.(39), one gets the Helmholtz formula

$$p_{in} + \iint_S \left[ p(y) \frac{\partial g(x, y)}{\partial n(y)} - \frac{\partial p(y)}{\partial n(y)} g(x, y) \right] ds = \begin{cases} p(x), & x \in B_e \\ \frac{1}{2} p(x), & x \in S \\ 0, & x \in B_i \end{cases} \quad (43a)$$

$$(43b)$$

$$(43c)$$

for the total pressure  $p$ . Assuming that the surface of the scatterer is rigid, the pressure gradient  $\partial p / \partial n = -j\omega\rho_0 v$  on the surface is zero. Hence, for a rigid scatterer the boundary integral equation O.5.(43b) can be written as

$$p(x) = 2 \iint_S p(y) \frac{\partial g(x, y)}{\partial n(y)} ds(y) + 2p_{in} . \quad (44)$$


For an arbitrary surface velocity distribution  $v$ , Eq. O.5.(43b), takes the form

$$p(x) = 2 \iint_S p(y) \frac{\partial g(x, y)}{\partial n(y)} ds(y) + 2 \iint_S j\omega\rho_0 v(y) g(x, y) ds(y) + 2p_i . \quad (45)$$

For the general impedance boundary value problem, the normal impedance  $Z = p/v$  is introduced at each point on the surface  $S$  of the scatterer. Substitution of the normalized impedance  $\bar{Z} = Z/(\rho_0 c_0)$  into Eq. O.5.(45) gives the boundary integral equation

$$p(x) = 2 \iint_S p(y) \frac{\partial g(x, y)}{\partial n(y)} ds(y) + 2 \iint_S \frac{j k_0}{\bar{Z}(y)} p(y) g(x, y) ds(y) + 2p_{in} \quad (46)$$

for an impedance scatterer. It should be emphasised that the local impedance  $\bar{Z}(y)$  can vary with the surface point  $y$ . Calculations for structures with varying normal surface impedance based on an iterative BE solver can be found in [Makarov/Ochmann (1998)].

The transmission problem is described in  Sect. O.3.5. The total pressure  $p_1 := p$  in the surrounding medium with constants  $c_1$  and  $\rho_1$  has to satisfy Eq. O.5.(43b) in the form

$$p_1(x) = 2 \iint_S p_1(y) \frac{\partial g_1(x, y)}{\partial n(y)} ds(y) - 2 \iint_S \frac{\partial p_1(y)}{\partial n(y)} g_1(x, y) ds(y) + 2p_{in} \quad (47)$$

with

$$g_1(x, y) = \frac{1}{4\pi\tilde{r}} e^{-jk_1\tilde{r}} \quad \text{with} \quad \tilde{r} = \|x - y\| \quad \text{and} \quad k_1 = \frac{\omega}{c_1} . \quad (48)$$

The pressure  $p_2 := p_i$  inside of the scattering body with constants  $c_2$  and  $\rho_2$  must satisfy Eq. O.5.(39b)

$$p_2(x) = -2 \iint_S p_2(y) \frac{\partial g_2(x, y)}{\partial n(y)} ds(y) + 2 \iint_S \frac{\partial p_2(y)}{\partial n(y)} g_2(x, y) ds(y) \quad (49)$$

with

$$g_2(x, y) = \frac{1}{4\pi\tilde{r}} e^{-jk_2\tilde{r}} \quad \text{with} \quad \tilde{r} = \|x - y\| \quad \text{and} \quad k_2 = \frac{\omega}{c_2} . \quad (50)$$

For  $f = g = 0$ , the transmission Conditions O.3.(23) and O.3.(24) take the form

$$p_1 = p_2 ; \quad \frac{\partial p_1}{\partial n} = \frac{1}{\varsigma} \frac{\partial p_2}{\partial n} ; \quad \varsigma = \rho_2 / \rho_1 . \quad (51, 52)$$

By introducing Eqs. O.5.(51) and O.5.(52) into Eqs. O.5.(47) and O.5.(48), two coupled integral equations are obtained

$$p_1(x) = 2 \iint_S p_1(y) \frac{\partial g_1(x, y)}{\partial n(y)} ds(y) - 2 \iint_S \frac{\partial p_1(y)}{\partial n(y)} g_1(x, y) ds(y) + 2p_{in}, \quad (53)$$

$$p_1(x) = -2 \iint_S p_1(y) \frac{\partial g_2(x, y)}{\partial n(y)} ds(y) + 2\zeta \iint_S \frac{\partial p_1(y)}{\partial n(y)} g_2(x, y) ds(y) \quad (54)$$

for the determination of the surface variables  $p_1$  and  $\partial p_1 / \partial n$ .

For equal sound velocities  $c_1 = c_2$ , the Green's functions also are equal  $g_1(x, y) = g_2(x, y)$ , and one single integral equation can be derived by combining Eqs. O.5.(53) and O.5.(54) in a suitable way

$$p_1(x) = \frac{2(\zeta - 1)}{\zeta + 1} \iint_S p_1(y) \frac{\partial g_1(x, y)}{\partial n(y)} ds(y) + 2 \frac{\zeta}{\zeta + 1} p_{in}. \quad (55)$$

The as yet unpublished boundary integral Eq. O.5.(55) was derived by S. Makarov (Worcester Polytechnic Institute, MA, USA) and communicated to the author.

For  $\zeta \rightarrow \infty$ , i.e.  $\rho_2 \gg \rho_1$ , the integral Eq. O.5.(44) for the rigid scatterer is obtained as expected for physical reasons.

Additional recent formulations and numerical implementations of the BEM can be found in the book [Estorff (2000)].

## **O.6 The Finite Element Method (FEM)**

### **O.6.1 Introduction**

The finite element method (FEM) is especially suited for the numerical calculation of sound fields in irregularly formed inner spaces, since such spaces are of finite dimensions. Originally, the FEM was developed for predicting the static or dynamical response of structures under certain loads in mechanical engineering. Several high-developed FEM packages exist which are commercially available. Some of these programs contain modules for acoustical computations. In principle, acoustical calculations can be directly performed with programs which were originally developed for structural computations, since a mechanical analogy for fluid motion can be used, [Gockel (1983)]. Consider the acoustical wave equation for the pressure with spatial varying fluid density  $\rho$  in Cartesian coordinates

$$\frac{\partial}{\partial x} \left( \frac{1}{\rho} \frac{\partial p}{\partial x} \right) + \frac{\partial}{\partial y} \left( \frac{1}{\rho} \frac{\partial p}{\partial y} \right) + \frac{\partial}{\partial z} \left( \frac{1}{\rho} \frac{\partial p}{\partial z} \right) = \frac{1}{\chi} \frac{\partial^2 p}{\partial t^2}, \quad (1)$$

where  $\chi = \rho c^2$  is the bulk modulus, and the equation for the equilibrium of stresses in a particular fixed direction  $x$

$$\frac{\partial \sigma_{xx}}{\partial x} + \frac{\partial \tau_{xy}}{\partial y} + \frac{\partial \tau_{xz}}{\partial z} = \rho_s \frac{\partial^2 u_x}{\partial t^2}, \quad (2)$$



where  $u_x$  is the structural displacement in the  $x$  direction,  $\sigma_{xx}$ ,  $\tau_{xy}$ ,  $\tau_{xz}$  are stress components, and  $\rho_s$  is the structural mass density. The acoustic-structural analogy can be established by comparing Eqs. O.6.(1) and O.6.(2) and taking

$$u_x = p; \quad \rho_s = 1/\chi,$$

$$\sigma_{xx} = \frac{1}{\rho} \frac{\partial p}{\partial x} = -\frac{\partial^2 w_x}{\partial t^2},$$

$$\tau_{xy} = \frac{1}{\rho} \frac{\partial p}{\partial y} = -\frac{\partial^2 w_y}{\partial t^2},$$

$$\tau_{xz} = \frac{1}{\rho} \frac{\partial p}{\partial z} = -\frac{\partial^2 w_z}{\partial t^2}.$$

Here, the acoustic equilibrium equation

$$\nabla p + \rho \frac{\partial^2 \vec{w}}{\partial t^2} = 0 \quad (3)$$

was taken into account, where  $\vec{w}$  is the particle displacement within the fluid. For completing the analogy, the structural displacement components  $u_y$  and  $u_z$  must be set equal to zero and the general stress-strain relationship must be modified in a suitable way (details can be found in [Gockel (1983)]). Hence, all the tools of classical FEM programs such as the variety of element types, solution methods etc. are available for the acoustical analysis, too.

Typical areas of application of the acoustical FEM are sound fields in small rooms at low frequencies as mentioned in ► Sect. O.3.3 where aspects of wave propagation play an essential role. Also, all problems involving fluid-structure interaction are treated by the FEM with preference.

At first, the principle of FEM will be explained for the simple example of an air-filled enclosure with rigid boundaries. Afterwards, more advanced applications will be shortly discussed.

## O.6.2 The Sound Field in Irregular Shaped Cavities with Rigid Walls

This problem belongs to the standard problems described in ► Sect. O.3.3, where the notation is explained. The Helmholtz equation O.3.(1) has to be satisfied in the interior  $B_i$  of the cavity. The whole boundary  $S$  is assumed to be rigid with  $\partial p / \partial n = 0$ . For simplicity, only the two-dimensional case is considered. Since no acoustical sources are specified, the eigenmodes and eigenfrequencies of the cavity are quantities which should be calculated. Following the presentation given in [Schwarz (1980)], the starting point of the FEM calculation is a variational principle for the Helmholtz equation, which must be minimized. In the present case, the functional [Gladwell/Zimmermann (1966); Petyt (1982); Petyt (1983)]

$$L = \frac{1}{2} \iint_B [(\text{grad } p)^2 - k_0^2 p^2] dv \quad (4)$$

must be minimised, where the integral has to be extended over the volume (or area in two dimensions)  $B$ , and the gradient is denoted by  $\text{grad}$ . The functional  $L$  can be interpreted as a Lagrange function, i.e. as the difference between kinetic and potential energy of the vibrating fluid. Hence, the minimisation of  $L$  corresponds to Hamilton's principle. Therefore, the Helmholtz equation is the Euler-Lagrange equation of the functional O.6.(4). The rigid boundary conditions are so-called natural boundary conditions and will be automatically satisfied.

The second step consists in dividing the cavity  $B$  into simple elements. In the following, only triangular elements are used. It is important to note that the process of triangularization should be adapted to the particular problem. This means, for example, that parts of the area, in which the solution changes more rapidly, should be modelled with more and smaller elements than other parts, where the change of the solution is slower. In addition, the triangular elements should not have too acute angles. Such requirements will be checked automatically in most commercial FE programs. If  $B$  is divided into  $N$  triangular elements  $E_n$ , the discretized functional is given by:

$$L_D = \frac{1}{2} \sum_{n=1}^N \iint_{E_n} [(\text{grad } p)^2 - k_0^2 p^2] dv. \quad (5)$$

The third step is to choose approximate functions for the sound pressure at each single element. Frequently, polynomials are used satisfying certain continuity conditions between adjacent elements. For fulfilling such continuity conditions in selected points of the element, named nodal points or nodes, the approximate function  $p^{(e)}$  for the  $e$ -th element is represented by:

$$p^{(e)}(x, y) = \sum_{k=1}^{K_e} p_k^{(e)} N_k^{(e)}(x, y) = P^{(e)T} N^{(e)}(x, y), \quad (6)$$

where the so-called nodal variables  $p_k^{(e)}$  are the sound pressure values in the nodes (for example, in the three corner points ( $K_e = 3$ ) of the triangular element), and the  $N_k^{(e)}$  are the shape functions. Moreover, the vectors

$$P^{(e)T} = (p_1^{(e)}, p_2^{(e)}, \dots, p_{K_e}^{(e)}), \quad (7a)$$

$$N^{(e)T}(x, y) = (N_1^{(e)}, N_2^{(e)}, \dots, N_{K_e}^{(e)}) \quad (7b)$$

were introduced, where the superscript  $T$  denotes transposition. The shape functions have to satisfy the interpolation property

$$N_i^{(e)}(x_k^{(e)}, y_k^{(e)}) = \begin{cases} 1 & \text{for } i = k \\ 0 & \text{for } i \neq k \end{cases} \quad (8)$$

in the nodal points  $Q_i^{(e)} = (x_i^{(e)}, y_i^{(e)})$  of the  $e$ -th element. The global representation of pressure  $p$  in the whole area  $B$  is composed of all element pressures  $p^{(e)}$ . By numbering all nodes lying in  $B$  from 1 to  $K$  successively, one obtains:

$$p(x, y) = \sum_{k=1}^K p_k N_k(x, y), \quad (9)$$

where the so-called global shape functions  $N_k(x, y)$  consist of the union of all element shape functions  $N_k^{(e)}(x, y)$  which possess the value 1 at the nodal point  $Q_k$ . It follows from O.6.(8) that the global shape functions are different from zero only in a small part of  $B$ , i.e. they are functions with local support, which is a key property of the FEM.

For example, if the linear substitution

$$p(x, y) = c_1 + c_2x + c_3y \quad (10)$$

is used in the unit triangle, the shape functions

$$N_1(x, y) = 1 - x - y; \quad N_2(x, y) = x; \quad N_3(x, y) = y \quad (11)$$

are obtained (see [Schwarz (1980), p. 90]).

The fourth step is to introduce the approximation O.6.(9) into the discretized functional O.6.(5). The integrals have to be performed element by element and can be solved analytically for polynomial shape functions. For a given triangle  $T_n$  with nodes  $Q_k(x_k, y_k)$ ,  $k = 1, 2, 3$  and the linear substitution O.6.(10) the following results are obtained (see [Schwarz (1980), p. 71]):

$$\iint_{T_n} \left[ \left( \frac{\partial p}{\partial x} \right)^2 + \left( \frac{\partial p}{\partial y} \right)^2 \right] dx dy = P^{(e)T} S_e P^{(e)}, \quad (12)$$

$$\iint_{T_n} p^2 dx dy = P^{(e)T} M_e P^{(e)}, \quad (13)$$

where the stiffness matrix  $S_e$  and the mass matrix  $M_e$  are composed of the four basis matrices

$$S_1 = \frac{1}{2} \begin{pmatrix} 1 & -1 & 0 \\ -1 & 1 & 0 \\ 0 & 0 & 0 \end{pmatrix}; \quad S_2 = \frac{1}{2} \begin{pmatrix} 2 & -1 & -1 \\ -1 & 0 & 1 \\ -1 & 1 & 0 \end{pmatrix}; \quad (14)$$

$$S_3 = \frac{1}{2} \begin{pmatrix} 1 & 0 & -1 \\ 0 & 0 & 0 \\ -1 & 0 & 1 \end{pmatrix}; \quad S_4 = \frac{1}{24} \begin{pmatrix} 2 & 1 & 1 \\ 1 & 2 & 1 \\ 1 & 1 & 2 \end{pmatrix}$$

in the following way

$$S_e = aS_1 + bS_2 + cS_3 \quad \text{and} \quad M_e = JS_4, \quad (15)$$

where the constants

$$a = \left[ (x_3 - x_1)^2 + (y_3 - y_1)^2 \right] / J, \quad (16a)$$

$$b = - \left[ (x_3 - x_1)(x_2 - x_1) + (y_3 - y_1)(y_2 - y_1) \right] / J, \quad (16b)$$

$$c = \left[ (x_2 - x_1)^2 + (y_2 - y_1)^2 \right] / J, \quad (16c)$$



$$J = (x_2 - x_1)(y_3 - y_1) - (x_3 - x_1)(y_2 - y_1) \quad (16d)$$

only depend on the geometry of the triangle considered.

Hence, the contribution of a single triangular element to the whole functional is given by:

$$L_D^{(e)} = \frac{1}{2} P^{(e)T} S_e P^{(e)} - \frac{1}{2} k_0^2 P^{(e)T} M_e P^{(e)}. \quad (17)$$

Summing up all contributions element by element leads to the discretized global functional of quadratic form:

$$L_D = \frac{1}{2} P^T S P - \frac{1}{2} k_0^2 P^T M P, \quad (18)$$

where  $P$  is the vector of all nodal pressure variables.  $S$  and  $M$  are the global stiffness and mass matrix, respectively. The requirement that  $L_D$  takes a minimum leads to the equation:

$$S P = k_0^2 M P, \quad (19)$$

which is a generalised eigenvalue problem for the eigenvalue parameter  $\lambda = k_0^2$ . Such a problem was solved in [Schwarz (1980)] with three different numerical methods for an idealised automobile passenger compartment. For this specific example, it was shown that the simultaneous inverse vector iteration was the most efficient method. Details about numerical methods for solving the generalised eigenvalue problem can be found in [Schwarz (1980)].

A great advantage of the FEM is the fact that the global matrices  $S$  and  $M$  are symmetric and weakly populated, in contrast to the BEM. By using optimal numbering procedures such as the algorithms of Rosen or Cuthill-McKee (see [Schwarz (1980)]) for the nodal variables, the bandwidth of such sparse matrices can be minimised which leads to a large reduction of computer time and storage capacity.

### 0.6.3 Supplementary Aspects and Fluid-Structure Coupling


The simple model problem of a rigid two-dimensional cavity, which is discretised with triangular elements, can be extended into different directions. For example, elements or shape functions of higher orders can be used. Also, the generalization to the three-dimensional case can be easily done. Especially, the sound field in enclosures and automobile passenger compartment was investigated by several authors: Craggs [Craggs (1972)] used tetrahedral and cuboid finite elements with a linear variation of the pressure between the nodes in order to find the eigenfrequencies and modes of a three-dimensional enclosure. Shuku and Ishihara [Shuku/Ishihara (1973)] used triangular elements with cubic polynomial functions for the pressure. Petyt et al. [Petyt/Lea/Koopmann (1976)] developed a twenty-node, isoparametric acoustic finite element for analysing the acoustics modes of irregular shaped cavities. Richards and Jha [Richards/Jha (1979)] preferred quadratic triangular elements with six nodes.


If only the part  $S_0$  of the surface  $S$  is rigid, whereas the normal velocity  $v$  is prescribed on  $S_1$  and an absorbing material with impedance  $Z$  is specified on  $S_2$ , the following boundary conditions are obtained:

$$\frac{\partial p}{\partial n} = 0 \quad \text{on } S_0; \quad \frac{\partial p}{\partial n} = -j\omega \rho_0 v \quad \text{on } S_1; \quad \frac{\partial p}{\partial n} = -j\omega \rho_0 \frac{p}{Z} \quad \text{on } S_2. \quad (20)$$

Instead of Eq. O.6.(4) the corresponding variational principle is now given by [Petyt (1983)]:

$$L = \frac{1}{2} \iiint_B [(\text{grad } p)^2 - k_0^2 p^2] dv + \int_{S_1} j\omega \rho_0 p v ds + \frac{1}{2} \iint_{S_2} j\omega \rho_0 \frac{p^2}{Z} ds, \quad (21)$$


which is minimised according to the same rules as described in  Sect. O.1. The resulting system of equations can be used for the investigation of passenger compartments or silencers which are partially lined with absorbing material (see [Petyt (1983)] and [Munjaj (1987)], where more references can be found). In Eq. O.6.(21), the three-dimensional case is considered, and hence the first integral is extended about the volume  $B$ . In [Schulze Hobbeling (1989)], wave propagation within the porous absorber is taken into account.

The coupled fluid-structure interaction problem is described in  Sect. O.3.4 as the fourth standard problem. A mathematically rigorous description of the corresponding finite dimension approximation, which can be associated with a finite element mesh, is given by Soize [Soize, Eur.J. Mech. A/Solids (1998); Soize, J. Acoust. Soc. Amer. (1998); Soize (1999)]. Instead, the method of Everstine and Henderson [Everstine/Henderson (1990)] will be described here, which is based on a coupled FE/BE approach. A very similar formulation was given by Smith, Hunt, and Barach [Smith/Hunt/Barach (1973)]. The structure is assumed to be modeled with finite elements. This leads to a matrix equation of motion for the structural degrees of freedom:

$$Z_s V_s = F_s - G A_s P, \quad (22)$$

where  $Z_s$  is the structural impedance matrix,  $V_s$  is the global velocity vector,  $F_s$  is the vector of mechanical forces applied to the structure,  $G$  is a transformation matrix in order to transform a vector of outward normal forces at the so-called wet points (which are in contact with the fluid) to a vector of forces at all points in the selected coordinate system,  $A_s$  is the diagonal matrix of areas for the wet surface, and  $P$  is the vector of total acoustic pressures. Equation O.6.(22) can be derived in a similar way as described in the last section for the acoustical case. The structural impedance matrix  $Z_s$  is given by:

$$Z_s = \frac{1}{j\omega} (-\omega^2 M_s + j\omega D_s + K_s), \quad (23)$$

where  $M_s$ ,  $D_s$  and  $K_s$  are the structural mass, damping and stiffness matrices, respectively. The integral equation of the scattering problem for an incident pressure wave  $p_i$  was derived in  Sect. O.5.6 and is given by (see Eq. O.5.(45)):

$$p(x) = 2 \iint_S p(y) \frac{\partial g(x, y)}{\partial n(y)} ds(y) + 2 \iint_S j\omega \rho_0 v(y) g(x, y) ds(y) + 2p_i. \quad (24)$$

Corresponding to the BE approach described by Eqs. O.5.(16)–O.5.(18), the discretised version of the integral equation O.6.(24) is

$$-AP = MV + P_i \quad \text{with} \quad A := D - 0.5I, \quad (25)$$

where  $P_i$  is the vector of incident pressures,  $V$  is the vector of normal velocities, and  $D$  and  $M$  are the dipole and monopole matrices, respectively, defined in Eqs. O.5.(17). According to Everstine and Henderson [Everstine/Henderson (1990)] the vector of normal velocities  $V$  is transformed into the vector  $V_s$  of total structural velocities by applying the transposed matrix  $G^T$  to  $V_s$ :

$$V = G^T V_s. \quad (26)$$

Now, by combining Eqs. O.6.(22), O.6.(25), and O.6.(26), the velocity vectors  $V$  and  $V_s$  can be eliminated, which leads to the coupled fluid–structure equation

$$HP = Q + P_i \quad (27)$$

with

$$H := -A + MG^T Z_s^{-1} G A_s \quad \text{and} \quad Q = MG^T Z_s^{-1} F_s. \quad (28, 29)$$

Having solved system O.6.(27) for the pressure  $P$ , the vector  $V_s$  of structural velocities is obtained from Eq. O.6.(22) by solving the equation

$$V_s = Z_s^{-1} F_s - Z_s^{-1} G A_s P. \quad (30)$$

With the knowledge of the fluid surface variables  $P$  and  $V$  all acoustics quantities in the exterior field can be calculated by evaluating the exterior Helmholtz formula O.5.(43a).

In [Hunt/Knittel/Barach (1974); Kirsch/Monk (1990); Masmoudi (1987)], a combined finite element and spectral approach is proposed: the FEM is used for calculating the vibration of the elastic structure and the acoustic field inside of a finite fluid sphere which totally surrounds the vibrating structure. At the boundary of the sphere, a perfect absorption condition is given explicitly in terms of the spherical wave functions O.4.(5). This method was generalised and implemented into the structural analysis code NAS-TRAN resulting in a commercially available FEM package. Some recent results of this technique can be found in [Zimmer/Ochmann/Holzheuer (2001)].

Another interesting idea is to use absorbing boundary condition operators [Gan/Levin/Ludwig(1993)] on the artificial boundary of the finite domain instead of coupling with analytical wave functions. The perfect absorbing boundary condition is modeled by the so-called BGT operator named after Bayliss, Gunzburger and Turkel [Bayliss/Gunzburger/Turkel (1982)]. The first-order operator  $B_1$  is defined by:

$$B_1 p := \left( \frac{\partial}{\partial R} + jk_0 + \frac{1}{2R} \right) p, \quad (31)$$

where  $p$  is the radiated sound pressure.  $R$  and  $k_0$  are defined as in the Sommerfeld radiation condition O.3.(3) which is approximated with increasing accuracy for increasing order of the BGT operator. The second operator  $B_2$  is given by:

$$B_2 p := \left( \frac{\partial}{\partial R} + jk_0 + \frac{5}{2R} \right) \left( \frac{\partial}{\partial R} + jk_0 + \frac{1}{2R} \right) p, \quad (32)$$

and, in general, the  $m$ -th order operator can be introduced by [Bayliss/Gunzburger/Turkel (1982), Gan/Levin/Ludwig(1993)]:

$$B_m := \prod_{\ell=1}^m \left( \frac{\partial}{\partial R} + \frac{2\ell - \frac{3}{2}}{R} + jk_0 \right). \quad (33)$$

It can be shown [Bayliss/Gunzburger/Turkel (1982), Gan/Levin/Ludwig(1993)] that the operator  $B_m$  annihilates terms in  $1/r$  of the asymptotic far field solution  $p_s$

$$p_s = \frac{e^{-jk_0 R}}{\sqrt{R}} \left( a_0 + \frac{a_1(\varphi)}{R} + \frac{a_2(\varphi)}{R^2} + \dots \right) \quad (34)$$


such that the accuracy in approximating the radiation condition is

$$B_m p_s = O \left( \frac{1}{r^{2m+1+1/2}} \right). \quad (35)$$

Here,  $a_0$  is a constant, and  $a_1(\varphi)$ ,  $a_2(\varphi)$ , ... are functions of the polar angle  $\varphi$ . These formulas are given for the two-dimensional case. The incorporation into a finite element model is described in [Gan/Levin/Ludwig(1993)].

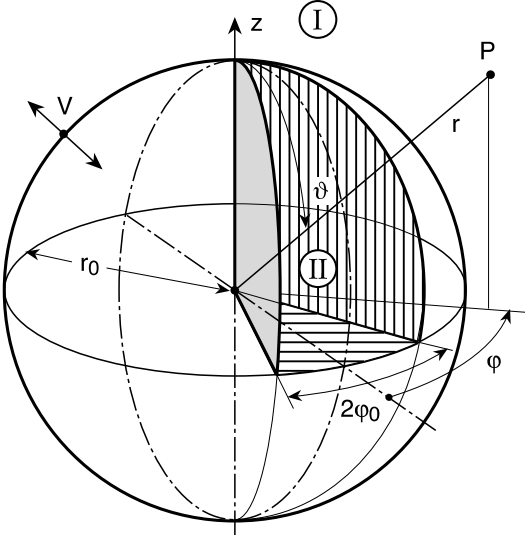
Some more special examples from the huge number of papers dealing with the application of the FEM to acoustical problems should be mentioned: The formulation of the FEM for cavities with fluid-structure interaction can be found in [Nefske/Wolf JR/Howell (1982); Soize (1999)], for example. The sound transmission between enclosures using plate and acoustic finite elements is studied in [Craggs/Stead (1976)]. A comparison between FEM and BEM for the calculation of sound fields is performed in [Becker/Waller (1986)].

## 0.7 The Cat's Eye Model

Many variations and improvements of numerical methods are studied in the literature. It is helpful to have benchmark models available for which analytical solutions are known, and which are not over-simplified, so that comparisons between different variants of numerical methods can be performed. One favourite benchmark model is the Cat's Eye model for which the analytical solution of the sound field will be described in this Section. An other model, with somewhat more simple geometry is the "Orange" model which will be described in  Sect. 0.8. Both Sections treat the radiation problem for the special case of a modal surface velocity pattern of the sphere (radiation problem). It will be explained at the end of this Section, how multi-mode radiation problems and scattering problems can be treated.

### 0.7.1 Cat's Eye Model and General Fundamental Solutions<sup>\*)</sup>

The Cat's Eye model is a sphere with one octant of the sphere taken away.



An octant with cuts at  $\varphi = \pm\varphi_0$ ;  $\vartheta = \pi/2$  is taken away of a sphere with radius  $r_0$ . The walls of the cuts are hard.

The remainder of the spherical surface oscillates with a velocity pattern of a spherical mode  $m_0, n_0$ . Radiation problems with a more general vibration pattern and scattering problems can be reduced to a repeated solution of the single-mode radiation problem.

Target quantities are :

- the sound field in the outer zone (I);
- the sound field in the inner zone (II).

A spherical co-ordinate system  $r, \vartheta, \varphi$  is used, with the co-ordinate axis  $\varphi = 0$  in the middle of the sector. A common time factor  $e^{j\omega t}$  is dropped. The particle velocity of a sound pressure field  $p$  is given by:

$$\mathbf{v} = \frac{j}{k_0 Z_0} \text{grad } p, \quad (1)$$

$$v_r = \frac{j}{k_0 Z_0} \frac{\partial p}{\partial r}; \quad v_\vartheta = \frac{j}{k_0 Z_0} \frac{1}{r} \frac{\partial p}{\partial \vartheta}; \quad v_\varphi = \frac{j}{k_0 Z_0} \frac{1}{r \sin \vartheta} \frac{\partial p}{\partial \varphi} \xrightarrow{\vartheta \rightarrow \pi/2} \frac{j}{k_0 Z_0} \frac{1}{r} \frac{\partial p}{\partial \varphi}.$$

The wave equation separates in spherical co-ordinates, therefore the fundamental solutions can be written as a product:

$$p(r, \vartheta, \varphi) = R(k_0 r) \cdot \Theta(\vartheta) \cdot \Phi(\varphi), \quad (2)$$

<sup>\*)</sup> See Preface to the 2<sup>nd</sup> edition.



in which the factors are linear combinations of elementary solutions:

$$\begin{aligned} R(k_0 r) &= A \cdot \mathfrak{R}_v^{(1)}(k_0 r) + B \cdot \mathfrak{R}_v^{(2)}(k_0 r), \\ \Theta(\vartheta) &= a \cdot P_v^H(\cos \vartheta) + b \cdot Q_v^H(\cos \vartheta), \\ \Phi(\varphi) &= \alpha \cdot \sin(\mu \varphi) + \beta \cdot \cos(\mu \varphi). \end{aligned} \quad (3)$$

Therein are:

$$\begin{aligned} \mathfrak{R}_v^{(i)}(k_0 r) & \quad 2 \text{ linear independent spherical Bessel functions;} \\ P_v^H(x); \quad Q_v^H(x) & \quad \text{Legendre functions of the first and second kind, with } x = \cos \vartheta. \end{aligned}$$

To simplify the formulations, we suppose the excitation to be symmetrical relative to  $\varphi = 0$ ; i.e., we suppose  $\Phi(\varphi) = \cos(\mu \varphi)$ .

*Outer field in (I):*

From Sommerfeld's condition follows:

$$\mathfrak{R}_v(k_0 r) = h_v^{(2)}(k_0 r)$$

(spherical Hankel function of second kind). The  $Q_v^H(z)$  have logarithmic singularities at  $z = \pm 1$ , i.e., at  $\vartheta = 0, \vartheta = \pi$ ; the sound field should be regular there, consequently the  $Q_v^H(z)$  are dropped. The outer field is periodic in  $\vartheta, \varphi$  with a period  $2\pi$ ; consequently the  $v, \mu = n, m = 0, 1, 2, \dots$  are integer numbers.

Thus the field in (I) can be formulated as a mode sum:

$$p^{(I)}(r, \vartheta, \varphi) = \sum_{n, m \geq 0} a_{n, m} \cdot h_n^{(2)}(k_0 r) \cdot P_n^m(\cos \vartheta) \cdot \cos(m \varphi), \quad (4a)$$

$$Z_0 v_r^{(I)}(r, \vartheta, \varphi) = j \sum_{n, m \geq 0} a_{n, m} \cdot h_n^{\prime(2)}(k_0 r) \cdot P_n^m(\cos \vartheta) \cdot \cos(m \varphi) \quad (4b)$$

(a prime indicates the derivative with respect to the argument).

$$\text{To be noticed:} \quad P_n^m(\cos \vartheta) = 0 \quad \text{for} \quad m > n, \quad (5)$$

$$\text{which follows from:} \quad P_n^m(x) = (-1)^m (1 - x^2)^{m/2} \frac{d^m P_n(x)}{dx^m} \quad (6)$$

for  $m, n = \text{integers}$ , with Legendre polynomials of  $n$ -th degree  $P_n(x)$ ; i.e.,  $m > n$  is excluded.

The strength of the excitation by the modal pattern with indices  $n_0, m_0$  either can be described by a sound pressure amplitude  $P_e$  or by the particle velocity  $V$  at the surface of the sphere. They are interrelated by:

$$\begin{aligned} Z_0 v_{er}(r_0, \vartheta, \varphi) &= j P_e \cdot h_{n_0}^{\prime(2)}(k_0 r_0) \cdot P_{n_0}^{m_0}(\cos \vartheta) \cdot \cos(m_0 \varphi) \\ &:= Z_0 V \cdot P_{n_0}^{m_0}(\cos \vartheta) \cdot \cos(m_0 \varphi), \end{aligned} \quad (7a)$$

whence the reference velocity  $V$  follows as:

$$Z_0 V = j P_e \cdot h_{n_0}^{\prime(2)}(k_0 r_0). \quad (7b)$$

Another kind of reference is the sound pressure which a full sphere with the exciting mode  $n_0, m_0$  would produce in the field point  $P = (r, \vartheta, \varphi)$ :

$$\begin{aligned} p_{\text{ref}}(r, \vartheta, \varphi) &= P_e \cdot h_{n_0}^{(2)}(k_0 r) \cdot P_{n_0}^{m_0}(\cos \vartheta) \cdot \cos(m_0 \varphi) \\ &= -jZ_0 V \frac{h_{n_0}^{(2)}(k_0 r)}{h_{n_0}^{(2)}(k_0 r_0)} \cdot P_{n_0}^{m_0}(\cos \vartheta) \cdot \cos(m_0 \varphi). \end{aligned} \quad (7c)$$

*Interior field in (II):*

From regularity at  $r = 0$ :

$$\Re_v(k_0 r) = j_v(k_0 r) \quad (8)$$

with spherical Bessel functions.

$$\text{From symmetry in } \varphi: \quad \Phi(\varphi) = \cos(\mu \varphi). \quad (9)$$

Regularity at  $\vartheta = 0$  again excludes the  $Q_v^\mu(z)$ .

The condition  $v_\varphi \xrightarrow{\varphi \rightarrow \pm \varphi_0} 0$  has the consequence:

$$\sin(\mu \varphi_0) \stackrel{!}{=} 0 \quad \Rightarrow \quad \mu \varphi_0 = m\pi; \quad m = 0, 1, 2, \dots \quad \Rightarrow \quad \mu = \frac{m\pi}{\varphi_0} \xrightarrow{\varphi_0 \rightarrow \pi/4} 4m. \quad (10)$$

The angle  $\varphi_0$  is restricted henceforth to an integer part of  $\pi$ ,  $\varphi_0 = \pi/N$ ;  $N = 2, 3, 4, \dots$ , from which condition follows:

$$\mu = m \cdot N. \quad (11)$$

The condition  $v_\vartheta \xrightarrow{\vartheta \rightarrow \pi/2} 0$  implies:

$$\Theta'(\vartheta) \Big|_{\vartheta=\pi/2} \sim P_v^\mu(0) \stackrel{!}{=} 0, \quad (12)$$

from which, with the relation

$$P_v^\mu(0) = \frac{2^{\mu+1}}{\sqrt{\pi}} \sin((v+\mu)\pi/2) \frac{\Gamma(v/2 + \mu/2 + 1)}{\Gamma(v/2 - \mu/2 + 1/2)} \quad (13)$$

follows:

$$\sin((v+\mu)\pi/2) \stackrel{!}{=} 0. \quad (14)$$

This is satisfied for integer  $\mu$  with

$$v = \text{integer}; \quad \mu + v \stackrel{!}{=} \text{even}. \quad (15)$$

Thus the sum of the mode indices in (II) must be an even number,  $v + \mu = \text{even}$ , i. e.,  $v, \mu$  both are either even or odd.

The relation

$$P_v^\mu(-x) = P_v^\mu(x) \cdot \cos((v+\mu)\pi) - \frac{2}{\pi} \sin((v+\mu)\pi) \cdot Q_v^\mu(z) \xrightarrow{v+\mu=\text{even}} P_v^\mu(x) \quad (16)$$

guarantees, because of  $v + \mu = \text{even}$ , a sound field in (II) which is symmetrical relative to the hard cut at  $\vartheta = \pi/2$ .

One consequently has the following sound field formulation in the interior zone (II) which satisfies the conditions of regularity and the boundary conditions at the hard walls of the cut:

$$p^{(II)}(r, \varphi, \vartheta) = \sum_{v, \mu} b_{v, \mu} \cdot j_v(k_0 r) \cdot P_v^\mu(\cos \vartheta) \cdot \cos(\mu \varphi); \quad (17a)$$

$$v = 0, 1, 2, \dots; \quad \mu = \eta \cdot N; \quad \eta = 0, 1, 2, \dots; \quad \mu + v \stackrel{!}{=} \text{even};$$

$$Z_0 v_r^{(II)}(r, \varphi, \vartheta) = j \sum_{v, \mu} b_{v, \mu} \cdot j'_v(k_0 r) \cdot P_v^\mu(\cos \vartheta) \cdot \cos(\mu \varphi). \quad (17b)$$

### 0.7.2 Mode Orthogonality

Because of symmetry in  $\varphi$  only the range  $0 \leq \varphi \leq \pi$  must be considered.

*In  $\varphi$  direction:*

In the outer zone (I):

$$\begin{aligned} \frac{1}{\pi} \int_0^\pi \cos(m\varphi) \cdot \cos(m'\varphi) d\varphi &= \frac{1}{2} \left[ \frac{\sin((m+m')\pi)}{(m+m')\pi} + \frac{\sin((m-m')\pi)}{(m-m')\pi} \right] \\ &= \begin{cases} 1; & m = m' = 0 \\ 1/2; & m = m' \neq 0 \\ 0; & m \neq m' \end{cases} = \frac{\delta_{m, m'}}{\delta_m} \end{aligned} \quad (18a)$$

with Kronecker's symbol  $\delta_{n, m} = 0; n \neq m; \delta_{n, m} = 1; n = m$  and Heaviside's symbol  $\delta_{n=0} = 1; \delta_{n \neq 0} = 2$ .

In the interior zone (II), where  $\mu\varphi_0 = m\pi; \mu'\varphi_0 = m'\pi$  the orthogonality integral holds:

$$\begin{aligned} \frac{1}{\varphi_0} \int_0^{\varphi_0} \cos(\mu\varphi) \cdot \cos(\mu'\varphi) d\varphi &= \frac{1}{2} \left[ \frac{\sin((\mu+\mu')\varphi_0)}{(\mu+\mu')\varphi_0} + \frac{\sin((\mu-\mu')\varphi_0)}{(\mu-\mu')\varphi_0} \right] \\ &= \frac{1}{2} \left[ \frac{\sin((m+m')\pi)}{(m+m')\pi} + \frac{\sin((m-m')\pi)}{(m-m')\pi} \right] = \frac{\delta_{m, m'}}{\delta_m}. \end{aligned} \quad (18b)$$

The orthogonality in  $\vartheta$ -direction in the outer zone (I) is a consequence of:

$$\int_{-1}^1 P_v^\mu(x) \cdot P_{v'}^\mu(x) dx = \begin{cases} 0; & v \neq v' \\ N_v^\mu; & v = v' \end{cases} = \delta_{v, v'} N_v^\mu; \quad v, v', \mu = \text{integer} \quad (19)$$

with the norms:

$$N_k^i = \int_{-1}^1 (P_k^i(x))^2 dx = \frac{2(k+i)!}{(2k+1)(k-i)!}. \quad (20)$$

In the interior zone (II) is  $v + \mu = \text{even}$ ; the Legendre functions are symmetrical with respect to  $x = 0$ ; therefore the orthogonality 0.7.(19) also holds in (II) over  $x = (0, 1)$ , i. e.,  $\vartheta = (0, \pi/2)$  with a halved value of the norm.

### 0.7.3 Remaining Boundary Conditions

One is left, after the above preparations, with two sets of unknown mode amplitudes  $a_{n,m}$ ,  $b_{v,\mu}$  and has for their determination two boundary conditions of field matching:

$$p^{(II)}(r_0, \vartheta, \varphi) \stackrel{!}{=} p^{(I)}(r_0, \vartheta, \varphi) \quad \text{in} \quad \vartheta = (0, \pi/2) \text{ \& } \varphi = (-\varphi_0, +\varphi_0), \quad (21)$$

$$Z_0 v_r^{(II)}(r_0, \vartheta, \varphi) \stackrel{!}{=} \begin{cases} Z_0 v_r^{(II)}(r_0, \vartheta, \varphi) & \text{in} \quad \vartheta = (0, \pi/2) \text{ \& } \varphi = (-\varphi_0, +\varphi_0), \\ Z_0 v_{er}(r_0, \vartheta, \varphi) & \text{in} \quad \text{rest of the sphere.} \end{cases} \quad (22)$$

One uses in 0.7.(21) the mode orthogonality in (II) and in 0.7.(22) the mode orthogonality in (I). In doing that, one multiplies both sides of the matching conditions at the zone limit with a mode of the relevant zone with arbitrary but fixed mode indices  $v, \mu$  or  $n, m$ , respectively, and integrates over the range of orthogonality which agrees with the range of definition of the boundary condition. One will obtain two linear systems of equations for the  $a_{n,m}$ ,  $b_{v,\mu}$ ; after their solution the sound fields will be determined.

Beginning with the matching condition 0.7.(21) for the *sound pressures* to each other, with:

$$p^{(II)}(r, \varphi, \vartheta) = \sum_{v,\mu} b_{v,\mu} \cdot j_v(k_0 r) \cdot P_v^\mu(\cos \vartheta) \cdot \cos(\mu \varphi),$$

$$p^{(I)}(r, \vartheta, \varphi) = \sum_{n,m \geq 0} a_{n,m} \cdot h_n^{(2)}(k_0 r) \cdot P_n^m(\cos \vartheta) \cdot \cos(m \varphi)$$

apply on both sides the integral

$$\frac{1}{\varphi_0} \int_0^{\varphi_0} d\varphi \int_0^1 \dots \cdot P_\kappa^l(x) \cdot \cos(\imath \varphi) \, dx$$

with  $\imath, \kappa$  from the range of values of  $\mu, v$ . This will give on the left-hand side:

$$\begin{aligned} \sum_{v,\mu} b_{v,\mu} \cdot \frac{\delta_{\mu,\imath}}{\delta_\imath} \cdot j_v(k_0 r_0) \int_0^1 P_v^\mu(x) \cdot P_\kappa^\imath(x) \, dx \\ = \sum_v b_{v,\imath} \cdot \frac{j_v(k_0 r_0)}{\delta_\imath} \int_0^1 P_v^\imath(x) \cdot P_\kappa^\imath(x) \, dx = \frac{N_\kappa^\imath}{2\delta_\imath} \cdot b_{\kappa,\imath} \cdot j_\kappa(k_0 r_0), \end{aligned} \quad (23a)$$

and on the right-hand side:

$$\sum_{n,m \geq 0} a_{n,m} \cdot h_n^{(2)}(k_0 r_0) \cdot K_{n,\kappa}^{m,\imath} \cdot I_{m,\imath}, \quad (23b)$$

where the following integrals are introduced:

$$I_{m,\imath} = \frac{1}{\varphi_0} \int_0^{\varphi_0} \cos(m \varphi) \cdot \cos(\imath \varphi) \, d\varphi, \quad (24)$$

$$K_{n,\kappa}^{m,\imath} = \int_0^1 P_n^m(x) \cdot P_\kappa^\imath(x) \, dx. \quad (25)$$

Thus the matching condition for the sound pressures leads to:

$$\frac{N_k^i}{2\delta_i} \cdot b_{k,i} \cdot j_k(k_0 r_0) = \sum_{n,m \geq 0} a_{n,m} \cdot h_n^{(2)}(k_0 r_0) \cdot K_{n,k}^{m,i} \cdot I_{m,i}. \quad (26)$$

This is a linear homogeneous system of equations for the vector  $\{b_{k,i}, a_{n,m}\}$  of solutions.

Next we apply on the matching condition O.7.(22) for the *particle velocities*, with

$$Z_0 v_r^{(I)}(r, \vartheta, \varphi) = j \sum_{n,m \geq 0} a_{n,m} \cdot h_n^{(2)}(k_0 r) \cdot P_n^m(\cos \vartheta) \cdot \cos(m\varphi),$$

$$Z_0 v_r^{(II)}(r, \varphi, \vartheta) = j \sum_{v,\mu} b_{v,\mu} \cdot j'_v(k_0 r) \cdot P_v^\mu(\cos \vartheta) \cdot \cos(\mu\varphi),$$

$$Z_0 v_{er}(r_0, \vartheta, \varphi) = j P_e \cdot h_{n_0}^{(2)}(k_0 r_0) \cdot P_{n_0}^{m_0}(\cos \vartheta) \cdot \cos(m_0 \varphi)$$

$$:= Z_0 V \cdot P_{n_0}^{m_0}(\cos \vartheta) \cdot \cos(m_0 \varphi),$$

the integral

$$\frac{1}{\pi} \int_0^\pi d\varphi \int_{-1}^1 \dots P_k^i(x) \cdot \cos(i\varphi) dx,$$

in which  $i, k$  are from the range of values of  $m, n$ . The left-hand side will give:

$$\begin{aligned} j \sum_{n,m \geq 0} a_{n,m} \cdot \frac{\delta_{m,i}}{\delta_i} \cdot h_n^{(2)}(k_0 r_0) \int_{-1}^1 P_n^m(x) \cdot P_k^i(x) dx \\ = j \sum_{n \geq 0} a_{n,i} \cdot \frac{h_n^{(2)}(k_0 r_0)}{\delta_i} \int_{-1}^1 P_n^i(x) \cdot P_k^i(x) dx \\ = j \frac{N_k^i}{\delta_i} \cdot h_k^{(2)}(k_0 r_0) \cdot a_{k,i}, \end{aligned} \quad (27a)$$

and the first line of the right-hand side of O.7.(22) by the integral

$$\frac{1}{\pi} \int_0^{\varphi_0} d\varphi \int_0^1 Z_0 v_r^{(II)}(r_0, \varphi, \vartheta) \cdot P_k^i(x) \cdot \cos(i\varphi) dx \quad (28)$$

will contribute:

$$j \sum_{v,\mu} b_{v,\mu} \cdot j'_v(k_0 r_0) \cdot L_{k,v}^{i,\mu} \cdot J_{i,\mu}, \quad (27b)$$

where the integrals are introduced:

$$J_{i,\mu} = \frac{1}{\pi} \int_0^{\varphi_0} \cos(i\varphi) \cdot \cos(\mu\varphi) d\varphi = \frac{\varphi_0}{\pi} I_{i,\mu}, \quad (29)$$



$$L_{k,v}^{i,\mu} = \int_0^1 P_k^i(x) \cdot P_v^\mu(x) dx = K_{k,v}^{i,\mu}. \quad (30)$$

The second line of the right-hand side of O.7.(22) takes the form:

$$\begin{aligned} & \frac{1}{\pi} \int_0^\pi d\varphi \int_{-1}^1 Z_0 v_{er}(r_0, \vartheta, \varphi) \cdot P_k^i(x) \cdot \cos(i\varphi) dx \\ & - \frac{1}{\pi} \int_0^{\varphi_0} d\varphi \int_0^1 Z_0 v_{er}(r_0, \vartheta, \varphi) \cdot P_k^i(x) \cdot \cos(i\varphi) dx, \end{aligned} \quad (31)$$

whereof the first line contributes:

$$Z_0 V \cdot \frac{\delta_{m_0,i}}{\delta_{m_0}} \delta_{n_0,k} N_{n_0}^{m_0}, \quad (27c)$$

and the second line gives the contribution:

$$Z_0 V \cdot J'_{i,m_0} \cdot K_{k,n_0}^{i,m_0} \quad (27d)$$

(the apostrophe at J, K shall indicate that  $m_0, n_0$  generally are not members of  $\mu, \nu$ ). In total, the boundary condition for  $v_r$  gives:

$$\begin{aligned} & j \frac{N_k^i}{\delta_i} \cdot h_k^{(2)}(k_0 r_0) \cdot a_{k,i} \\ & = j \sum_{\nu, \mu} b_{\nu, \mu} \cdot j'_\nu(k_0 r_0) \cdot L_{k,\nu}^{i,\mu} \cdot J_{i,\mu} + Z_0 V \cdot \frac{\delta_{m_0,i} \cdot \delta_{n_0,k}}{\delta_{m_0}} N_{n_0}^{m_0} - Z_0 V \cdot J'_{i,m_0} \cdot K_{k,n_0}^{i,m_0}. \end{aligned} \quad (27)$$

This is a second linear inhomogeneous system of equations for  $\{a_{k,i}, b_{\nu,\mu}\}$ . Either one packs the systems O.7.(26), O.7.(27) together to a compound system for the  $\{a_{n,m}, b_{\nu,\mu}\}$  or, preferably, one next tries a reduction of the systems of equations (see below). Before doing that, the mode coupling integrals shall be discussed.

## 0.7.4 Mode Coupling Integrals

In principle, the coupling integrals can be evaluated numerically, since the integration interval is finite. But because the integrands oscillate, analytical solutions are preferable.

The integrals from O.7.(24) and O.7.(29), with  $\mu = \eta \cdot N; i, \eta = 0, 1, 2, \dots$  have the values:

$$\begin{aligned} I_{i,\mu} &= \frac{1}{\varphi_0} \int_0^{\varphi_0} \cos(i\varphi) \cdot \cos(\mu\varphi) d\varphi = \frac{\pi}{\varphi_0} J_{i,\mu} \\ &= \frac{1}{2} \left[ \frac{\sin((i + \eta N)\varphi_0)}{(i + \eta N)\varphi_0} + \frac{\sin((i - \eta N)\varphi_0)}{(i - \eta N)\varphi_0} \right] \\ &\xrightarrow{i=\eta N=0} 1; \quad \xrightarrow{i=\eta N \neq 0} \frac{1}{2} \left[ 1 + \frac{\sin(2\eta N\varphi_0)}{2\eta N\varphi_0} \right] = \frac{1}{2} \left[ 1 + \frac{\sin(2\eta\pi)}{2\eta\pi} \right] = \frac{1}{2}. \end{aligned} \quad (32)$$

The integrals from (27d), with  $i, m = 0, 1, 2, \dots$  are:

$$J'_{i,m} = \frac{1}{\pi} \int_0^{\varphi_0} \cos(i\varphi) \cdot \cos(m\varphi) d\varphi = \frac{\varphi_0}{2\pi} \left( \frac{\sin((i+m)\varphi_0)}{(i+m)\varphi_0} + \frac{\sin((i-m)\varphi_0)}{(i-m)\varphi_0} \right) \quad (33)$$

$$\xrightarrow{i=m \neq 0} \frac{\varphi_0}{2\pi} \left( 1 + \frac{\sin(2m\varphi_0)}{2m\varphi_0} \right) \xrightarrow{i=m=0} \frac{\varphi_0}{\pi}.$$

There still remain the integrals from O.7.(25), O.7.(30):

$$L_{n,v}^{m,\mu} = \int_0^1 P_n^m(x) \cdot P_v^\mu(x) dx = K_{n,v}^{m,\mu},$$

Solutions can be found in integral tables only for a few special values of the indices. An algorithm for the integration starts from the representation of Legendre functions for integer  $n, m$  and real  $x$  (with  $|x| < 1$ ):

$$P_n^m(x) = (-1)^m (1-x^2)^{m/2} \frac{d^m P_n(x)}{dx^m}. \quad (34)$$

The Legendre polynomials  $P_n(x)$  are polynomials of  $n$ -th degree in  $x$ . Therefore  $P_n^m(x) = 0$  for  $m > n$ . The Legendre polynomials have the form:

$$P_n(x) = \sum_{k=0}^{[n/2]} \beta_k \cdot x^{n-2k} = \frac{1}{2^n} \sum_{k=0}^{[n/2]} \frac{(-1)^k (2n-2k)!}{k! \cdot (n-k)! \cdot (n-2k)!} x^{n-2k}, \quad (35)$$

where  $[n/2]$  = largest integer  $\leq n/2$ . The  $m$ -th derivative thereof is ( $m \leq n$ ):

$$\begin{aligned} \frac{d^m P_n(x)}{dx^m} &= \sum_{k=0}^{[(n-m)/2]} \beta_k \frac{(n-2k)!}{(n-2k-m)!} \cdot x^{n-2k-m} \\ &= \frac{1}{2^n} \sum_{k=0}^{[(n-m)/2]} \frac{(-1)^k (2n-2k)!}{k! \cdot (n-k)! (n-2k-m)!} x^{n-2k-m}. \end{aligned} \quad (36)$$

Thus the Legendre functions become:

$$P_n^m(x) = \frac{(-1)^m (1-x^2)^{m/2}}{2^n} \sum_{k=0}^{[(n-m)/2]} \frac{(-1)^k (2n-2k)!}{k! \cdot (n-k)! (n-2k-m)!} x^{n-2k-m}. \quad (37)$$

If one has available a computer program for mathematics which can perform symbolic operations (like *Mathematica*® or *Maple*®) one can imagine to have the factor  $(1-x^2)^{m/2}$  multiplied under the sum and expanded the sum terms with  $x$  remaining symbolic. After multiplication two sums for two Legendre functions (and expanding again) the program can integrate term-wise. This indeed is an easy method, but it will take long computing times, because the number of integrals to be evaluated roughly increases with the fourth power of the upper limits of the used mode orders (and the number of terms in the sums increases linearly with those limits). Therefore explicit solutions for the integrals shall be given here, even if the result becomes lengthy.



One starts from the representation:

$$P_n^m(x) = \frac{(-1)^m (1-x^2)^{m/2}}{2^n} \sum_{k=0}^{[(n-m)/2]} \frac{(-1)^k (2n-2k)!}{k! \cdot (n-k)! (n-2k-m)!} x^{n-2k-m}$$

and similarly after the substitutions  $m \rightarrow \mu$ ;  $n \rightarrow v$ ;  $k \rightarrow i$ . The indefinite integral of their product then becomes (by multiplication of the sums, expanding the product, and term-wise integration):

$$\begin{aligned} \int_x P_n^m(x) \cdot P_v^\mu(x) dx &= \frac{(-1)^{1+m+\mu} x^{1+n+v-m-\mu}}{2^{n+v}} \cdot \sum_{k=0}^{[(n-m)/2]} \sum_{i=0}^{[(v-\mu)/2]} \\ &\frac{(-1)^{i+k} (2n-2k)! \cdot (2v-2i)! \cdot x^{-2i-2k}}{(-1+2i+2k+m+\mu-n-v) \dots} \\ &\dots \\ &\dots \cdot (i! \cdot k! \cdot (n-k)! \cdot (v-i)! \cdot (n-m-2k)! \cdot (v-\mu-2i)!) \\ &\cdot {}_2F_1 \left( (1-2i-2k-m-\mu+n+v)/2, -(m+\mu)/2; \right. \\ &\left. 1 + (1-2i-2k-m-\mu+n+v)/2; x^2 \right), \end{aligned} \quad (38)$$

where  ${}_2F_1(a, b; c; z)$  are hypergeometric functions.

The definite integral is:

$$\begin{aligned} \int_0^1 P_n^m(x) \cdot P_v^\mu(x) dx &= \frac{(-1)^{m+\mu}}{2^{n+v}} \cdot \sum_{k=0}^{[(n-m)/2]} \sum_{i=0}^{[(v-\mu)/2]} \\ &\frac{(-1)^{1+i+k} (2n-2k)! \cdot (2v-2i)!}{(1+n+v-m-\mu-2i-2k) i! \cdot k! \cdot (n-k)! \cdot (v-i)! \dots} \\ &\dots \\ &\dots \cdot (n-m-2k)! \cdot (v-\mu-2i)! \\ &\cdot \frac{[\Gamma((3+n+v-2i-2k)/2) - \Gamma((2+m+\mu)/2)] \dots}{\Gamma((3+n+v-2i-2k)/2)} \\ &\dots \cdot \frac{\Gamma((3+n+v-m-\mu-2i-2k)/2)}{\dots} \end{aligned} \quad (39)$$

with the Gamma function  $\Gamma(z)$ .



### 0.7.5 Reduction of the System of Equations

Eliminate the  $b_{k,i}$  from 0.7.(26) and to insert them into 0.7.(27):

$$b_{v,\mu} = \frac{2\delta_\mu}{N_v^\mu \cdot j_v(k_0 r_0)} \sum_{n,m \geq 0} a_{n,m} \cdot h_n^{(2)}(k_0 r_0) \cdot K_{n,v}^{m,\mu} \cdot I_{m,\mu}. \quad (40)$$

After insertion in 0.7.(27) and rearrangement that equation becomes:

$$\begin{aligned} j \sum_{n,m \geq 0} & \left[ -\delta_{m,i} \cdot \delta_{n,k} \cdot \frac{N_k^i}{\delta_i} \cdot h_k^{(2)}(k_0 r_0) \right. \\ & \left. + \frac{\varphi_0}{\pi} h_n^{(2)}(k_0 r_0) \sum_{v,\mu} \frac{2\delta_\mu \cdot j'_v(k_0 r_0)}{N_v^\mu \cdot j_v(k_0 r_0)} \cdot I_{m,\mu} \cdot I_{i,\mu} \cdot K_{n,v}^{m,\mu} \cdot K_{k,v}^{i,\mu} \right] \cdot a_{n,m} \\ & = Z_0 V \cdot \left( I'_{i,m_0} \cdot K_{k,n_0}^{i,m_0} - \frac{\delta_{m_0,i} \cdot \delta_{n_0,k}}{\delta_{m_0}} N_{n_0}^{m_0} \right); \quad k \in \{n\}; \quad i \in \{m\} \leq k. \end{aligned} \quad (41a)$$

This is a two-dimensional system of equations for the  $a_{n,m}$ ; in every sub-system the  $i, k$  have fixed values  $0, 1, 2, \dots$ . By the variation of  $n, k = 0, 1, 2, \dots, n_{hi}$  every line of the system contains the unknowns  $a_{n,m}$ , because of the requirements  $i \leq k, m \leq n$ , in an arrangement like:

$$\{a_{n,m}\} = \{\{a_{0,0}\}, \{a_{1,0}, a_{1,1}\}, \{a_{2,0}, a_{2,1}, a_{2,2}\}, \{a_{3,0}, a_{3,1}, a_{3,2}, a_{3,3}\}, \dots\}.$$

The system 0.7.(41a) of equations in principle has an infinite size. It must converge if a truncation shall be possible. A sufficient condition for convergence is a decrease (or constant value) of the elements on the main diagonal, together with a decrease of the other elements with increasing distance to the main diagonal, and a decrease of the right-hand side elements. The first condition is violated by the norms  $N_k^i$  in the first term in the brackets, because they assume huge values for larger indices. Therefore the lines are divided by  $N_k^i$ . Introducing the reference amplitude  $P_e$  instead of  $Z_0 V$  one gets the system of equations:

$$\begin{aligned} \sum_{n,m} & \left[ -\frac{\delta_{m,i} \cdot \delta_{n,k}}{\delta_i} \cdot h_k^{(2)}(k_0 r_0) \right. \\ & \left. + \frac{\varphi_0}{\pi} \frac{h_n^{(2)}(k_0 r_0)}{N_k^i} \sum_{v,\mu} \frac{2\delta_\mu \cdot j'_v(k_0 r_0)}{N_v^\mu \cdot j_v(k_0 r_0)} \cdot I_{m,\mu} \cdot I_{i,\mu} \cdot K_{n,v}^{m,\mu} \cdot K_{k,v}^{i,\mu} \right] \cdot a_{n,m} \\ & = P_e \cdot \frac{h_{n_0}^{(2)}(k_0 r_0)}{N_k^i} \left( \frac{\varphi_0}{\pi} \cdot I'_{i,m_0} \cdot K_{k,n_0}^{i,m_0} - \frac{\delta_{m_0,i} \cdot \delta_{n_0,k}}{\delta_{m_0}} N_{n_0}^{m_0} \right); \end{aligned} \quad (41b)$$

$$\begin{cases} k \in \{n\}; & i \in \{m\} \leq k \\ m \leq n; & \mu \leq v \end{cases}.$$

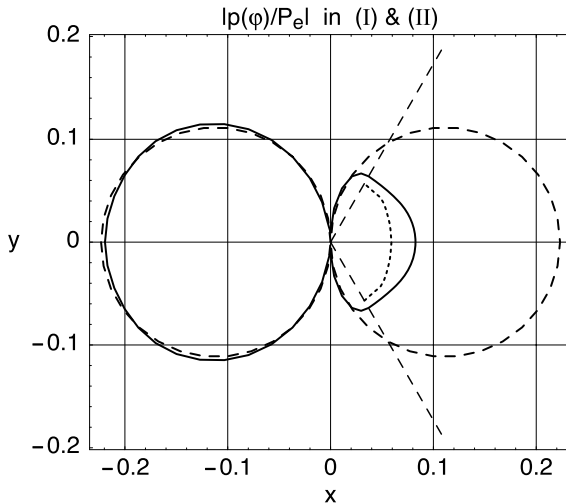
If one symbolises the matrix elements with  $X_{k,n}^{i,m}$  and the elements of the right-hand side with  $Y_k^i$  the system O.7.(41b) at its beginning has the form:

$$\begin{aligned}
 X_{0,0}^{0,0} \cdot a_{0,0} + (X_{0,1}^{0,0} \cdot a_{1,0} + X_{0,1}^{0,1} \cdot a_{1,1}) + (X_{0,2}^{0,0} \cdot a_{2,0} + X_{0,2}^{0,1} \cdot a_{2,1} + X_{0,2}^{0,2} \cdot a_{2,2}) + \dots &= Y_0^0, \\
 X_{1,0}^{0,0} \cdot a_{0,0} + (X_{1,1}^{0,0} \cdot a_{1,0} + X_{1,1}^{0,1} \cdot a_{1,1}) + (X_{1,2}^{0,0} \cdot a_{2,0} + X_{1,2}^{0,1} \cdot a_{2,1} + X_{1,2}^{0,2} \cdot a_{2,2}) + \dots &= Y_1^0, \\
 X_{1,0}^{1,0} \cdot a_{0,0} + (X_{1,1}^{1,0} \cdot a_{1,0} + X_{1,1}^{1,1} \cdot a_{1,1}) + (X_{1,2}^{1,0} \cdot a_{2,0} + X_{1,2}^{1,1} \cdot a_{2,1} + X_{1,2}^{1,2} \cdot a_{2,2}) + \dots &= Y_1^1, \\
 X_{2,0}^{0,0} \cdot a_{0,0} + (X_{2,1}^{0,0} \cdot a_{1,0} + X_{2,1}^{0,1} \cdot a_{1,1}) + (X_{2,2}^{0,0} \cdot a_{2,0} + X_{2,2}^{0,1} \cdot a_{2,1} + X_{2,2}^{0,2} \cdot a_{2,2}) + \dots &= Y_2^0, \\
 X_{2,0}^{1,0} \cdot a_{0,0} + (X_{2,1}^{1,0} \cdot a_{1,0} + X_{2,1}^{1,1} \cdot a_{1,1}) + (X_{2,2}^{1,0} \cdot a_{2,0} + X_{2,2}^{1,1} \cdot a_{2,1} + X_{2,2}^{1,2} \cdot a_{2,2}) + \dots &= Y_2^1, \\
 X_{2,0}^{2,0} \cdot a_{0,0} + (X_{2,1}^{2,0} \cdot a_{1,0} + X_{2,1}^{2,1} \cdot a_{1,1}) + (X_{2,2}^{2,0} \cdot a_{2,0} + X_{2,2}^{2,1} \cdot a_{2,1} + X_{2,2}^{2,2} \cdot a_{2,2}) + \dots &= Y_2^2.
 \end{aligned} \tag{41c}$$

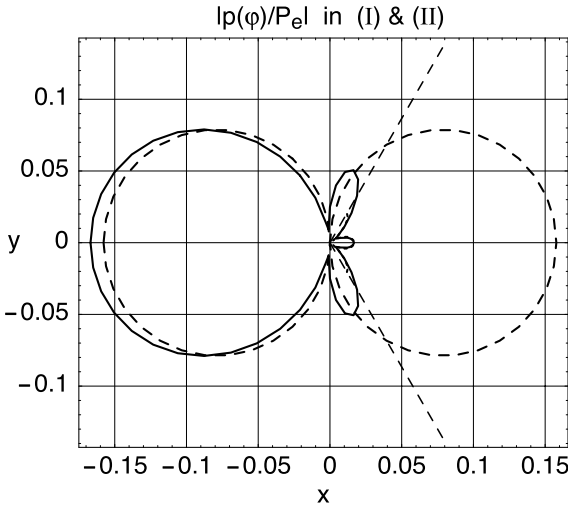
An important aspect, both for the precision and the computing time, are the upper limits of the mode orders  $n_{hi}$  and  $\mu_{hi} = \eta_{hi} \cdot N$ . In the outer zone (I) at least the orders  $n_0$ ,  $m_0$  of the exciting mode must be exceeded. In the sector (II) a rather low number of modes often may be sufficient. In turn, the mode index  $m$  in (I) should reach the order  $\mu_{hi} = \eta_{hi} \cdot N$ ; i.e.,  $n_{hi} \geq \mu_{hi} = \eta_{hi} \cdot N$ .

After solution of this system of equations for the  $a_{n,m}$ , the  $b_{v,\mu}$  are obtained by insertion in O.7.(40). Thus the sound field in and around the Cat's Eye is known.

The formulas above are derived for the radiation problem in the simple case of a mono-modal excitation. For any given distribution  $V(\vartheta, \varphi)$  first expand that distribution as sum of multipole sources. Then solve the multipole radiation task for each sum term and add the results.



Sound pressure magnitude  $|p(\varphi)/P_e|$  on a  $\varphi$ -orbit around a cat's eye with higher mode excitation  $m_0 = 1$ ;  $n_0 = 1$  at elevation  $\vartheta = 90^\circ$ .  $k_0 r_0 = 4$ ;  $N = 3$ ;  $\varphi_0 = 60^\circ$ ;  $n_0 = 1$ ;  $m_0 = 1$ ;  $k_0 r = 4$ ;  $\vartheta = 90^\circ$ ;  $n_{hi} = 12$ ;  $\eta_{hi} = 4$



As above, but elevation  $\vartheta = 45^\circ$

In a scattering task, e.g. for an incident plane wave, first expand the plane wave in spherical harmonics:

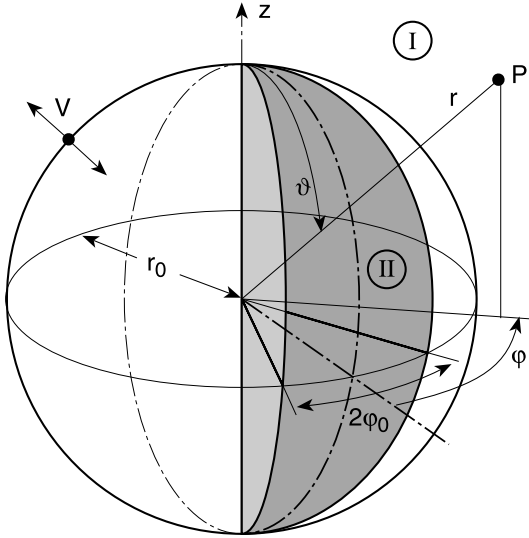
$$e^{-j\mathbf{k}\cdot\mathbf{r}} = \sum_{n=0}^{\infty} (-j)^n (2n+1) \sum_{m=0}^{\infty} \delta_m \frac{(n-m)!}{(n+m)!} \cos(m(\varphi - v)) \cdot P_n^m(\cos u) P_n^m(\cos \vartheta) j_n(k_0 r), \quad (42)$$

where the vector  $\mathbf{r}$  shows from the origin to the field point  $P = (r, \varphi, \vartheta)$ , and the wave number vector  $\mathbf{k}$  has the length  $k_0$  and has the spherical angles  $\vartheta = u, \varphi = v$ . The particle velocities of the terms at the surface  $r = r_0$  are considered as given velocities of a multipole radiation task; these are solved in turn, and the fields are added.

The presented numerical examples show  $|p(\varphi)/P_e|$  (as full lines) on orbits with varying  $\varphi$  and fixed  $r, \vartheta$ . For orientation, the sound pressure  $|p_e(\varphi)/P_e|$  is also shown (as dashed curve) which the exciting mode  $n_0, m_0$  on a full sphere would produce at  $r$ , and the flanks of the cut out at  $\pm\varphi_0$  are also indicated as dashed straight lines. Both  $|p^{(I)}(\varphi)/P_e|$  (full line) and  $|p^{(II)}(\varphi)/P_e|$  (with short dashes) are plotted.

## O.8 The Orange Model

For tests of some numerical methods the Orange model with a simpler geometry may be sufficient also. This model consists of a sphere with “orange slices” taken away.



A sphere with radius  $r_0$  has at its surface the radial velocity distribution  $V$  of a spherical mode with mode indices  $n_0, m_0$ . A sector is cut at  $\varphi = \pm\varphi_0$ . The walls of the cut are hard.

Target quantities are:

- outer sound field (in (I));
- sound field in the cut ((II)).

The time factor  $e^{i\omega t}$  dropped.

The problem be symmetrical in  $\varphi$  relative to  $\varphi = 0$ .

### O.8.1 Elementary Solutions and Field Formulations

The sound field *in the outer zone (I)* is formulated as a sum of spherical modes with spherical Hankel functions of second kind  $h_n^{(2)}(k_0 r)$  as radial functions and tesseral Legendre functions  $P_n^m(\cos \vartheta)$  in the polar direction  $\vartheta$ , and the even azimuthal functions  $\cos(m\varphi)$  along  $\varphi$ . With integer indices  $n, m = 0, 1, 2, \dots$  the sum terms satisfy the wave equation, Sommerfeld's far field condition and the periodicity in  $\varphi$  with period  $2\pi$ .

$$p^{(I)}(r, \vartheta, \varphi) = \sum_{n, m \geq 0} a_{n, m} \cdot h_n^{(2)}(k_0 r) \cdot P_n^m(\cos \vartheta) \cdot \cos(m\varphi), \quad (1a)$$

$$Z_0 v_r^{(I)}(r, \vartheta, \varphi) = j \sum_{n, m \geq 0} a_{n, m} \cdot h_n'^{(2)}(k_0 r) \cdot P_n^m(\cos \vartheta) \cdot \cos(m\varphi). \quad (1b)$$

The sound field which the exciting mode with mode indices  $n_0, m_0$  on a full sphere would produce in (I) is, with arbitrary amplitude  $P_e$ :

$$p_e(r, \vartheta, \varphi) = P_e \cdot h_{n_0}^{(2)}(k_0 r) \cdot P_{n_0}^{m_0}(\cos \vartheta) \cdot \cos(m_0 \varphi). \quad (2)$$

A corresponding radial reference velocity  $V$  may be defined by the relations:

$$\begin{aligned} Z_0 v_{er}(r_0, \vartheta, \varphi) &= jP_e \cdot h_{n_0}^{(2)}(k_0 r_0) \cdot P_{n_0}^{m_0}(\cos \vartheta) \cdot \cos(m_0 \varphi) \\ &:= Z_0 V \cdot P_{n_0}^{m_0}(\cos \vartheta) \cdot \cos(m_0 \varphi), \end{aligned} \quad (3)$$

$$Z_0 V = jP_e \cdot h_{n_0}^{(2)}(k_0 r_0).$$

The special case of constant surface velocity belongs to the mode indices  $n_0, m_0 = 0, 0$ , because of  $P_0^0(x) = 1$ .

A formulation of the *field in (II)* as sum of modes satisfying the symmetry in  $\varphi$  around  $\varphi = 0$ , and being regular at  $r = 0$  reads:

$$p^{(II)}(r, \varphi, \vartheta) = \sum_{v, \mu} b_{v, \mu} \cdot j_v(k_0 r) \cdot P_v^\mu(\cos \vartheta) \cdot \cos(\mu \varphi), \quad (4a)$$

$$Z_0 v_r^{(II)}(r, \varphi, \vartheta) = j \sum_{v, \mu} b_{v, \mu} \cdot j'_v(k_0 r) \cdot P_v^\mu(\cos \vartheta) \cdot \cos(\mu \varphi) \quad (4b)$$

with spherical Bessel functions  $j_v(k_0 r)$ . The boundary condition of zero azimuthal particle velocity at the flanks of the cut-out sector leads to the conditions:

$$v_\varphi \xrightarrow[\varphi \rightarrow \pm \varphi_0]{} 0 \Rightarrow \sin(\mu \varphi_0) \stackrel{!}{=} 0 \Rightarrow \mu \varphi_0 = n\pi; \quad n = 0, 1, 2, \dots \quad (5a)$$

A restriction of  $\varphi_0$  to integer fractions of  $\pi$ ,  $\varphi_0 = \pi/N$ ;  $N = 2, 3, 4, \dots$ ; makes also  $\mu$  an integer:

$$\mu = n \cdot N. \quad (5b)$$

The modes in (II) are symmetrical or anti-symmetrical in  $\vartheta$  relative to  $\vartheta = \pi/2$  if  $v + \mu$  is even or odd, respectively. This requires an integer  $v$  for integer values of  $\mu$ .

## 0.8.2 Orthogonality of Modes

The mode terms of the fields in (I) and (II) are orthogonal in both directions  $\varphi$  and  $\vartheta$ . This follows *in  $\varphi$  direction* for the *zone (I)* from:

$$\begin{aligned} \frac{1}{\pi} \int_0^\pi \cos(m\varphi) \cdot \cos(m'\varphi) d\varphi &= \frac{1}{2} \left[ \frac{\sin((m+m')\pi)}{(m+m')\pi} + \frac{\sin((m-m')\pi)}{(m-m')\pi} \right] \\ &= \begin{cases} 1; & m = m' = 0 \\ 1/2; & m = m' \neq 0 \\ 0; & m \neq m' \end{cases} = \frac{\delta_{m,m'}}{\delta_m} \end{aligned} \quad (6)$$

with Kronecker symbols  $\delta_{n,m} = 0$ ;  $n \neq m$ ;  $\delta_{n,m} = 1$ ;  $n = m$ ; and Heaviside symbols  $\delta_{n=0} = 1$ ;  $\delta_{n \neq 0} = 2$ .

In the *zone (II)*, with  $\mu \varphi_0 = n\pi$ ;  $\mu' \varphi_0 = n'\pi$ ;  $n, n' = 0, 1, 2, \dots$  (see 0.8.(5a)):

$$\begin{aligned} \frac{1}{\varphi_0} \int_0^{\varphi_0} \cos(\mu \varphi) \cdot \cos(\mu' \varphi) d\varphi &= \frac{1}{2} \left[ \frac{\sin((\mu + \mu')\varphi_0)}{(\mu + \mu')\varphi_0} + \frac{\sin((\mu - \mu')\varphi_0)}{(\mu - \mu')\varphi_0} \right] \\ &= \frac{1}{2} \left[ \frac{\sin((n + n')\pi)}{(n + n')\pi} + \frac{\sin((n - n')\pi)}{(n - n')\pi} \right] = \frac{\delta_{n,n'}}{\delta_n}. \end{aligned} \quad (7)$$

In  $\vartheta$  direction, with  $P_v^H(\cos \vartheta) = P_v^H(x)$ , and  $x = \cos \vartheta$ , exists orthogonality in  $\vartheta$  direction for integer orders  $\mu, v \rightarrow m, n$  only when the polar orders  $m, m'$  agree; this follows from the relation:

$$\int_{-1}^1 P_v^H(x) \cdot P_{v'}^H(x) dx = \begin{cases} 0; & v \neq v' \\ N_v^H; & v = v' \end{cases} = \delta_{v,v'} N_v^H; \quad v, v', \mu = \text{integer}, \quad (8)$$

which defines the mode norms  $N_v^H$  (evaluation see below).

### 0.8.3 Field Matching

Matching of the fields in (I) and (II) of sound pressure and radial velocity at  $r = r_0$  to each other and to the excitation on the “rest of the sphere” implies the two boundary conditions:

$$p^{(II)}(r_0, \vartheta, \varphi) \stackrel{!}{=} p^{(I)}(r_0, \vartheta, \varphi) \quad \text{in } \vartheta = (0, \pi) \text{ \& } \varphi = (-\varphi_0, +\varphi_0), \quad (9)$$

$$Z_0 v_r^{(II)}(r_0, \vartheta, \varphi) \stackrel{!}{=} \begin{cases} Z_0 v_r^{(I)}(r_0, \vartheta, \varphi) & \text{in } \vartheta = (0, \pi) \text{ \& } \varphi = (-\varphi_0, +\varphi_0) \\ Z_0 v_{er}(r_0, \vartheta, \varphi) & \text{in rest of the sphere} \end{cases}. \quad (10)$$

Apply in 0.8.(9) the orthogonality in (II), and in 0.8.(10) the orthogonality in (I); then the ranges of orthogonality will agree with the ranges of definition of the relevant boundary condition. For doing that multiply on both sides of a boundary condition with a mode function of the respective co-ordinate for arbitrary fix values  $v, \mu$ , or  $n, m$ , respectively, and then integrate over the range of orthogonality in  $\varphi, \vartheta$ , i.e., in 0.8.(9) over the surface of the sector, and in 0.8.(10) over the sphere (or, because of the  $\varphi$ -symmetry over  $0 \leq \varphi \leq \pi$ ). So one will get two linear inhomogeneous systems of equations for the mode amplitudes  $a_{n,m}, b_{v,\mu}$ .

*p-matching in the sector:*

Apply the sound pressure formulations (at  $r = r_0$ ):

$$p^{(II)}(r_0, \varphi, \vartheta) = \sum_{v,\mu} b_{v,\mu} \cdot j_v(k_0 r_0) \cdot P_v^H(\cos \vartheta) \cdot \cos(\mu\varphi), \quad (11)$$

$$p^{(I)}(r_0, \vartheta, \varphi) = \sum_{n,m \geq 0} a_{n,m} \cdot h_n^{(2)}(k_0 r_0) \cdot P_n^m(\cos \vartheta) \cdot \cos(m\varphi) \quad (12)$$

in 0.8.(9) and perform on both sides of that equation the integrals:

$$\frac{1}{\varphi_0} \int_0^{\varphi_0} d\varphi \int_{-1}^1 \dots \cdot P_\kappa^l(x) \cdot \cos(l\varphi) dx \quad (13)$$

with  $l, \kappa$  from the range of values of  $\mu, v$ . Using the definitions of the mode coupling integrals

$$I_{m,l} = \frac{1}{\varphi_0} \int_0^{\varphi_0} \cos(m\varphi) \cdot \cos(l\varphi) d\varphi, \quad K_{n,\kappa}^{m,l} = \int_{-1}^1 P_n^m(x) \cdot P_\kappa^l(x) dx, \quad (14, 15)$$

one gets from the p-condition the linear, homogeneous system of equations for the combined vector of mode amplitudes  $\{b_{\kappa,1}, a_{n,m}\}$ :

$$\frac{N_{\kappa}^i}{\delta_i} \cdot b_{\kappa,1} \cdot j_{\kappa}(k_0 r_0) = \sum_{n,m \geq 0} a_{n,m} \cdot h_n^{(2)}(k_0 r_0) \cdot K_{n,\kappa}^{m,1} \cdot I_{m,1}. \quad (16)$$

*v<sub>r</sub>-matching on the whole sphere:*

Apply in O.8.(10) the formulations of the radial particle velocities:

$$Z_0 v_r^{(I)}(r_0, \vartheta, \varphi) = j \sum_{n,m \geq 0} a_{n,m} \cdot h_n^{(2)}(k_0 r_0) \cdot P_n^m(\cos \vartheta) \cdot \cos(m\varphi), \quad (17)$$

$$Z_0 v_r^{(II)}(r_0, \varphi, \vartheta) = j \sum_{v,\mu} b_{v,\mu} \cdot j'_v(k_0 r_0) \cdot P_v^{\mu}(\cos \vartheta) \cdot \cos(\mu\varphi), \quad (18)$$

and of the exciting mode:

$$\begin{aligned} Z_0 v_{er}(r_0, \vartheta, \varphi) &= j P_e \cdot h_{n_0}^{(2)}(k_0 r_0) \cdot P_{n_0}^{m_0}(\cos \vartheta) \cdot \cos(m_0 \varphi) \\ &:= Z_0 V \cdot P_{n_0}^{m_0}(\cos \vartheta) \cdot \cos(m_0 \varphi). \end{aligned} \quad (19)$$

Perform on both sides of O.8.(10) (with  $k, i$  = integers from the range of  $n, m$ ) the integration:

$$\frac{1}{\pi} \int_0^{\pi} d\varphi \int_{-1}^1 \dots \cdot P_k^i(x) \cdot \cos(i\varphi) dx. \quad (20)$$

With the definitions of the mode coupling integrals

$$J_{i,\mu} = \frac{1}{\pi} \int_0^{\varphi_0} \cos(i\varphi) \cdot \cos(\mu\varphi) d\varphi = \frac{\varphi_0}{\pi} I_{i,\mu}, \quad (21)$$

$$Q_{i,m_0} = \frac{1}{\pi} \int_{\varphi_0}^{\pi} \cos(i\varphi) \cdot \cos(m_0 \varphi) d\varphi, \quad (22)$$

one gets the linear inhomogeneous system of equations for the  $\{b_{\kappa,1}, a_{n,m}\}$ :

$$j \frac{N_{\kappa}^i}{\delta_i} \cdot h_{\kappa}^{(2)}(k_0 r_0) \cdot a_{\kappa,i} = j \sum_{v,\mu} b_{v,\mu} \cdot j'_v(k_0 r_0) \cdot K_{\kappa,v}^{i,\mu} \cdot J_{i,\mu} + Z_0 V \cdot Q_{i,m_0} K_{\kappa,n_0}^{i,m_0} \quad (23)$$

(The prime at  $K_{\kappa,n_0}^{i,m_0}$  shall recall that  $n_0, m_0$  in general are not in the range of  $\kappa, 1$ ). Both systems of equations O.8.(16), O.8.(23) can be solved for the mode amplitudes  $a_{n,m}, b_{v,\mu}$ .

### 0.8.4 Mode Coupling Integrals and Mode Norms

In O.8.(14) and O.8.(21) with  $\mu = \eta \cdot N$ ;  $i, \eta = 0, 1, 2, \dots$ :

$$\begin{aligned} I_{i,\mu} &= \frac{1}{\varphi_0} \int_0^{\varphi_0} \cos(i\varphi) \cdot \cos(\mu\varphi) d\varphi = \frac{\pi}{\varphi_0} J_{i,\mu} \\ &= \frac{1}{2} \left[ \frac{\sin((i + \eta N)\varphi_0)}{(i + \eta N)\varphi_0} + \frac{\sin((i - \eta N)\varphi_0)}{(i - \eta N)\varphi_0} \right] \end{aligned} \quad (24)$$

$$\xrightarrow{i=\eta N=0} 1; \quad \xrightarrow{i=\eta N \neq 0} \frac{1}{2} \left[ 1 + \frac{\sin(2\eta N\varphi_0)}{2\eta N\varphi_0} \right] = \frac{1}{2} \left[ 1 + \frac{\sin(2\eta\pi)}{2\eta\pi} \right] = \frac{1}{2}.$$

In O.8.(22) with  $i, m = 0, 1, 2, \dots$ :


$$\begin{aligned} Q_{i,m} &= \frac{1}{\pi} \int_0^{\pi} \cos(i\varphi) \cdot \cos(m\varphi) d\varphi \\ &= \frac{1}{2} \left[ \frac{\sin((i - m)\pi)}{(i - m)\pi} + \frac{\sin((i + m)\pi)}{(i + m)\pi} - \frac{\varphi_0}{\pi} \left( \frac{\sin((i - m)\varphi_0)}{(i - m)\varphi_0} + \frac{\sin((i + m)\varphi_0)}{(i + m)\varphi_0} \right) \right] \\ &= \begin{cases} 1 - \frac{\varphi_0}{\pi}; & i = m = 0 \\ \frac{1}{2} - \frac{\varphi_0}{2\pi} \left( 1 + \frac{\sin(2m\varphi_0)}{2m\varphi_0} \right); & i = m \neq 0 \\ -\frac{\varphi_0}{2\pi} \left( \frac{\sin((i - m)\varphi_0)}{(i - m)\varphi_0} + \frac{\sin((i + m)\varphi_0)}{(i + m)\varphi_0} \right); & i \neq m \end{cases} \end{aligned} \quad (25)$$

In O.8.(8) with  $i, k = 0, 1, 2, \dots$ :

$$N_k^i = \int_{-1}^1 (P_k^i(x))^2 dx = \frac{2(k + i)!}{(2k + 1)(k - i)!}. \quad (26)$$

In O.8.(15) with  $k, i, v, \mu = \text{integer}$ :

$$K_{k,v}^{i,\mu} = \int_{-1}^1 P_k^i(x) \cdot P_v^\mu(x) dx. \quad (27)$$

This integral can be evaluated with the help of Eq. O.7.(38) in  Sect. O.7.4.

### 0.8.5 Reduction of the Systems of Equations

Eliminate the  $b_{v,\mu}$  from O.8.(16):

$$b_{v,\mu} = \frac{\delta_\mu}{N_v^\mu \cdot j_v(k_0 r_0)} \sum_{n,m \geq 0} a_{n,m} \cdot h_n^{(2)}(k_0 r_0) \cdot K_{n,v}^{m,\mu} \cdot I_{m,\mu} \quad (28)$$



and insert in O.8.(23), leading to the system of equations for the  $a_{n,m}$ :

$$\sum_{n,m \geq 0} \left[ -\delta_{m,i} \cdot \delta_{n,k} \cdot \frac{N_k^i}{\delta_i} \cdot h_k^{(2)}(k_0 r_0) + \frac{\varphi_0}{\pi} h_n^{(2)}(k_0 r_0) \sum_{v,\mu} \frac{\delta_\mu \cdot j'_v(k_0 r_0)}{N_v^\mu \cdot j_v(k_0 r_0)} \cdot I_{m,\mu} \cdot I_{i,\mu} \cdot K_{n,v}^{m,\mu} \cdot K_{k,v}^{i,\mu} \right] \cdot a_{n,m} \quad (29)$$

$$= jZ_0 V \cdot Q_{i,m_0} K_{k,n_0}^{i,m_0}; \quad k \in \{n\}; \quad i \in \{m\} \leq k.$$

With  $P_e$  instead of  $Z_0 V$  (from O.8.(3)) as reference amplitude, O.8.(29) may be written as:

$$\sum_{n \geq 0, m \leq n} \left[ -\frac{\delta_{m,i} \cdot \delta_{n,k}}{\delta_i} + \frac{\varphi_0}{\pi} \frac{h_n^{(2)}(k_0 r_0)}{N_k^i \cdot h_k^{(2)}(k_0 r_0)} \sum_{v,\mu \leq v} \frac{\delta_\mu \cdot j'_v(k_0 r_0)}{N_v^\mu \cdot j_v(k_0 r_0)} \cdot I_{m,\mu} \cdot I_{i,\mu} \cdot K_{n,v}^{m,\mu} \cdot K_{k,v}^{i,\mu} \right] \cdot a_{n,m} \quad (30)$$

$$= -P_e \cdot \frac{h_{n_0}^{(2)}(k_0 r_0)}{h_k^{(2)}(k_0 r_0)} \cdot Q_{i,m_0} \frac{K_{k,n_0}^{i,m_0}}{N_k^i}; \quad k \in \{n\}; \quad i \in \{m\} \leq k.$$

This is a two-dimensional system of linear, inhomogeneous systems of equations for the  $a_{n,m}$ ; in each subsystem  $i, k$  have fix values  $0, 1, 2, \dots$ . Through the variations  $n, k = 0, 1, 2, \dots, n_{hi}$  each equation contains the unknown  $a_{n,m}$ , because of the requirement  $i \leq k, m \leq n$ , in an arrangement:

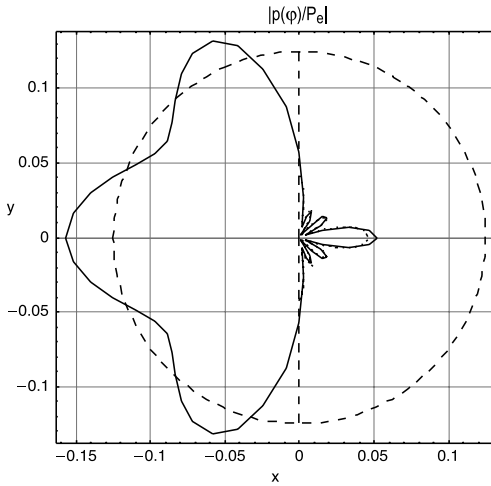
$$\{a_{n,m}\} = \{\{a_{0,0}\}, \{a_{1,0}, a_{1,1}\}, \{a_{2,0}, a_{2,1}, a_{2,2}\}, \{a_{3,0}, a_{3,1}, a_{3,2}, a_{3,3}, \dots\}.$$

$$\sum_{kk=0}^{n_{hi}} (1 + kk) = \frac{(n_{hi} + 1)(n_{hi} + 2)}{2} \text{ lines of equations will arise by the variation of } k, i \leq k.$$

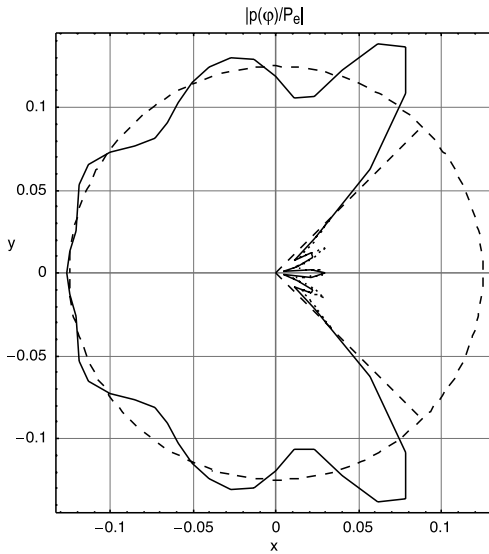
In total, there will arise a system with a square matrix having this number as side length. The upper limit of the  $\mu, \nu = 0, 1 \cdot N, 2 \cdot N, \dots, n_{hi} \cdot N$  may be selected independently.

## O.8.6 Numerical Examples

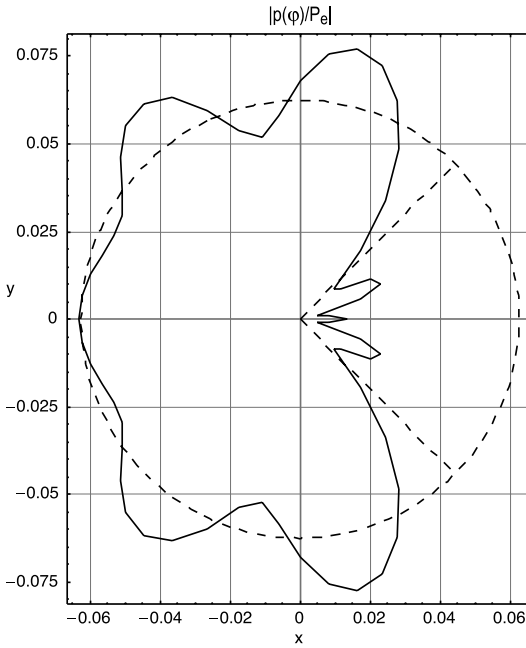
The numerical examples will display  $|p(\varphi)/P_e|$  on  $\varphi$ -orbits (as full curves, represented by the radial distance from the origin) for  $r, \vartheta = \text{const}$ . The diagrams also indicate as dashed straight lines the flanks of the sector at  $\pm\varphi_0$ , and as dashed curves the sound pressure which a full sphere with the vibration pattern of the  $n_0, m_0$  mode would generate in the field point  $P = (r, \vartheta, \varphi)$ . If  $r = r_0$  the sound pressure orbit in zone (II) is shown with short dashes.



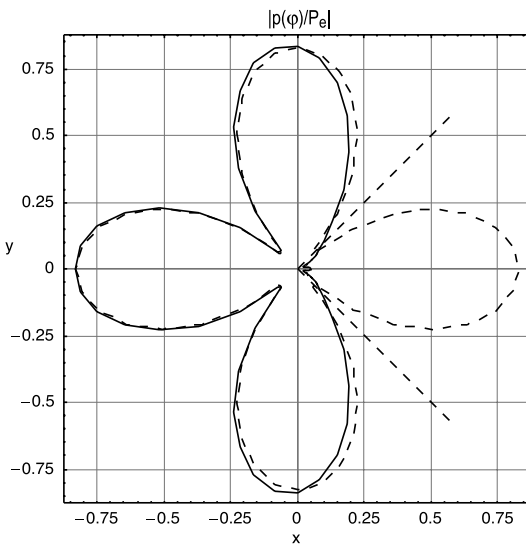
Hemisphere, excited with constant radial velocity,  $n_0 = 0$ ;  $m_0 = 0$ ;  $k_0 r_0 = 8$ ;  $N = 2$ ;  $\varphi_0 = 90^\circ$ ;  $k_0 r = 8$ ;  $\vartheta = 90^\circ$ ;  $\Delta\varphi = 6^\circ$ ;  $n_0 = 0$ ;  $m_0 = 0$ ;  $n_{hi} = 6$ ;  $m_{hi} = 6$



Sphere with sector  $2\varphi_0 = 90^\circ$ , excited with constant radial velocity,  $n_0 = 0$ ;  $m_0 = 0$ ;  $\varphi$ -orbit at sphere radius  $r = r_0$ .  $k_0 r_0 = 8$ ;  $N = 4$ ;  $\varphi_0 = 45^\circ$ ;  $k_0 r = 8$ ;  $\vartheta = 90^\circ$ ;  $\Delta\varphi = 6^\circ$ ;  $n_0 = 0$ ;  $m_0 = 0$ ;  $n_{hi} = 12$ ;  $m_{hi} = 3$



Sphere with sector  $2\varphi_0 = 90^\circ$ , excited with constant radial velocity,  $n_0 = 0$ ;  $m_0 = 0$ ;  $\varphi$ -orbit at double sphere radius  $r = 2r_0$ .  $k_0 r_0 = 8$ ;  $N = 4$ ;  $\varphi_0 = 45^\circ$ ;  $k_0 r = 16$ ;  $\vartheta = 90^\circ$ ;  $\Delta\varphi = 6^\circ$ ;  $n_0 = 0$ ;  $m_0 = 0$ ;  $n_{hi} = 12$ ;  $m_{hi} = 3$



Sphere with sector  $2\varphi_0 = 90^\circ$ , excited with mode pattern  $n_0 = 2$ ;  $m_0 = 2$ .  $k_0 r_0 = 4$ ;  $N = 4$ ;  $\varphi_0 = 45^\circ$ ;  $k_0 r = 4$ ;  $\vartheta = 90^\circ$ ;  $\Delta\varphi = 6^\circ$ ;  $n_0 = 2$ ;  $m_0 = 2$ ;  $n_{hi} = 12$ ;  $m_{hi} = 3$

## References

### Section O.3:

Colton, D., Kress, R.: *Integral Equations in Scattering Theory* Wiley-Interscience Publication, New York (1983)

Junger, M.C., Feit, D.: *Sound, Structures, and their Interaction*. The Massachusetts Institute of Technology Press, Cambridge (1972)

Koopmann, G.H., Perraud, J.C.: Crack location by means of surface acoustic intensity measurements. ASME publication for presentation at the Winter Annual Meeting, Washington, (1981)

Seybert, A.F., Cheng, C.Y., Wu, T.W.: The solution of coupled interior/exterior acoustic problems using the boundary element method. *J. Acoust. Soc. Amer.* **88**, 1612–1618 (1990)

Soize, C.: Reduced models in the medium-frequency range for general external structural-acoustic systems. *J. Acoust. Soc. Amer.* **103**, 3393–3406 (1998)

Soize, C.: Reduced models for structures in the medium-frequency range coupled with internal acoustic cavities. *J. Acoust. Soc. Amer.* **106**, 3362–3374 (1999)

Urick, R.J.: *Principles of Underwater Sound* McGraw-Hill, New York, 3rd ed. (1983)

### Section O.4:

Abramowitz, M. and Stegun, I.A.: *Handbook of Mathematical Functions*, 9th Printing, Dover Publications, Inc., New York (1972)

Attala, N., Winkelmann, G., and Sgard, F.: A multiple multipole expansion approach for predicting the sound power of vibrating structures. *Acustica/Acta Acustica*, **85**, 47–53 (1999)

Bobrovnikskii, Yu.I., Tomilina, T.M.: Calculation of radiation from finite elastic bodies by the method of auxiliary sources. *Sov. Phys. Acoust.*, **36**, 334–338 (1990)

Bobrovnikskii, Yu.I., Tomilina, T.M.: General properties and fundamental errors of the method of equivalent sources. *Acoust. Physics*, **41**, 649–660 (1995)

Colton, D., Kress, R.: *Integral Equations in Scattering Theory*, Wiley-Interscience Publication, New York (1983)

Cremer, L., Wang, M.: Synthesis of spherical wave fields to generate the sound radiated from bodies of arbitrary shape, its realisation by calculation and experiment. *Acustica* **65**, (1988) in German

Cunefare, A.K., Koopmann, G.H., and Brod, K.: A boundary element method for acoustic radiation valid for all wavenumbers. *J. Acoust. Soc. Amer.* **85**, 39–48 (1989)

Erez, E., Leviatan, Y.: Analysis of scattering from structures containing a variety of length scales using a source-model technique. *J. Acoust. Soc. Amer.*, **93**, 3027–3031 (1993)

Fahnlne, J.B., Koopmann, G.H.: A numerical solution for the general radiation problem based on the combined methods of superposition and singular-value decomposition. *J. Acoust. Soc. Amer.* **90**, 2808–2819 (1991)

Guyader, J.L.: Methods to reduce computing time in structural acoustic prediction. *Proc. of the 3rd Int. Congress on Air- and Structure-Borne Sound and Vibration*, ed. M. Crocker, Vol. 1, International Scientific Pub., Auburn, pp. 5–20 (1994)

Hackman, R.H.: The transition matrix for acoustic and elastic wave scattering in prolate spheroidal coordinates. *J. Acoust. Soc. Amer.* **75**, 35–45 (1984)

Heckl, M.: Remarks on the calculation of sound radiation using the method of spherical wave synthesis. *Acustica* **68**, 251–257 (1989), in German

Higgins, J.R.: *Completeness and Basis Properties of Sets of Special Functions*, Cambridge University Press, Cambridge (1977)

Homm, A., Ochmann, M.: Sound scattering of a rigid test cylinder using the source simulation technique for numerical calculations. *Proc. of the 4th Int. Congress on Sound and Vibration*, eds. M. J. Crocker and N.I. Ivanov, International Scientific Pub., Auburn, pp. 133–138 (1996)

Homm, A., Schneider, H.-G.: Application of BE and coupled FE/BE in underwater acoustics, in: *Boundary Elements in Acoustics, Advances and Applications* (ed. by Otto von Estorff, *Advances in Boundary Element Series*), Chapter 13, WIT Press, Computational Mechanics Publications, Southampton, Boston (2000)



- Hwang, J., Chang, S.: A retracted boundary integral equation for exterior acoustic problem with unique solution for all wave numbers. *J. Acoust. Soc. Amer.* **90**, 1167–1179 (1991)
- Jeans, R., Mathews, I.C.: The wave superposition method as a robust technique for computing acoustic fields. *J. Acoust. Soc. Amer.* **92**, 1156–1166 (1992)
- Johnson, M.E., Elliott, S.J., Baek, K.-H., Garcia-Bonito, J.: An equivalent source technique for calculating the sound field inside an enclosure containing scattering objects. *J. Acoust. Soc. Amer.* **104**, 1221–1231 (1998)
- Karageorghis, A., Fairweather, G.: The method of fundamental solutions for axisymmetric acoustic scattering and radiation problems. *J. Acoust. Soc. Amer.* **104**, 3212–3218 (1998)
- Kleinman, R.E., Roach, G.F., Ström, S.E.G.: The null field method and modified Green functions. *Proc. Roy. Soc. Lond., A* **394**, 121–136 (1984)
- Koopmann, G., Song, L., and Fahnlne, J.: A method for computing acoustic fields based on the principle of wave superposition. *J. Acoust. Soc. Amer.* **86**, 2433–2438 (1989)
- Kress, R., Mohsen, A.: On the simulation source technique for exterior problems in acoustics, *Math. Meth. in the Appl. Sci.* **8**, 585–597 (1986)
- Kropp, W., Svensson, U.: Application of the time domain formulation of the method of equivalent sources to radiation and scattering problems. *Acustica* **81**, 528–543 (1995)
- Makarov, A.N., and Ochmann, M.: An iterative solver of the Helmholtz integral equation for high-frequency acoustic scattering. *J. Acoust. Soc. Am.* **103**, 742–750 (1998)
- Martin, P.A.: Acoustic scattering and radiation problems, and the null-field method. *Wave Motion* **4**, 391–408 (1982)
- Masson, P., Redon, E., Priou, J.-P., Gervais, Y.: The application of the Trefftz Method to acoustics. *Proc. of the 3rd Int. Congress on Air- and Structure-Borne Sound and Vibration*, ed. M. Crocker, Vol. 3, International Scientific Pub., Auburn, pp. 1809–1816 (1994)
- Millar, R.F.: On the completeness of sets of solutions to the Helmholtz equation. *IMA J. Appl. Math.* **30**, 27–37 (1983)
- Morse, P.M., Feshbach, H.: *Methods of Theoretical Physics, Part I*, McGraw-Hill, New York (1953)
- Ochmann, M.: Multipole radiator synthesis - an effective method for calculating the radiated sound field of vibrating structures of arbitrary surface configuration. *Acustica* **72**, 233–246 (1990), in German
- Ochmann, M.: Calculation of sound radiation from complex machine structures with application to gearboxes, VDI-Berichte Number 816, pp. 801–810 (1990), in German
- Ochmann, M.: Calculation of sound radiation from complex structures using the multipole radiator synthesis with optimized source locations. *Proc. of the 2nd Int. Congress on Recent Developments in Air- and Structure-Borne Sound and Vibration*, ed. by M. Crocker, International Scientific Pub., Auburn, pp. 1887–1194, (1992)
- Ochmann, M.: The source simulation technique for acoustic radiation problems, *Acustica* **81**, 512–527 (1995)
- Ochmann, M.: The multipole method: Contributions of Manfred Heckl and new developments for high-frequency acoustic scattering, *Proc. of the 16th ICA and the 135th meeting of the ASA*, eds. P.K. Kuhl, L.A. Crum, ASA, New York, pp. 1223–1224 (1998)
- Ochmann, M.: The full-field equations for acoustic radiation and scattering. *J. Acoust. Soc. Am.* **105**, 2574–2584 (1999)
- Ochmann, M.: Source simulation techniques for solving boundary element problems, in: *Boundary Elements in Acoustics, Advances and Applications* (ed. by Otto von Estorff, *Advances in Boundary Element Series*), Ch. 7, WIT Press, Computational Mechanics Publications, Southampton, Boston (2000)
- Ochmann, M.: Complex source point method for computing the Green's function over an arbitrary impedance plane, *Proceedings of the NOVEN 2005*, St. Raphael, France (2005)
- Ochmann, M., Heckl, M.: Numerical methods in technical acoustics, Ch. 3, *Taschenbuch der Technischen Akustik*, eds. M. Heckl and H.A. Müller, 2nd Printing, Springer, Berlin, Heidelberg, New York (1994), in German
- Ochmann, M., Homm, A.: The source simulation technique for acoustic scattering. *Acustica / Acta Acustica* **82**, Suppl. 1, p. 159 (1996)

Ochmann, M., Homm, A.: Calculation of sound scattering from bodies with variable surface impedance and multiple reflections. Proc. of the 23rd German Acoustics DAGA Conference, ed. P. Wille, Fortschritte der Akustik, DEGA, Oldenburg, pp. 167–168 (1997), in German

Ochmann, M., Homm, A.: Calculation of the acoustic radiation from a propeller using the multipole method. Proc. of the 3rd Int. Congress on Air- and Structure-Borne Sound and Vibration, ed. M. Crocker, Vol. 2, International Scientific Pub., Auburn, pp. 1215–1220 (1994)

Ochmann, M., Piscoya, R.: The source simulation technique with complex source points for computing acoustic radiation problems, Proceedings of the “13th International Congress on Sound and Vibration (ICSV13)”, July 2006, Wien, Austria (auf CD-ROM)

Ochmann, M., Wellner, F.: Calculation of sound radiation from complex machine structures using the multipole radiator synthesis and the boundary element multigrid method. Revue Francaise de Mécanique, Numéro spécial 1991, pp. 457–471 (1991)

Pärt-Enander, E., Sjöberg, A., Melin, B., Isaksson, P.: The MATLAB® *Handbook*, Addison-Wesley, Harlow (1996)

Piscoya, R., Ochmann, M.: Calculation of sound radiation using the equivalent source method with complex source points, in preparation.

Press, W.H., Flannery, B.P., Teukolsky, S.A., Vetterling, W.T.: Numerical Recipes, the Art of Scientific Computing, Cambridge University Press, Cambridge, 2nd ed. (1990)

Schenck, H.A.: Improved integral formulation for acoustic radiation problems. J. Acoust. Soc. Amer. **44**, 41–58 (1968)

Stepanishen, P.R.: A generalized internal source density method for the forward and backward projection of harmonic pressure fields from complex bodies. J. Acoust. Soc. Am. **101**, 3270–3277 (1997)

Stupfel, B., Lavie, A., Decarpigny, J.N.: Combined integral formulation and null-field method for the exterior acoustic problem. J. Acoust. Soc. Amer. **83**, 927–941 (1988)

Tobocman, W.: Comparison of the T-matrix and Helmholtz integral equation methods for wave scattering calculations. J. Acoust. Soc. Amer. **77**, 369–374 (1985)

Vekua, N.P.: On the completeness of the system of metaharmonic functions. Dokl. Akad. Nauk SSSR **90**, 715–718 (1953) (in Russian)

Waterman, P.C.: New formulation of acoustic scattering. J. Acoust. Soc. Amer. **45**, 1417–1429 (1969)

Wu, S.F., Yu, J.: Reconstructing interior acoustic pressure fields via Helmholtz equation least-squares method. J. Acoust. Soc. Amer. **104**, 2054–2060 (1998)

## Section 0.5:

---

Akyol, T.P.: Schallabstrahlung von Rotationskörpern. *Acustica* **61**, 200–212 (1986)

Angell, T.S., Kleinman, R.E.: Boundary integral equations for the Helmholtz equation: The third boundary value problem. Math. Meth. in the Appl. Sci. **4**, 164–193 (1982)

Burton, A.J., Miller, G.F.: The application of integral equation methods to the numerical solution of some exterior boundary-value problems. Proc. Roy. Soc. Lond. A **323**, 201–210 (1971)

Chen, L.H., Schweikert, D.G.: Sound radiation from an arbitrary body. J. Acoust. Soc. Amer. **35**, 1626–1632 (1963)

Chertock, G.: Convergence of iterative solutions to integral equations for sound radiation. Quart. Appl. Math. **26** (1968)

Colton, D., Kress, R.: Integral Equations in Scattering Theory, Wiley-Interscience Publication, New York (1983)

Colton, D., Kress, R.: The unique solvability of the null field equations of acoustics. Q.J. Mech. Appl. Math. **36**, 87–95 (1983)

Colton, D., Kress, R.: Inverse Acoustic and Electromagnetic Scattering Theory. Springer, Berlin, Heidelberg, New York (1992)

Copley, L.G.: Fundamental results concerning integral representations in acoustic radiation. J. Acoust. Soc. Amer. **44**, 28–32 (1968)

Estorff, O.V. (ed.): Boundary Elements in Acoustics, Advances and Applications, (Advances in Boundary Element Series), WIT Press, Computational Mechanics Publications, Southampton, Boston (2000)

- Everstine, G.C., Henderson, F.M.: Coupled finite element/boundary element approach for fluid-structure interaction. *J. Acoust. Soc. Amer.* **87**, 1938–1947 (1990)
- Jones, D.S.: Integral equation for the exterior acoustic problem. *Q.J. Mech. Appl. Math.* **27**, 129–142 (1974)
- Kleinman, R.E., Roach, G.F.: Boundary integral equations for the three-dimensional Helmholtz equation. *Siam Review* **16**, 214–236 (1974)
- Kleinman, R.E., Roach, G.F.: On modified Green functions in exterior problems for the Helmholtz equation. *Proc. Roy. Soc. Lond. A* **383**, 313–323 (1982)
- Kleinman, R.E., Roach, G.F.: Iterative solutions of boundary integral equations in acoustics, *Proc. Roy. Soc. Lond. A* **417**, 45–57 (1988)
- Kleinman, R.E., Roach, G.F., Schuetz, L.S., Shirron, J.: An iterative solution to acoustic scattering by rigid objects. *J. Acoust. Soc. Amer.* **84**, 385–391 (1988)
- Kleinman, R.E., Wendland, W.L.: On Neumann's method for the exterior Neumann problem for the Helmholtz equation. *J. Math. Anal. Appl.* **57**, 170–202 (1977)
- Koopmann, G.H., Benner, H.: Method for computing the sound power of machines based on the Helmholtz integral. *J. Acoust. Soc. Amer.* **71**, 78–89 (1982)
- Kress, R., Spassow, W.: On the condition number of boundary integral operators for the exterior Dirichlet problem for the Helmholtz equation. *Numer. Math.* **42**, 77–95 (1983)
- Kupradse, W.D.: *Randwertaufgaben der Schwingungstheorie und Integralgleichungen*, VEB Deutscher Verlag der Wissenschaften, Berlin (1956)
- Lam, Y.W., Hodgson, D.C.: The prediction of the sound field due to an arbitrary vibrating body in a rectangular enclosure. *J. Acoust. Soc. Amer.* **88**, 1993–2000 (1990)
- Makarov, A.N., Ochmann, M.: An iterative solver of the Helmholtz integral equation for high-frequency acoustic scattering. *J. Acoust. Soc. Amer.* **103**, 742–750 (1998)
- Makarov, S., Ochmann, M., Ludwig, R.: Comparison of GMRES and CG iterations on the normal form of magnetic field integral equation, submitted
- Makarov, S., Ochmann, M., Ludwig, R.: An iterative solution for magnetic field integral equation, submitted
- Marburg, S.: Six elements per wavelength – is that enough?, accepted for publication in *Journal of Computational Acoustics*
- Martin, P.A.: On the null field equations for the exterior problems of acoustics. *Q.J. Mech. Appl. Math.* **33**, 385–396 (1980), **83**, 927–941 (1988)
- Mechel, F.P.: *Schallabsorber, Band I: Äußere Schallfelder – Wechselwirkungen*, Hirzel, Stuttgart (1989)
- Morse, P.M., Ingard, K.U.: *Theoretical acoustics*, McGraw-Hill, New York (1968), Ch. 9, pp. 579–580
- Ochmann, M.: The complex equivalent source method for sound propagation over an impedance plane. *J. Acoust. Soc. Am.* **116**, 3304–3311 (2004)
- Ochmann, M., Homm, A., Semenov, S., Makarov, S.: An iterative GMRES-based solver for acoustic scattering from cylinder-like structures, will appear in: *Proc. of the 8th Int. Congress on Sound and Vibration (ICSV8)*, Hong Kong, China, July (2001)
- Ochmann, M., Wellner, F.: Calculation of sound radiation from complex machine structures using the multipole radiator synthesis and the boundary element multigrid method. *Revue Française de Mécanique, Numéro spécial* 1991, pp. 457–471 (1991)
- Peter, J.: Iterative solution of the direct collocation BEM equations, *Proc. of the seventh Int. Congress on Sound and Vibration (ICSV7)*, Garmisch-Partenkirchen, Germany, on CD-ROM, pp. 2077–2084, July (2000)
- Press, W.H., Flannery, B.P., Teukolsky, S.A., Vetterling, W.T.: *Numerical recipes, the art of scientific computing*, Cambridge University Press, Cambridge (1990)
- Rao, S.M., Raju, P.K.: Application of the method of moments to acoustic scattering from multiple bodies of arbitrary shape. *J. Acoust. Soc. Amer.* **86**, 1143–1148 (1989)
- Rosen, E.M., Canning, X.C., Couchman, L.S.: A sparse integral equation method for acoustic scattering. *J. Acoust. Soc. Amer.* **98**, 599–610 (1995)
- Schenck, H.A.: Improved integral formulation for acoustic radiation problems. *J. Acoust. Soc. Amer.* **44**, 41–58 (1968)

Schwarz, H.R.: Methode der finiten Elemente, Teubner, Stuttgart (1980)

Seybert, A.F., Cheng C.Y.R.: Applications of the boundary element method to acoustic cavity response and muffler analysis. *J. Vib. Acoust. Stress Reliab. Design* **109**, 15–21 (1987)

Seybert, A.F., Cheng, C.Y.R., Wu, T.W.: The solution of coupled interior/exterior acoustic problems using the boundary element method. *J. Acoust. Soc. Amer.* **88**, 1612–1618 (1990)

Seybert, A.F., Soenarko, B.: Radiation and scattering of acoustic waves from bodies of arbitrary shape in a three-dimensional half space. *ASME Trans. J. Vib. Acoust. Stress Reliab. Design.* **110**, 112–117 (1988)

Seybert, A.F., Soenarko B., Rizzo, F.J., Shippy, D.J.: An advanced computational method for radiation and scattering of acoustic waves in three dimensions. *J. Acoust. Soc. Amer.* **77**, 362–368 (1985)

Seybert, A.F., Soenarko B., Rizzo, F.J., Shippy, D.J.: A special integral equation formulation for acoustic radiation and scattering for axisymmetric bodies and boundary conditions. *J. Acoust. Soc. Amer.* **80**, 1241–1247 (1986)

Seybert, A.F., Wu, T.W.: Modified Helmholtz integral equation for bodies sitting on an infinite plane. *J. Acoust. Soc. Amer.* **85**, 19–23 (1989)

Skudrzyk, E.: The foundations of acoustics. Springer, Wien, New York (1971)

Smirnov, W.I.: Lehrgang der Höheren Mathematik, Teil IV, VEB Deutscher Verlag der Wissenschaften, Berlin (1977)

Stummel, F., and Hainer, K.: Praktische Mathematik, Teubner, Stuttgart (1971)

Stupfel, B., Lavie, A., Decarpigny, J.N.: Combined integral equation formulation and null-field method for the exterior acoustic problem. *J. Acoust. Soc. Amer.* **83**, 927–941 (1988)

Ursell, F.: On the exterior problems of acoustics. *Proc. Camb. Phil. Soc.* **74**, 117–125 (1973)

Ursell, F.: On the exterior problems of acoustics: II. *Proc. Camb. Phil. Soc.* **84**, 545–548 (1978)

## Section O.6:

Bayliss, A., Gunzburger, M., Turkel, E.: Boundary conditions for the numerical solution of elliptic equations in exterior regions. *SIAM J. Appl. Math.* **42**, 430–451 (1982)

Becker, P., Waller, H.: Vergleich der Methoden der Finiten Elemente und der Boundary-Elemente bei der numerischen Berechnung von Schallfeldern. *Acustica* **60**, 21–33 (1986)

Craggs, A.: The use of simple three-dimensional acoustic finite elements for determining the natural modes and frequencies of complex shaped enclosures. *J. Sound Vib.* **23**, 331–339 (1972)

Craggs, A., Stead, G.: Sound transmission between enclosures – a study using plate and acoustic finite elements. *Acustica* **35**, 89–98 (1976)

Everstine, G.C., Henderson, F.M.: Coupled finite element/boundary element approach for fluid-structure interaction. *J. Acoust. Soc. Amer.* **87**, 1938–1947 (1990)

Gan, H., Levin, P.L., Ludwig, R.: Finite element formulation of acoustic scattering phenomena with absorbing boundary condition in the frequency domain. *J. Acoust. Soc. Amer.* **94**, 1651–1662 (1993)

Gladwell, G.M.L., Zimmermann, G.: On energy and complementary energy formulations of acoustic and structural vibration problems. *J. Sound Vib.* **3**, 233–241 (1966)

Gockel, M.A. (ed.): Handbook for dynamic analysis. Ch. 7.3, (MSC/NASTRAN) Los Angeles: The Mac Neal-Schwendler Corporation (1983)

Hunt, T.J., Knittel, M.R., Barach, D.: Finite element approach to acoustic radiation from elastic structures. *J. Acoust. Soc. Amer.* **55**, 269–280 (1974)

Kirsch, A., Monk, P.: Convergence analysis of a coupled finite element and spectral method in acoustic scattering. *IMA J. Numer. Anal.* **9** 425–447 (1990)

Masmoudi, M.: Numerical solution for exterior problems. *Numer. Math.* **51**, 87–101 (1987)

Munjal, M.L.: Acoustics of ducts and mufflers New York, John Wiley (1987)

Nefske, D.J., Wolf, J.A. JR, Howell, L.J.: Structural-acoustic finite element analysis of the automobile passenger compartment: a review of current practice. *J. Sound Vib.* **80**, 247–266 (1982)



Petyt, M., Lea, J., Koopmann, G.H.: A finite element method for determining the acoustic modes of irregular shaped cavities. *J. Sound Vib.* **45**, 495–502 (1976)

Petyt, M.: Finite element techniques for structural vibration and acoustics, Chap. 15, 16 in: *Noise and vibration*, (ed. R.G. White, J.G. Walker) New York, John Wiley (1982)

Petyt, M.: Finite element techniques for acoustics, Ch. 2 In: *Theoretical acoustics and numerical techniques*, (ed. P. Filippi) Wien, New York, Springer (1983)

Richards, T.L., Jha, S.K.: A simplified finite element method for studying acoustic characteristics inside a car cavity. *J. Sound Vib.* **63**, 61–72 (1979)

Schwarz, H.R.: *Methode der finiten Elemente*. Stuttgart, Teubner (1980)

Schulze Hobbeling, H.: Berechnung komplexer Absorptions-/ Reflexions-Schalldämpfer mit Hilfe der Finite-Element-Methode. *Acustica* **67**, 275–283 (1989)

Shuku, T., Ishihara, K.: The analysis of the acoustics field in irregularly shaped rooms by the finite element method. *J. Sound Vib.* **29**, 67–76 (1973)

Smith, R.R., Hunt, J.T., Barach, T.: Finite element analysis of acoustically radiating structures with applications to sonar transducers. *J. Acoust. Soc. Amer.* **54**, 1277–1288 (1973)

Soize C.: Reduced models in the medium frequency range for general dissipative structural-dynamics systems. *Eur. J. Mech. A/Solids* **17**, 657–685 (1998)

Soize C.: Reduced models in the medium-frequency range for general external structural-acoustic systems. *J. Acoust. Soc. Amer.* **103**, 3393–3406 (1998)

Soize C.: Reduced models for structures in the medium-frequency range coupled with internal acoustic cavities. *J. Acoust. Soc. Amer.* **106**, 3362–3374 (1999)

Zimmer, H., Ochmann, M., Holzheuer, C.: A finite element approach combined with analytical wave functions for acoustic radiation from elastic structures. *Proc. 17th Int. Congress on Acoustics (ICA)*, Rome, Italy (2001), to appear

## Sections 0.7 & 0.8:

---

Mechel, F.P.: Das Orangen-Modell. *Acta Acustica* **90**, 564–572 (2004)

Mechel, F.P.: The Cat's Eye Model. *Acta Acustica* **91**, 653–660 (2005)